Dynamic wind turbine models in power system simulation tool DIgSILENT

Anca D. Hansen, Clemens Jauch, Poul Sørensen, Florin Iov, Frede Blaabjerg

Abstract

The present report describes the dynamic wind turbine models implemented in the power system simulation tool DIgSILENT (Version 12.0). The developed models are a part of the results of a national research project, whose overall objective is to create a model database in different simulation tools. This model database should be able to support the analysis of the interaction between the mechanical structure of the wind turbine and the electrical grid during different operational modes.

The report provides a description of the wind turbines modelling, both at a component level and at a system level. The report contains both the description of DIgSILENT built-in models for the electrical components of a grid connected wind turbine (e.g. induction generators, power converters, transformers) and the models developed by the user, in the dynamic simulation language DSL of DIgSILENT, for the non-electrical components of the wind turbine (wind model, aerodynamic model, mechanical model). The initialisation issues on the wind turbine models into the power system simulation are also presented. However, the main attention in this report is drawn to the modelling at the system level of two wind turbine concepts:

1. **Active stall wind turbine with induction generator**
2. **Variable speed, variable pitch wind turbine with doubly-fed induction generator**

These wind turbine concept models can be used and even extended for the study of different aspects, e.g. the assessment of power quality, control strategies, connection of the wind turbine at different types of grid and storage systems. For both these two concepts, control strategies are developed and implemented, their performance assessed and discussed by means of simulations.

The report has passed the internal review performed by:

Henrik Bindner

Contents

Preface

This report describes the results of the project titled "Simulation Platform to model, optimize and design wind turbines". The project was carried out in a cooperation between Risø National Laboratory and Aalborg University, funded by the Danish Energy Agency contract number ENS-1363/01-0013.

1 Introduction

The present report describes the dynamic wind turbine models implemented in the power system simulation tool DIgSILENT (Version 12.0), which provides both an extensive library for grid components and a dynamic simulation language (DSL) for the modelling of each wind turbine component. The development of these models is a part of the results of a national Danish research project, whose overall objective is to create a model database of electrical components mainly, in different simulation tools in order to enhance the design and the optimisation of the wind turbines.

The developed model database is able to support the analysis of the interaction between the mechanical structure of the wind turbine and the electrical grid both during normal operation of the wind turbine and during transient grid fault events. Such models make it possible to simulate the dynamic interaction between a wind turbine/wind farm and a power system. They enable both the potential wind turbine owners and the grid utility technical staff to perform the necessary studies before investing and connecting wind turbines (farms) to the grid. Simulation of the wind turbine interaction with the grid may thus provide valuable information and may even lower the overall grid connection costs.

The motivation for this research project is the ever-increasing wind power penetration into power networks. In recent years the trend has been moved from installations with a few wind turbines to the planning of large wind farms with several hundred MW of capacity. This increased and concentrated penetration makes the power network more dependent on, and vulnerable to, the wind energy production. This situation means that future wind farms must be able to replace conventional power stations, and thus be active controllable elements in the power supply network. In other words, wind farms must develop power plant characteristics (Sørensen P. et al., 2000). The two utilities responsible for the transmission systems in Denmark, Eltra and Elkraft System, have issued requirements (Eltra, 2000) that focus on the influence of wind farms on grid stability and power quality, and on the control capabilities of wind farms.

Another consequence of the increased future size of wind farms is that the large wind farms will be connected directly to the high voltage transmission grid. Until now, wind turbines and wind farms have been connected to the distribution system, which typically has either 10/20 kV or 50/60 kV grids. Therefore, the main focus has been on the influence of the wind farms on the power quality of the distribution system. For example in Denmark, this has been regulated by the Danish Utilities Research Institute (DEFU) requirements for grid connection of wind turbines to the distribution system (DEFU, 1998). However, the transmission system operators in Denmark now issue more strict connection requirements for large wind farms if they are connected directly to the transmission system. Moreover, national standards for power quality of wind turbines have recently been supplemented by a new standard for measurement and assessment of power quality of grid connected wind turbines, namely (IEC 61400-21,2001).

A large part of the report is dedicated to the description of two wind turbine concepts with their control strategies, namely:

1. Active stall wind turbine with induction generator
2. Variable speed, variable pitch wind turbine with doubly-fed induction generator.

The report is organised as follows. First, the power system simulation tool DIgSILENT is shortly described. Then the wind turbine modelling in DIgSILENT is presented. The description and implementation of the two mentioned

wind turbine concepts in the power simulation tool DIgSILENT is then presented, their performance assessed and analysed by means of simulations.

2 Wind turbine modelling in DIgSILENT

After a short description of the power system simulation tool, the goal of this chapter is to describe the wind turbine modelling in DIgSILENT at component level, namely the modelling of each wind turbine component.

2.1 Power system simulation tool - DIgSILENT

The increasing capacity of wind power penetration is one of today's most challenging aspects in power-system control. Computer models of power systems are widely used by power-system operators to study load flow, steady state voltage stability, dynamic and transient behaviour of power systems. Today these tools must incorporate extensive modelling capabilities with advanced solution algorithms for complex power-system studies, as in the case of wind power applications. An example of such a tool is the power system simulation tool DIgSILENT (DIgSILENT GmbH, 2002).

DIgSILENT has the ability to simulate load flow, RMS fluctuations and transient events in the same software environment. It provides models on a different level of detailing. It combines models for electromagnetic transient simulations of instantaneous values with models for electromechanical simulations of RMS values. This makes the models useful for studies of both (transient) grid fault and (longer-term) power quality and control issues.

DIgSILENT provides a comprehensive library of models of electrical components in power systems. The library includes models of e.g. generators, motors, controllers, dynamic loads and various passive network elements (e.g. lines, transformers, static loads and shunts). Therefore, in the present work, the grid model and the electrical components of the wind turbine model are included as standard components in the existing library. The models of the wind speed, the mechanics, aerodynamics and the control systems of the wind turbines are written in the dynamic simulation language DSL of DIgSILENT. The DSL makes it possible for users to create their own blocks either as modifications of existing models or as completely new models. These new models can be collected into a library, which can be easily used further in the modelling of other wind farms with other wind turbines.

The program DIgSILENT has been extended and further developed for wind power applications, based on extensive communication and collaboration between DIgSILENT and Risø National Laboratory.

In the following, the two types of models in DIgSILENT are presented:
1. Built-in models, which are standard electrical component models, already existing in the DIgSILENT library.
2. DSL models, which are created by the user in the dynamic simulation language DSL.

2.2 Built-in models in DIgSILENT

The built-in models are standard models existing in DIgSILENT for different electrical components. The internal details of these models (e.g. equations, assumptions, approximations) are not directly accessible for the user and therefore they can only be used as black boxes with predefined inputs and outputs.

During the implementation of different wind turbine models in DIgSILENT, different built-in models are used for the grid components and for the electrical wind turbine components, e.g. generators, power converters, transformers and capacitors. The simulation results depend strongly on these built-in component models and they are therefore briefly described below, based on DIgSILENT documentation.

A grid can be modelled in a graphical programming environment, see Figure 1, where the power system component models (built-in models) are dragged, dropped and connected.
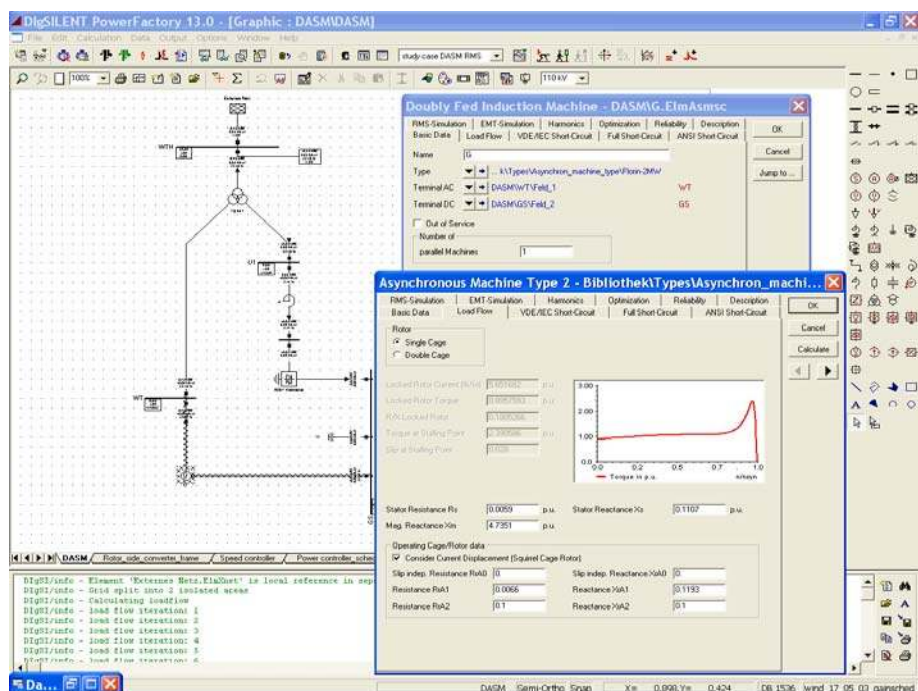
Figure 1: DIgSILENT graphical programming environment.

2.2.1 Electrical machinery

DIgSILENT provides models for induction (asynchronous) machines as well as for synchronous machines. In the present report, the induction generators are in focus.

DIgSILENT machine models are black boxes with predefined inputs and outputs. Figure 2 illustrates the built-in blocks, with the most relevant input and output signals for squirrel cage induction generator (SCIG) and for doubly-fed induction generator (DFIG).
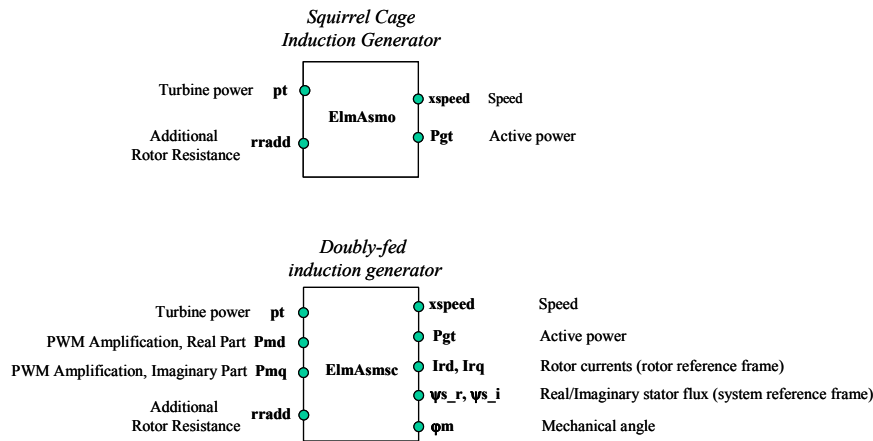
Figure 2: Squirrel cage induction generator (SCIG) and doubly-fed induction generator (DFIG) blocks.

1. *Squirrel cage induction generator model* (*ElmAsmo* asynchronous machine block model) – has the mechanical power of the wind turbine as primer mover input. An additional rotor resistance can be inserted if it is necessary. The outputs are   the generator speed and the electrical power. In the load flow calculation, used in the initialisation process of the system, the information on the generators active power has to be specified.

2. *Doubly-fed induction generator model* (*ElmAsmsc* slip controlled asynchronous machine block model) – has as inputs the mechanical power of the wind turbine, the pulse width modulation factors *Pmd*, *Pmq* and the additional rotor resistance. As outputs, besides the speed and the active power, the rotor currents, the stator flux and the mechanical angle of the rotor can be delivered. In the load flow calculation, the active power for the stator, the reactive power and the slip have to be specified. Internally, the corresponding modulation factors of the converter are calculated and together with power balance between the AC and DC side of the converter, DC voltage and DC current are obtained.

2.2.1.1   Squirrel cage induction generator (SCIG)

DIgSILENT uses different equivalent circuits to define the parameters in the induction generator model, as illustrated in Figure 3. It consists of a general model for the stator, which can be combined with three different rotor models, depending on the type of the generator. The model is thus basically a classical induction machine model including a slip dependent rotor impedance *Zrot*.
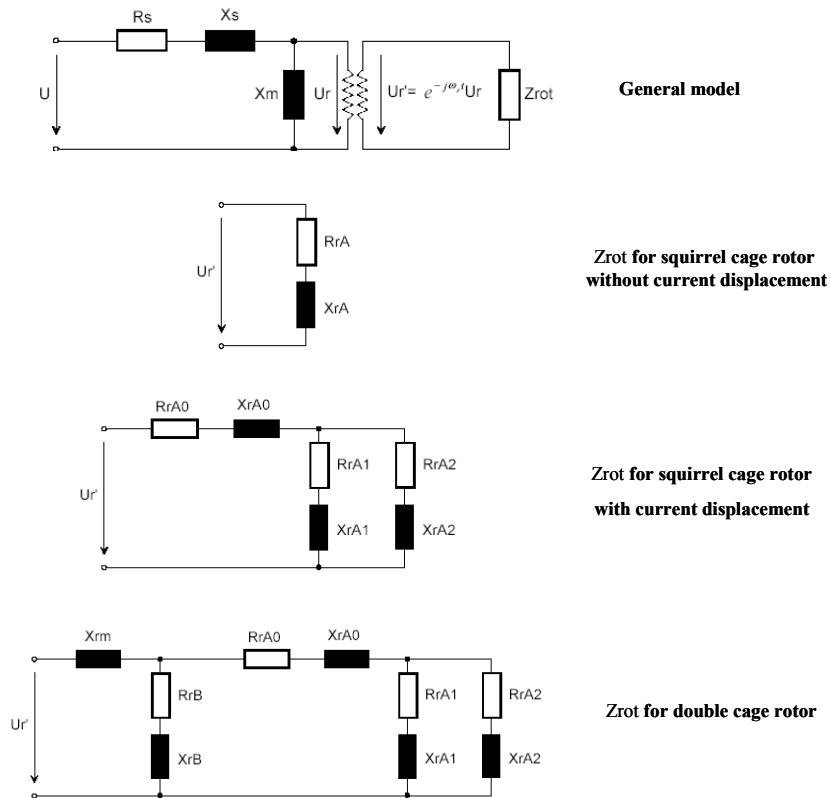
Figure 3: Squirrel cage induction generator diagram with the different definitions for the rotor impedance Zrot.

The model is characterized by the stator winding resistance R_s, the stator leakage reactance X_s, the magnetizing reactance X_m and the rotor impedance Z_{rot}. The rotor impedance Z_{rot} is frequency dependent and allows therefore the modeling over a wide speed/slip range. The rotor impedance can be approximated by parallel R-L elements. Different rotor circuit designs, depending on the rotor geometry, can thus be modeled by selecting a specific rotor impedance Z_{rot}.

Three different squirrel cage rotor types, as illustrated in Figure 3, can be used:

- Squirrel cage rotor without current displacement
- Squirrel cage rotor with current displacement
- Double cage rotor

Saturation is not available in the Version 12.0 of DIgSILENT.

The input parameters of the generator can be entered either by directly specifying the resistances and reactances of the equivalent circuit diagrams (if they are known e.g. from tests or other simulation programs) or by specifying characteristic points on the slip-torque and slip-current characteristic of the generator. When the electrical parameters are not available, they are automatically calculated from the nominal operation point and slip-torque/slip-current characteristics. The nominal operation point is specified by the rated mechanical power, the rated power factor, the efficiency at nominal operation and the nominal speed.

The dynamic model of the induction generator uses the steady state parameters defined in the equivalent diagram depicted in Figure 3. DIgSILENT provides a d-q model, expressed in the rotor reference frame:

$$u_s = R_s\, i_s + j\,\omega_{syn}\,\psi_s + \frac{d\psi_s}{dt}$$

$$0 = R_r\, i_r + j\,(\omega_{syn} - \omega_r)\,\psi_r + \frac{d\psi_r}{dt}$$

(1)

where u, i, and ψ are space vectors for the voltage, current and flux, respectively. ω_{syn} is the synchronous speed, while ω_r is the angular speed of the rotor.

As the rotor is short-circuited in the squirrel-cage induction generator, the rotor voltage is set to zero. The voltage equations are used in DIgSILENT in per unit quantities, as follows:

$$\underline{u}_s = \underline{R}_s\, \underline{i}_s + j\,\frac{\omega_{syn}}{\omega_n}\,\underline{\psi}_s + \frac{1}{\omega_n}\,\frac{d\underline{\psi}_s}{dt}$$

$$0 = \underline{R}_r\, \underline{i}_r + j\,\frac{(\omega_{syn} - \omega_r)}{\omega_n}\,\underline{\psi}_r + \frac{1}{\omega_n}\,\frac{d\underline{\psi}_r}{dt}$$

(2)

where ω_n is the nominal electrical frequency of the network.

As mentioned before, DIgSILENT provides models with different detailing levels. Depending on the goal of the analysis, it is possible to select the models of an appropriate detailing level, by choosing the type of simulation method. For stability analysis, power quality and control issues, RMS simulations are used. RMS simulations are based on simplified electromechanical transient models. In the case of induction generators, the RMS simulation is using a third order generator model, where the stator transients are neglected. For the analysis of the wind turbine's behavior during grid faults, electromagnetic transient EMT simulations of instantaneous values are used. For this purpose, models of higher detailing level e.g. a fifth order generator model are used.

The generator inertia is modeled inside the built-in induction machine model. The generator inertia is specified in the form of an acceleration time constant in the induction generator type.

The dynamic model of the induction generator is completed by the mechanical equation:

$$J\,\dot{\omega}_r = T_e - T_m$$

(3)

where J is generator inertia, T_e is the electrical torque, T_m is the mechanical torque. The mechanical equation can be rated to the nominal torque:

$$T_n = P_n / \left[\omega_n\,(1 - s_n)\right]$$

(4)

and thus the acceleration time constant T_{ag} can be expressed as:

$$T_{ag} = \frac{J\,(1 - s_n)\,\omega_n^2}{P_n}$$

(5)

where ω_n is the nominal electrical frequency of the network and s_n is the nominal slip.

The doubly-fed induction generator (DFIG) model in DIgSILENT, illustrated in Figure 3, extends the usual induction generator by a PWM rotor side converter in series to the rotor impedance Z_{rot} (DIgSILENT GmbH, 2002).
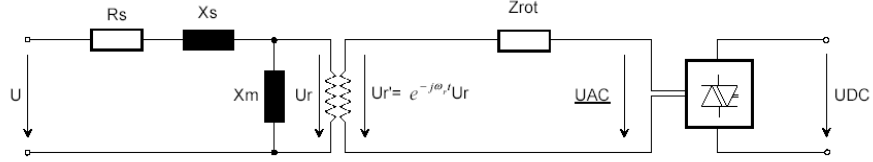

Figure 4: Doubly-fed induction machine with rotor side converter.

The PWM converter inserted in the rotor circuit allows for a flexible and fast control of the machine by modifying the magnitude and phase angle of the generator's AC voltage output U_{AC} on the rotor side. This is done by modifying the modulation factor *PWM*. Based on the power balance between the AC and DC side of the converter, the DC voltage and DC current can be then calculated (DIgSILENT note, 2003). The AC-DC relationship of the PWM converter is the following (the AC voltage is expressed as line-to-line voltage):

$$U_{ACr} = \frac{\sqrt{3}}{2\sqrt{2}} \cdot PWM_r \cdot U_{DC}$$

$$U_{ACi} = \frac{\sqrt{3}}{2\sqrt{2}} \cdot PWM_i \cdot U_{DC}$$

(6)

where PWM_r and PWM_i are the real and imaginary components of the modulation factor, respectively.

It is assumed that a standard bridge consisting of six transistors builds the converter and that an ideal sinusoidal pulse width modulation is applied. The relationship between AC and DC currents can be found by assuming that the PWM converter is loss free:

$$P_{AC} = \mathrm{Re}(U_{AC}\ I_{AC}^*) = U_{DC}\ I_{DC} = P_{DC}$$

(7)

During time domain simulations the converter is controlled through the pulse width modulation factors PWM_d and PWM_q, which define the ratio between DC-voltage and the AC-voltage at the slip rings.

The model equations of the doubly-fed machine can be derived from the normal induction machine equations by modifying the rotor-voltage equations:

$$\underline{u}_s = \underline{R}_s\,\underline{i}_s + j\frac{\omega_{syn}}{\omega_n}\underline{\psi}_s + \frac{1}{\omega_n}\frac{d\underline{\psi}_s}{dt}$$

$$\underline{u}_r\, e^{-j(\omega_{syn}-\omega_r)t} = \underline{R}_r\,\underline{i}_r + j\frac{(\omega_{syn}-\omega_r)}{\omega_n}\underline{\psi}_r + \frac{1}{\omega_n}\frac{d\underline{\psi}_r}{dt}$$

(8)

The per unit rotor voltage that appears in the above equation is related to the DC- voltage as follows:

$$\underline{u}_{rd} = \frac{\sqrt{3}}{2\sqrt{2}} \cdot PWM_d \cdot \frac{U_{DC}}{U_{rnom}}$$

$$\underline{u}_{rq} = \frac{\sqrt{3}}{2\sqrt{2}} \cdot PWM_q \cdot \frac{U_{DC}}{U_{rnom}}$$

(9)

where U_{rnom} is the nominal rotor voltage.

In the case of faults near the generator, rotor currents are increasing and risk to damage the rotor side converter. The rotor-side PWM-converter is therefore protected against such high rotor currents by a bypass-circuit (Pöller, M., 2003). If the rotor current exceeds the maximum allowed value, a bypass R-L-circuit is immediately inserted and the rotor side converter is blocked. All parameters of the bypass protection, including the time for its automatic removal can directly be entered in the input dialogue of the doubly fed induction machine (element).

Figure 5 illustrates the single line diagram of DFIG configuration in DIgSI-LENT.
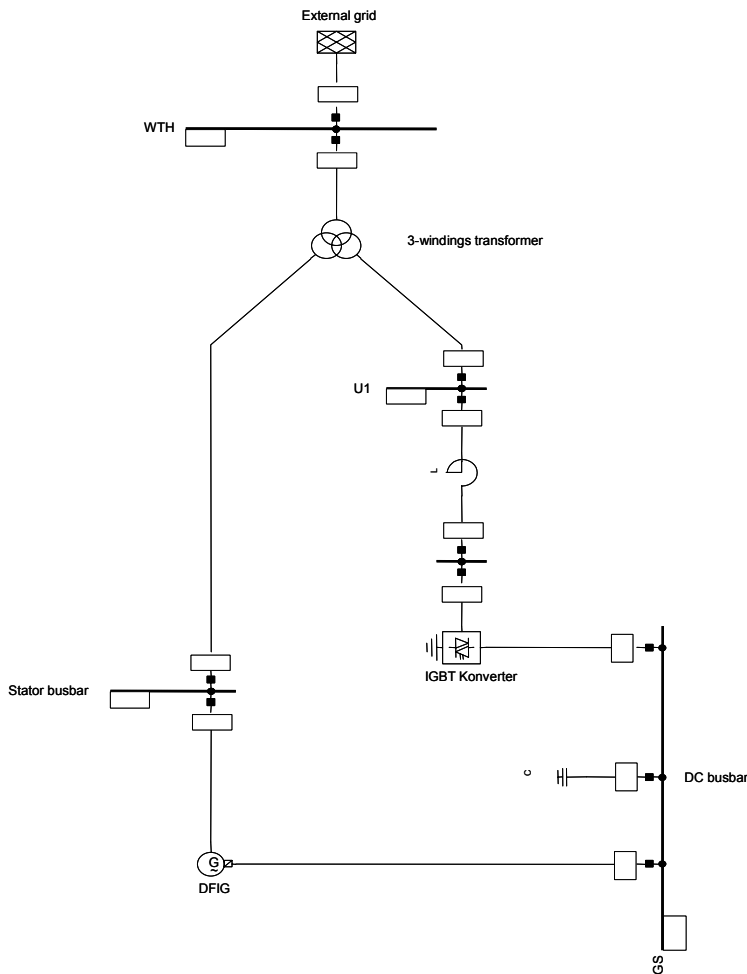
Figure 5: Single line diagram of the DFIG in DIgSILENT.

It contains a DFIG built-in model (the usual induction machine model extended with the PWM rotor side converter), a common DC – busbar, an IGBT grid side converter (independent component in DIgSILENT's library) and an inductor in series with the grid converter, used to smooth the converter currents. This inductor may also be integrated into the transformer.

The controllers of the rotor side converter and of the grid side converter are implemented as DSL models in DIgSILENT – see for details in Chapter 4.

2.2.2 Power converters

DIgSILENT provides models for different power converters such as: rectifiers/inverters, PWM converters, softstarter. They are briefly described below.

Rectifier/Inverter

The rectifier/inverter model is used to create DC power links, or for building power electronic devices such as variable speed drives (DIgSILENT GmbH, 2002). The rectifier and inverter models allow modelling of different types of frequency converters. For example, in the doubly-fed induction generator concept, the rotor circuit is connected to the grid through two PWM converters working back-to-back.

PWM converter

The power converters used in wind turbines are usually realised by self-commutated pulse-width modulated circuits – see Figure 6.
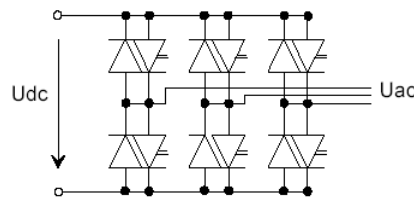
Figure 6: Generic PWM converter model.

These circuits are built by six valves with turn-off capability and six anti-parallel diodes. The valves are typically realised by IGBTs (insulated gate bipolar transistors) because they allow for higher switching frequencies than classical GTOs.

The general model of the PWM converter, that usually operated as a voltage source converter, is illustrated in Figure 7.
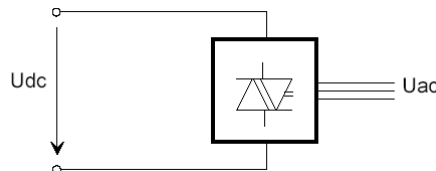
Figure 7: PWM converter - general model.

The model equations are expressed as follows:

$$U_{ACr} = K_0 \cdot PWM_r \cdot U_{DC}$$
$$U_{ACi} = K_0 \cdot PWM_i \cdot U_{DC}$$

(10)

where U_{ACr}, U_{ACi} are the real and the imaginary parts of the AC voltage, corresponding to the positive sequence component. PWM_r, PWM_i are the real and the imaginary modulation factors, while K_0 is the modulation factor, defined as follows:

- $K_0 = \dfrac{\sqrt{3}}{2\sqrt{2}}$ for a sinusoidal PWM

- $K_0 = \dfrac{\sqrt{2}\ \sqrt{3}}{\pi}$ for a rectangular PWM or for no modulation

    The input parameters for the converter are the rated AC or DC voltage, the rated power and the modulation factor K_0, which relates the fundamental component of the line to line AC voltage to the DC voltage. The equation (10) is valid for modulation factor $0 \leq |PWM| < 1$. For values higher than 1, the converter starts to saturate and the level of low-order harmonics starts increasing. In order to avoid the low-order harmonics the controllers of the converters usually limit the pulse-width modulation factor to 1.

    Assuming the PWM to be loss-less, the converter equation can be completed by the power conservation equation:

$$P_{AC} = \mathrm{Re}(U_{AC}\ I_{AC}^*) = U_{DC}\ I_{DC} = P_{DC} \tag{11}$$

    As the switching frequency of PWM converters is usually very high (5-10kHz), the switching losses are the predominant type of losses.

    DIgSILENT provides several control modes for the converter, as for example:

- U_{dc}-Q mode: regulates the dc-voltage and the reactive power. This mode is typical for the grid-side converter of a doubly fed induction machine.
- U_{ac}-phi mode: regulates the ac-voltage magnitude and angle on the DC side. This mode is typical for variable speed drive applications, when the converter drives an induction machine at the AC side.
- P-Q mode: regulates the active and reactive power.

Softstarter

The softstarter is a simple and cheap power electric component, used in the fixed speed wind turbine during connection or disconnection to the grid of its generator. The softstarter's function is to reduce the in-rush current and thereby limit the disturbances to the grid. Without a softstarter, the in-rush current can be up to 7-8 times the rated current, which can cause severe voltage disturbance in the grid.

    The softstarter contains two thyristors, as commutation devices in each phase. They are connected in anti-parallel for each phase. The smooth connection of the generator to the grid, during a predefined number of grid periods, is done by adjusting the firing angle (α) of the thyristors. The relationship between the firing angle (α) and the resulting amplification of the softstarter is highly non-linear and depends additionally on the power factor of the connected element. After in-rush, the thyristors are bypassed in order to reduce the losses of the overall system.

    The softstarter model in DIgSILENT is a dqo model, considering one phase and an RL source.

    There are many configurations of softstarters, which fed an induction machine, as for example: a) star connection b) delta connection and c) branch-delta connection. In wind turbine applications mainly the delta connection for the induction machine is used because the current rating of the stator windings can be reduced, and the third harmonic in the line currents is eliminated in this case.

    In delta branch connection, the softstarter is not in series to the induction generator lines, but it is built inside the delta of the generator, reducing thus the power rating of the thyristors. As in DIgSILENT, the softstarter and the generator blocks are two independent components, it is not possible directly to model the generator with delta branch softstarter. However, the delta branch connec-

tion could be possibly equivalent with an ideal delta/star transformer in series with the softstarter and a star connected induction generator.

Capacitor bank

The capacitor bank is an electrical component, which is supplying reactive power (i.e. to the induction generators or to the grid). Thus the reactive power absorbed by the generator from the grid is reduced.

The general compensation device is modelled in DIgSILENT by a series connection of a capacitor C, a reactor L and a resistance R. The user can choose between different types of shunt, e.g.: *C, R-L* or *R-L-C*. The capacitor can be connected in a star or delta configuration.

To represent a parallel connection of capacitors, several compensators in parallel must be connected to the same busbar, as illustrated in Figure 8.
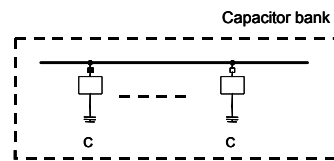
Figure 8: Capacitor bank in DIgSILENT.

The capacitor bank system is combinations of shunt capacitors, which can be switched on and off individually, depending on the load situation in response to changes in reactive power demands.

2.2.3   Transformer

DIgSILENT provides model blocks both for 2-windings transformer and for 3-windings transformer. The two/three winding transformer is a two/three -port element connecting two/three cubicles, respectively, in the power system. Both transformers include manual and automatic tap changers with voltage, active power or reactive power control.

In the following, the model of the 3- windings transformer is briefly illustrated. The representation of the positive sequence equivalent diagram is shown in Figure 9 and includes a generalised tap-changer model.

The magnetisation current may be chosen to be linear or piecewise linear, which is defined with a knee-current, a linear current and a saturated current.

The zero sequence equivalent models for three common winding connections are illustrated in Figure 10 to Figure 12.
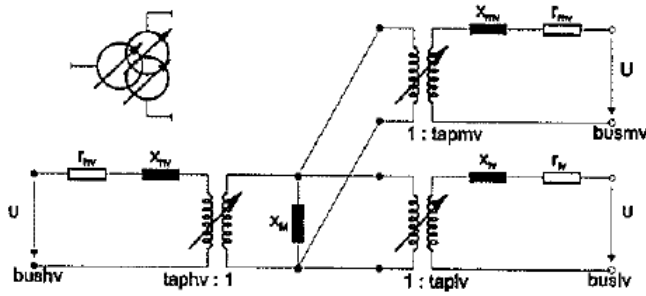
Figure 9: Positive sequence - three windings transformer equivalent model. Source: DIgSILENT Power Factory Manual. Version 12.0 (DIgSILENT GmbH,2001).

Figure 10: Zero sequence - grounded star/delta/delta connection. Source: DIgSILENT Power Factory Manual. Version 12.0 (DIgSILENT GmbH,2001).

Figure 11: Zero sequence - grounded star/grounded star/delta connection. Source: DIgSILENT Power Factory Manual. Version 12. (DIgSILENT GmbH,2001).

Figure 12: Zero sequence - grounded star/grounded star/ grounded star connection. DIgSILENT Power Factory Manual. Version 12.0 (DIgSILENT GmbH,2001).

2.3 DSL models of wind turbine in DIgSILENT

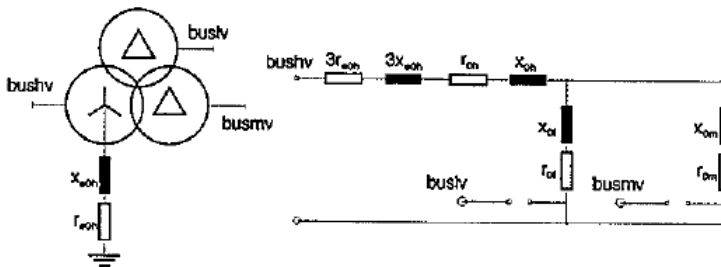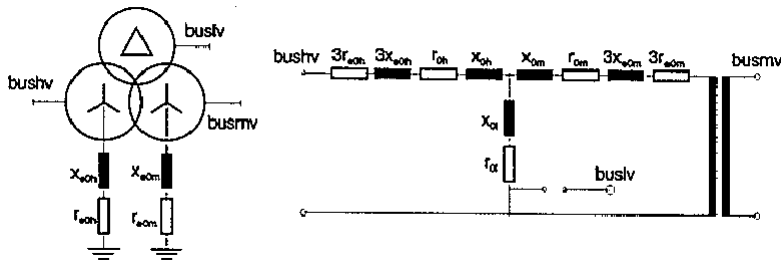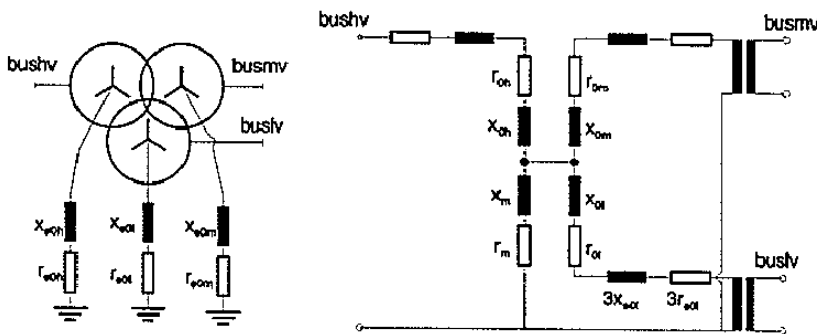Besides the models of the electrical components, already existing in DIgSI-LENT, as described in Section 2.2, the modelling of the wind turbine also requires models for wind speed, aerodynamic system, mechanical system and control system.

The Dynamic Simulation Language (DSL) is a powerful feature of DIgSI-LENT. It allows dynamic modelling of linear and non-linear systems. Thus, besides the modelling non-electrical wind turbine components (i.e. wind speed, aerodynamic system, mechanical system), DSL is also used to design and implement different types of controllers, such as capacitor bank (reactive power) controller, doubly-fed induction generator DFIG controller, active stall wind turbine controller and variable speed/variable pitch wind turbine controller.

In contrast to the built-in electrical models with initialisation procedures based on the load flow calculation, the initialisation of DSL models has to be carried out carefully by the user. Such initialisation is very useful to be able to evaluate the performance of the whole system (grid connected wind turbine), both during normal operation and during transient faults. The wind turbine and the electrical power system must be treated as a unified system, despite their formal separation at initialisation.

For illustration, a directly grid-connected blade angle-controlled wind turbine is used. Figure 13 depicts the overall structure of such a grid-connected wind turbine model. It contains (i) the wind speed model, (ii) the aerodynamic, mechanical, generator and grid model, and (iii) the control system models (i.e. blade angle control model, capacitor bank control model).
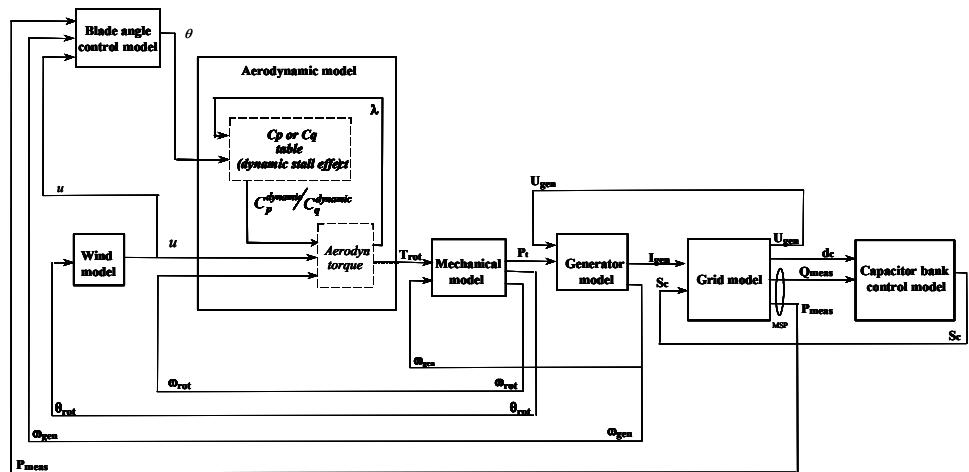
Figure 13: Example of grid-connected wind turbine model.

The aerodynamic model, extended with the dynamic stall effect, is fed with the equivalent wind speed u from the wind model, the rotor speed ω_{rot} from the mechanical model and the blade angle θ from the control model. The mechanical model describes the dynamics of the drive train and delivers the mechanical turbine power P_t to the generator model. Beside the mechanical turbine power P_t, the generator model has as input the voltage U_{gen} from the grid model. It delivers the rotational speed ω_{gen} and the current I_{gen} as outputs. The blade angle-control and capacitor-bank control systems constitute the overall control. The blade angle-control model delivers the blade angle θ to the aerodynamic model, by using information on the measured active power P_{meas}, the generator

speed ω_{gen} and the wind speed u. The capacitor-bank control model generates the capacitor switch control signals S_C to the grid model, based on information on the measured reactive power Q_{meas} and on the capacitor status signals d_c. The active and the reactive power P_{meas} and Q_{meas}, measured at the main switch point MSP of the wind turbine, are used by the control system.

2.3.1 Initialisation issues on the wind turbine DSL models

In this section, the initialisation procedure and the initialisation of each DSL component model of a wind turbine is presented. The initialisation procedure is described by using a blade angle-controlled wind turbine with a directly connected squirrel-cage induction generator, as an example. However, during the description of the initialisation procedure, some comments regarding the variable speed wind turbine are also made.

To integrate new models in the power-system simulation software, e.g. wind turbine and new controller models, the initialisation problem must be solved properly (Hansen A. D. et al., 2003). Correct initialisation of a model in a power-system simulation-tool avoids fictitious electrical transients and makes it possible to evaluate correctly the real dynamic performance of the system (even in the case of a grid transient event). A transient simulation requires very small time steps and consequently very long simulation time.

Power system simulations start with a load flow calculation. Load flow calculations provide the steady state condition of the system. For these calculations certain input data has to be provided by the user. For example, the load flow input data for a squirrel-cage induction generator includes the active power, while for a doubly-fed induction generator, the required load flow data are the stator's active power, reactive power and the slip. Once the load flow calculation is performed, and thus all electrical models are initialised (e.g. mechanical turbine power at the machine and generator speed are calculated), the initialisation of non-electrical turbine component models starts.

The initialisation of the grid-connected turbine model is a successive process. The main problem is to find the sequence in which the models have to be initialised one after another. The simulation equations are solved by setting time derivatives to zero and using the load flow results and additional non-electrical input data. It is necessary to identify which inputs, outputs and states are known and which have to be initialised. Once one model is initialised, the gathered information on its signals and states is used for the initialisation of the next model. A DIgSILENT command makes it possible to check if the initial conditions are transferred correctly from one component model to another. If the initialisation is not done properly, the state variables do not stay at the value at which they were initialised, but start changing at the start of the dynamic simulation. In this case, it may take time to reach a steady state, and even numerical instability can occur before the stationary state is reached. These initialisation transients are undesirable in the dynamic simulations, especially in the case when a real grid transient event appears, just before the system achieves its steady state. A correct evaluation of the dynamic performance is then quite difficult to achieve. To overcome these difficulties, an accurate calculation of the initial conditions of the dynamic wind turbine models is required.

While Figure 13 depicts the direction of the simulation flow, Figure 14 illustrates the initialisation flow of the turbine model. The input data necessary for the initialisation are:
- electrical input data (from grid side): e.g. the initial active power of the generator and the initial capacitor status information d_c. These electrical input data are used in the load flow calculation and in the initialisation of the electrical models.

- non-electrical input data (from turbine side): the initial value of the wind speed and the initial value of the blade angle.

These input data provide information about the operating point of the turbine at the simulation start. The single-dotted lines indicate the direction of the initialisation flow, for each component model; see Figure 14. The known signals at the simulation start, indicated by the double dotted lines, are:

- electrical signals - determined in the load flow calculation: mechanical power P_t, generator speed ω_{gen}, capacitor status signal d_c, generator current I_{gen}, generator voltage U_{gen}, the "measured" active power P_{meas} and reactive power Q_{meas} in MSP (Main Switch Point).
- initially (*a priori*) known non-electrical signals: the initial wind speed u and the initial blade angle θ.
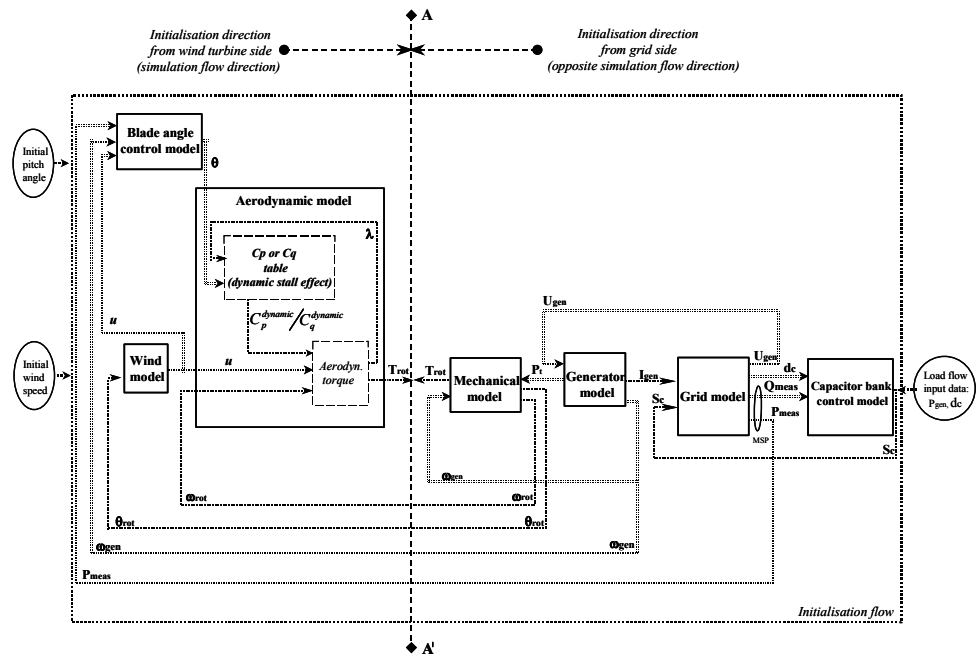
Figure 14: Initialisation flow of a blade angle controlled wind turbine with a directly connected squirrel-cage induction generator.

The non-electrical input data (from turbine side) and the load flow electrical input data (from the grid side) must correspond to each other, based on the static power curve of the wind turbine, on the generator efficiency and eventually losses in the system. The initial value of the wind speed is assumed known at the beginning of the initialisation sequence because, otherwise, its initialisation backward from the non-linear expression in wind speed of the aerodynamic torque would be quite difficult and with ambiguous solutions. The initial value of the blade angle is also assumed known (Hansen A. D. et al., 2003).

Two initialisation directions are distinguished in the initialisation procedure; see Figure 14. Some of the variables in the initialisation sequence are initialised in the opposite direction of the simulation (starting from the grid connection point towards the wind); while others are initialised in the same direction as the simulation is performed (starting from the wind to the grid). When the initialisation is performed in the opposite direction of the simulation flow, namely from the grid to the wind, the model is calculated from certain known outputs to inputs, based on load flow computations. The initial values of the inputs, outputs and state variables have thus to be calculated from the known outputs and from the model equations.

For example, in the "Mechanical model" block shown in Figure 14, the aerodynamic torque T_{rot} is initialised in the opposite direction of the simulation flow. It is based on the known outputs from the load flow calculation, i.e. the mechanical power P_t and the generator speed ω_{gen}.

When the initialisation is performed in the same direction as the simulation flow, the model initialisation is performed from certain known inputs to outputs. The initial values of the inputs are assumed known based on the non-electrical information about the system in the starting moment, as e.g. the initial wind speed and the initial blade angle.

During the initialisation process, initial values are successively calculated in two directions approaching each other. At the point where the initialisations from the two opposite directions meet, they should match each other. If they do, a steady state is obtained. Otherwise, fictive transients in the beginning of the dynamic simulation appear. These fictive transients have been minimised by choosing a point where the transients can be absorbed, e.g. big inertia in the mechanical system. The place between the aerodynamic model and the mechanical model has been chosen as a point where the two opposite initialisation directions meet. This is illustrated in Figure 14 by the borderline AA´. The reason for this choice is that the fictive transients in the low-speed shaft torque signal, in the case of an initialisation conflict, are absorbed due to the large inertia of the rotor.

The models are initialised one after another, starting with the mechanical model, followed by the wind model, blade angle control model and the aerodynamic model. The initialisation of the capacitor-bank control model is based on the load flow data only, i.e. independent of the initialisation of the other individual component models. Once one model is initialised, all its variables are known and can be used in the initialisation of the next models in the initialisation sequence.

In the following figures, concerning the models initialisation, the known signals in the moment of initialisation are illustrated by using double-dotted lines. Single-dotted lines illustrate the signals, which must be initialised.

2.3.2   Mechanical model

In the mechanical model, Figure 15, emphasis is put only on those parts of the dynamic structure of the wind turbine that contribute to the interaction with the grid. Therefore only the drive train is considered in the first place, because this part of the wind turbine has the most significant influence on the power fluctuations. The other parts of the wind turbine structure, e.g. tower and the flap bending modes, are thus neglected.
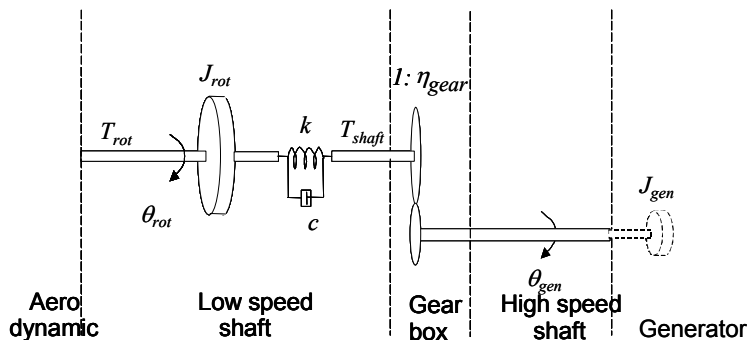

Figure 15: Drive train model in DIgSILENT.

The mechanical model is implemented as a DSL model in DIgSILENT. The drive train is essentially a two mass model (Hansen A.D. et al., 2002), (Sørensen P. et al., 2001a), namely a large mass corresponding to the rotor inertia J_{rot} and a small mass corresponding to the generator inertia J_{gen}, which is implemented as part of a DIgSILENT generator model. Thus, besides the electromagnetic description, the generator model in DIgSILENT also contains the mechanical inertia of the generator rotor J_{gen}. The low speed shaft is modelled by a stiffness k and a damping coefficient c, while the high-speed shaft is assumed stiff. Moreover, an ideal gear-box with a ratio ($1:n_{gear}$) is included.

The drive train converts the aerodynamic torque T_{rot} of the rotor into the torque on the low speed shaft T_{shaft}. The dynamical description of the mechanical model consists of three differential equations, namely:

$$\dot{\theta}_{rot} = \omega_{rot} \qquad\qquad [rad/s]$$

$$\dot{\theta}_k = \omega_{rot} - \frac{\omega_{gen}}{n_{gear}} \qquad\qquad [rad/s] \qquad\qquad (12)$$

$$\dot{\omega}_{rot} = (T_{rot} - T_{shaft})/J_{rot} \qquad\qquad [rad/s^2]$$

where $\theta_k = \theta_{rot} - \theta_{gen}/n_{gear}$ is the angular difference between the two ends of the flexible shaft. The mechanical torque on the low speed shaft and the mechanical power of the generator are:

$$T_{shaft} = c\,(\omega_{rot} - \frac{\omega_{gen}}{n_{gear}}) + k\,\theta_k \qquad\qquad [Nm]$$

$$\qquad\qquad (13)$$

$$P_t = \omega_{gen}\,\frac{T_{shaft}}{n_{gear}} \qquad\qquad [W]$$

The damping coefficient c is given by:

$$c = 2\,\xi\,\sqrt{k\,J_{rot}}$$

$$\qquad\qquad (14)$$

where ξ is the damping ratio and can be expressed using the logarithmic decrement δ_s:

$$\xi = \frac{\delta_s}{\sqrt{\delta_s^2 + 4\,\pi^2}} \qquad\qquad (15)$$

The logarithmic decrement is the logarithm of the ratio between the amplitude at the beginning of the period and the amplitude at the end of the next period of the oscillation:

$$\delta_s = \ln\left(\frac{a(t)}{a(t + t_p)}\right) \qquad\qquad (16)$$

where a denotes the amplitude of the signal.

Figure 16 illustrates the inputs and outputs of the mechanical model, which must be initialised. These are the aerodynamic torque T_{rot}, the rotor angle θ_{rot} and the rotor speed ω_{rot}. The mechanical power P_t^{lf} and the generator speed

ω_{gen}^{lf} are known (double dotted style) from the load flow calculation. The aerodynamic torque T_{rot} is initialised in the opposite direction to that of the simulation flow (i.e. *from* grid *to* wind, and not from wind to grid), while the rotor angle θ_{rot}, the rotor speed ω_{rot} and the internal states of the mechanical model are initialised in the same direction as the simulation flow.
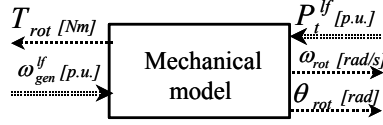
*Figure 16: Known and unknown inputs/outputs in the initialisation
of the mechanical model.*

Notice that the electrical data available from the load flow calculation and the equations of grid components are expressed in per unit in DIgSILENT. This aspect must be taken into account in the initialisation process of the turbine model, as the turbine equations are implemented in physical units. The per unit mechanical power P_t^{lf} and the generator speed ω_{gen}^{lf}, generated by the load flow are:

$$P_t^{lf} = \frac{P_t}{P_t^{base}} \qquad [p.u.]$$

$$\omega_{gen}^{lf} = \frac{\omega_{gen}}{\omega_{gen}^{base}} \qquad [p.u.] \tag{17}$$

where P_t^{base} is the rated mechanical power in *[W]* of the wind turbine, $\omega_{gen}^{base} = \frac{2\pi f}{p}$ is the synchronous speed of the generator in *[rad/s]*, with f as the grid frequency in *[Hz]* and p as the number of pole-pairs.

The initial steady states are determined by setting their derivatives to zero:

$$\dot{\theta}_k = 0 \qquad \Rightarrow \qquad \omega_{rot}^{initial} = \frac{\omega_{gen}}{n_{gear}} \qquad and \qquad T_{shaft}^{initial} = k\,\theta_k^{initial}$$

$$\dot{\omega}_{rot} = 0 \qquad \Rightarrow \qquad T_{rot}^{inital} = T_{shaft}^{inital} \qquad and \qquad T_{rot}^{initial} = \frac{P_t\,n_{gear}}{\omega_{gen}} \tag{18}$$

Notice that since the shaft is rotating, the derivative of the rotor position θ_{rot} cannot be zero. Its value can be initialised to any appropriate value.

The mechanical model, expressed in (12) and (13), is using physical units, while the signals determined in the load flow calculation are expressed in per unit. The initialisation of the inputs and states, based on equations (18), must take the transformations (17) into account, as follows:

$$T_{rot}^{\,initial} = n_{gear}\,\frac{P_t^{lf}\;P_t^{base}}{\omega_{gen}^{lf}\;\omega_{gen}^{base}} \qquad\qquad [Nm]$$

$$\omega_{rot}^{\,initial} = \frac{\omega_{gen}^{lf}\;\omega_{gen}^{base}}{n_{gear}} \qquad\qquad [rad\,/\,s] \qquad\qquad (19)$$

$$\theta_k^{\,initial} = \frac{T_{rot}^{initial}}{k} = n_{gear}\,\frac{P_t^{lf}\;P_t^{base}}{\omega_{gen}^{lf}\;\omega_{gen}^{base}}\,\frac{1}{k} \qquad\qquad [rad]$$

2.3.3 Aerodynamic model

As illustrated in Figure 14, the DSL aerodynamic model block contains two sub-model blocks. One sub-model block relates to the non-linear expression of the aerodynamic torque, and the other contains the power coefficient C_p or the torque coefficient C_q look-up tables. In the later sub-model block the modelling of the dynamic stall effect can be included or not. Figure 17 depicts the known and unknown inputs/outputs of the aerodynamic model and the initialisation direction.

The rotor speed ω_{rot} is determined in the initialisation of the mechanical model. The equivalent wind speed u is known from the initialisation of the wind speed model. The initial pitch angle θ is assumed known. Based on these known non-electrical signals, the tip speed ratio λ, the output aerodynamic torque T_{rot} and the internal states are further initialised. Notice that the aerodynamic torque T_{rot} is also initialised in the "Mechanical model", based on the electrical input data (load flow data); see equations (19).

Both Figure 14 and Figure 17 illustrate the borderline AA′, where the initialisation information from two opposite directions (wind turbine side and grid side) cross each other. In this place, a conflict can appear if the initialisation information provided by the non-electrical and the electrical signals don't match.
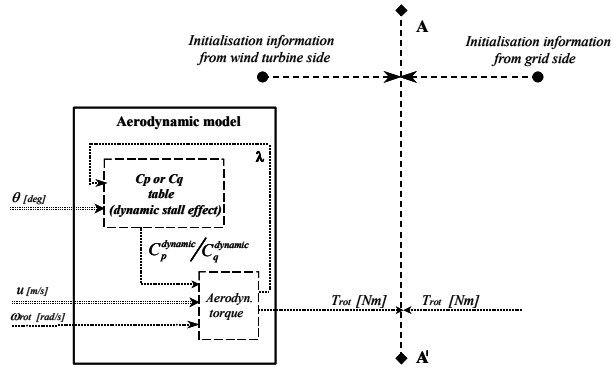
Figure 17: Known and unknown inputs/outputs in the initialisation of the aerodynamic model.

As mentioned before, this border position AA′ is chosen deliberately at the aerodynamic torque signal. The reason is that the transients in the aerodynamic torque, due to the possible discrepancy, can be absorbed by the large inertia of the rotor.

(a) Aerodynamic torque
Standard aerodynamic programs typically use blade element methods and therefore they require considerable computation time. The use of such standard aero-

dynamic programs to simulate wind farms with several wind turbines is therefore not attractive. A simplified aerodynamic model is preferably used instead when only the effect on the power, respectively the aerodynamic torque T_{rot} is taken into account. This simplified aerodynamic model is typically based on the aerodynamic power coefficient $C_p(\theta,\lambda)$ or on the torque coefficient $C_q(\theta,\lambda)$, provided by a standard aerodynamic program.

Thus, the aerodynamic torque developed on the main shaft of a wind turbine with rotor radius R at a wind speed u and air density ρ can be modelled by one of the following static relations:

$$T_{rot} = \frac{P_{rot}}{\omega_{rot}} = \frac{1}{2\,\omega_{rot}}\,\rho\,\pi\,R^2\,u^3\,C_p(\theta,\lambda), \tag{20}$$

or

$$T_{rot} = \frac{1}{2}\,\rho\,\pi\,R^3\,u^2\,C_q(\theta,\lambda), \tag{21}$$

where the aerodynamic power coefficient $C_p = C_p(\theta,\lambda)$ and the torque coefficient, respectively, $C_q = C_q(\theta,\lambda)$ are tabled as matrices, depending on the pitch angle θ and on the tip speed ratio λ, which initial value is:

$$\lambda^{initial} = \frac{R\,\omega_{rot}^{initial}}{u^{initial}} \tag{22}$$

Both torque expressions (20) and (21) can be used to express the aerodynamic torque. However, the aerodynamic torque expressed in (21) with the torque coefficient has the advantage that it is determined directly and not through power and therefore it can also be used in the case of standstill ($\omega_{rot} = 0$). This is important because at standstill the aerodynamic power is zero, while the aerodynamic torque is not. Both torque expressions (20) and (21) are presently implemented and can be independently used in DIgSILENT.

Notice that both aerodynamic torque expressions (20) and (21) contain the wind speed u both in explicit and implicit form (through λ). They are non-monotone, highly non-linear and with a maximum point. This means that if the initial wind speed is not known at the beginning of the initialisation, the wind speed would have to be determined backwards from the high non-linear and non-monotone aerodynamic torque expression. This calculation would be both complicated and have ambiguous solutions.

The aerodynamic torque expressions (20) and (21) are expressed in steady state operating points, based thus on steady state power coefficient or steady state torque coefficient. This simplification underestimates the actual power fluctuations in the stall region (Sørensen P. et al., 2001a), and therefore the aerodynamic model can be improved by taking the dynamic stall effects into account. A dynamic power coefficient $C_p^{dynamic}(\theta,\lambda)$ and a dynamic torque coefficient $C_q^{dynamic}(\theta,\lambda)$, respectively, are used instead.

(b) Dynamic stall model

The dynamic stall effects, described in (Sørensen P. et al., 2001a), (Hansen A.D. et al., 2002), appear because, at strong wind speeds, the dynamic power/wind speed slope is much steeper than the static power/wind speed slope. This is the reason why, at strong wind speeds, the power fluctuations in reality

are much larger than the power fluctuations estimated by using the standard power curve.

Figure 18 illustrates both the steady state power curve of a wind turbine and how large the dynamic power fluctuations are caused by wind speed fluctuations. Two situations are illustrated: low wind speed region ($u < 8$ m/s - case 1) and high wind speed region ($u > 8$ m/s - case 2). For low wind speeds (case 1) there is no significant difference between the static power P^{static} and the dynamic power $P^{dynamic}$, because the amplification factors of the fluctuations for both steady state and dynamic state are similar. This is not the case for the high wind speeds (case 2) in the stall region, where, due to the dynamic stall effects, fluctuations in wind speed, produce larger power fluctuations.
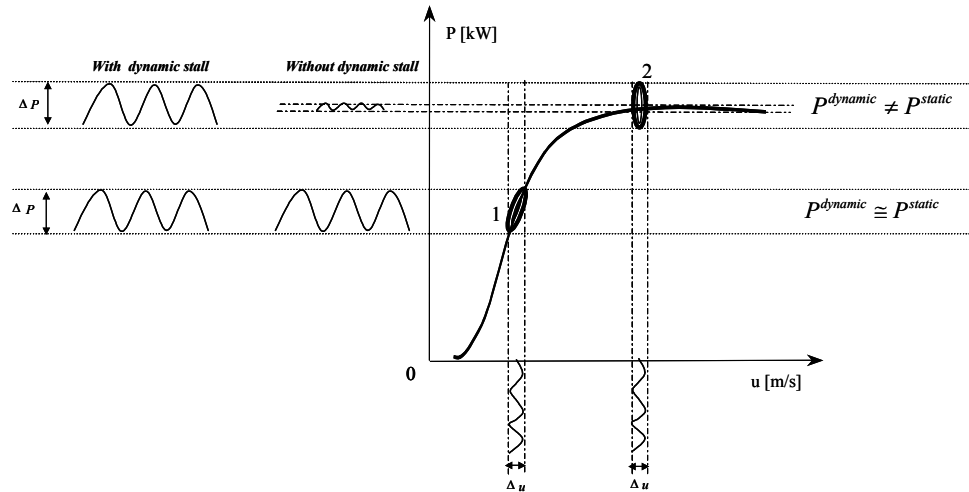

Figure 18: Power fluctuations in the stall region with and without dynamic stall.

The applied model for the dynamic stall is a slight modification of the method described by (Øye & S.,1991), where the dynamic stall is modelled as a time-lag of separation. According to this method, the lift coefficient for a blade section can be associated with different flows with different angles of attack:

(i) an attached (un-separated) flow, which corresponds to the steady state flow at low angles of attack;

(ii) a fully separated flow, which corresponds to the steady state flow at large angles of attack;

(iii) a steady state flow (static flow).

Instead of using lift coefficient C_L, as it is proposed by (Øye & S., 1991), the dynamic stall effect model can be based on the aerodynamic power coefficient C_p or on the torque coefficient C_q. In the following, only the generation of the dynamic aerodynamic power coefficient $C_p^{dynamic}$ is presented, as the generation of the dynamic aerodynamic power coefficient $C_q^{dynamic}$ is similar.

The dynamic power coefficient table, $C_p^{dynamic}$, is generated by using three other tables: one for the steady state (static) power coefficient, C_p^{static}, one for the attached power coefficient, $C_p^{attached}$ and one for the separated power coefficient, $C_p^{separated}$.

In order to illustrate these three power coefficients (static, attached and separated) and thus the influence of the dynamic stall effect over the whole wind speed range, a simulation of a single wind turbine is performed. In this example, the equivalent wind speed is designed (not modelled by the rotor wind

model) to have a sinusoidal variation with a 3p frequency, amplitude of 2 m/s and a linear increasing mean value, as it is illustrated in Figure 19. The simulation is performed with a constant pitch angle, which corresponds to 2 MW
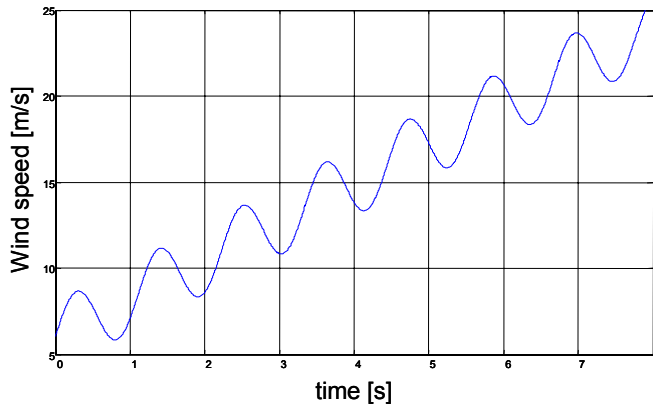
Figure 19: Designed equivalent wind speed - input for wind turbine simulation.

power at high wind speeds.

Figure 20 shows the profile of the dynamic power curve, modelled with and without dynamic stall. The cyclic behaviour of the sinusoidal wind speed input signal is transferred through the second order dynamic model of the transmission system to other signals, such as the aerodynamic power, the aerodynamic torque and the rotor speed ω with a corresponding phase shift. The significantly increased amplitude of the dynamic power fluctuations at high wind speeds illustrates that the dynamic stall effect is important at large wind speeds, while at small wind speeds it is not relevant. The improved aerodynamic model with the dynamic effect is thus able to simulate the larger fluctuations in the power in the stall region. It is also observed that even the power curve without dynamic stall has some cyclic behaviour. This is due to the sinusoidal wind speed input signal, which is transferred to the other state variables through the model dynamics. Beside the sinusoidal wind speed, the power coefficient without dynamic stall, expressed as a function of wind speed, $C_p(u,\theta)$, also influences the calculation of the small cycles in the power curve without dynamic stall.

Figure 20: Power curve with and without dynamic stall effect.

Figure 21 illustrates the power coefficient as a function of tip speed ratio, $\lambda = \omega R / u$, for the steady state, attached, separated and dynamic flow, simulated with the wind speed illustrated in Figure 19. It is observed that the steady state power coefficient, C_p^{static}, illustrated th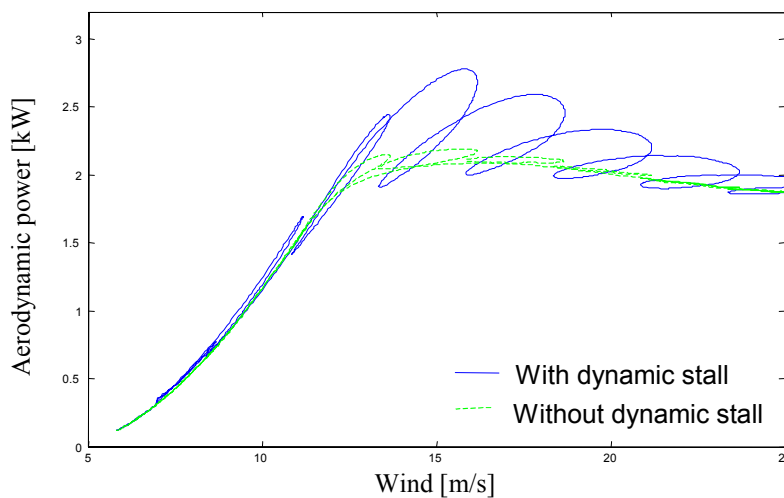is time as function of λ, does not contain any cycles. This is because C_p^{static} is an algebraic function of rotor speed ω, wind speed u and pitch angle θ. It is also noted that the steady state C_p^{static} converges to the attached $C_p^{attached}$ power coefficient at high λ values (low wind speeds), while at small λ values (high wind speeds), the steady state C_p^{static} converges to the separated $C_p^{separated}$. Moreover, at small wind speeds, the steady state C_p^{static} power coefficient and the dynamic power coefficient $C_p^{dynamic}$ do not differ significantly, because at small wind speeds the dynamic stall effect is not relevant. At high wind speeds (small λ values) the values of the dynamic power coefficient $C_p^{dynamic}$ are delayedwith the time constant τ of the first order filter, and then moved towards the steady state power coefficient C_p^{static} on an almost "parallel" curve with the attached and separated coefficient curves. The calculated value of $C_p^{dynamic}$ is interpolated between these "parallel" curves, which correspond to different separation ratios f (Sørensen P. et al., 2001a). The dynamic value $C_p^{dynamic}$ is the result of the first order filter, which physically corresponds to the fact that it cannot change instantaneously from one value to another, remaining thus on a specific intermediary curve for a time lag. Thus, at high wind speeds, the variation of $C_p^{dynamic}$ is different from that of C_p^{static}.

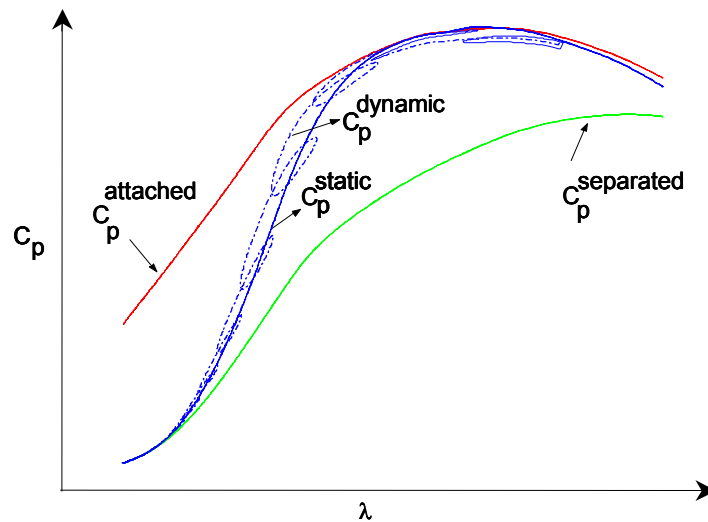*Figure 21: Steady state, attached, separated and dynamic power coefficient as a function of λ.*

The three power coefficients (static, attached and separated) are determined as follows. As illustrated in Figure 22, for a certain known blade angle θ and a known tip speed ratio λ, the three power coefficient look-up tables are providing the values for $C_p^{attached}$, C_p^{static} and $C_p^{separated}$.
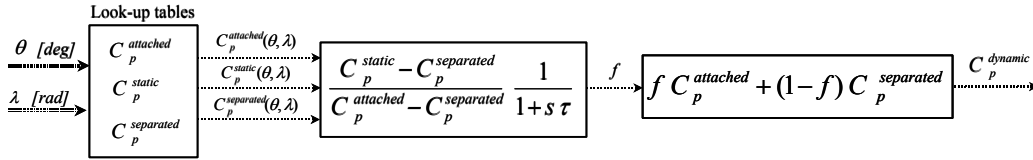
Figure 22: Known and unknown inputs/outputs in the initialisation of the dynamic stall model.

The dynamic separation factor f is defined as the following transfer function:

$$f = \frac{C_p^{static} - C_p^{separated}}{C_p^{attached} - C_p^{separated}} \; \frac{1}{1 + s\,\tau} \tag{23}$$

The dynamic power coefficient $C_p^{dynamic}$ is interpolated between the attached power coefficient, $C_p^{attached}$, and the separated coefficient $C_p^{separated}$:

$$C_p^{dynamic} \;=\; f\,C_p^{attached} \;+\; (1 - f)\; C_p^{separated} \tag{24}$$

The factor f is a dynamic separation ratio, obtained by using a low pass filter with a time constant (lag) τ, approximated, as in (Sørensen P. et al., 2001a), by $\tau = 4/u_0$, where u_0 is the mean wind speed.

With a known blade angle θ and an initialised tip speed ratio λ in (22), the initialisation of the dynamic power coefficient is performed in the simulation direction (see Figure 22), based on the expressions (23), (24) and on the final-value theorem (Laplace transformation):

$$C_p^{dynamic,\ initial} \;=\; C_p^{static}(\theta, \lambda) \tag{25}$$

Once the dynamic power coefficient is initialised, the aerodynamic torque T_{rot} can be also initialised:

$$T_{rot}^{initial} \;=\; \frac{1}{2\,\omega_{rot}^{initial}}\,\rho\,\pi\;R^2\;u^3\,C_p^{dynamic,\ initial} \tag{26}$$

Notice that there are two expressions, (19) and (26), which indicate the initial value of the aerodynamic torque. Nevertheless, the initial value of T_{rot} actually corresponds to (19), from which T_{rot} immediately steps to the value given by (26). In the case of mismatch between the initial input data (both from grid side and wind turbine side) in the initialisation sequence, the expressions (19) and (26) will yield different initial values of the aerodynamic torque. This produces a transient step in T_{rot}. However, due to the large inertia of the rotor, such a transient in the aerodynamic torque will be rapidly absorbed. This is why the delimitation border between the two opposite information sources (i.e. grid side or wind turbine side) is chosen deliberately to be at the aerodynamic torque signal.

2.3.4 Wind model

The wind model, implemented as DSL model in DIgSILENT, generates the equivalent wind speed u based on a spectral description of the turbulence and includes the rotational sampling turbulence and the tower shadow effect. The

wind model is described in details in several references, such e.g. (Sørensen P. et al., 2000), (Sørensen P. et al., 2001a), (Sørensen P. et al., 2001b).

The wind speed model is built as a two-step model – see Figure 23. The first is the hub wind model, which models the fixed point wind speed at hub height of the wind turbine. In this sub-model, possible park scale coherence can be taken into account if a whole wind farm is modelled (Sørensen P. et al., 2001a). The second step is the rotor wind model, which adds the effect of the averaging the fixed point fixed-speed over the whole rotor, the effect of the rotational turbulence and the effect of the tower shadow influence. One input of the rotor wind model block is the azimuth position of the turbine rotor θ_{rot}, which provides the frequency and the phase of the 3p fluctuation. The presence of the rotor position θ_{rot} in the model makes it directly applicable also for variable speed wind turbines.
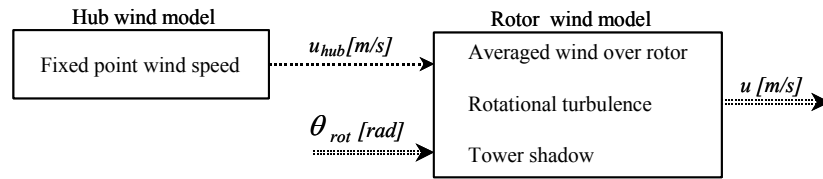

Figure 23: Simplified scheme of wind model with known and unknown inputs/outputs.

The rotational turbulence and the tower shadow are included in the model as they have a major impact on the dynamics. They cause fluctuations in the power with three times the rotational frequency (3p), which is the frequency that mainly contributes to flicker emission during continuous operation. The tower shadow is modelled as a 3p fluctuation with constant amplitude, whereas the rotational sampled turbulence is modelled as a 3p fluctuation with variable (stochastic) amplitude (Sørensen P. et al., 2000).

As indicated in Figure 23, the initialisation of the wind speed model is performed in the same direction as the simulation. The initial value of the equivalent wind speed u is the same as the initial wind speed value, inserted in the initialisation sequence in Figure 13. It corresponds to the active power of the generator, based on the static power curve of the turbine and on the generator efficiency. If a time series describing the wind speed is available, then this can directly replace the wind model. The first value in the time series is then used as the known initial wind speed value in the initialisation sequence.

The two sub-models of the wind speed model, the hub wind model and the rotor wind model, contain a cascade of second order filters (Langreder W., 1996), of the following transfer function form:

$$y_{out} = K \frac{s^2 T_4 + s T_3 + 1}{s^2 T_2 + s T_1 + 1} y_{in} \tag{27}$$

where y_{out} and y_{in} are the output and the input, respectively, while K, T_1, T_2, T_3, T_4 are estimated parameters (Langreder W., 1996). The key in the initialisation of this cascade of second order filters is the initialisation of each second order filter, and therefore the generic initialisation of a second order filter is presented shortly in the following. The second order transfer function (27) can be expressed in terms of the following canonical state space form:

$$\begin{bmatrix} \dot{x}_1 \\ \dot{x}_2 \end{bmatrix} = \begin{bmatrix} 0 & 1 \\ -\dfrac{1}{T_2} & -\dfrac{T_1}{T_2} \end{bmatrix} \begin{bmatrix} x_1 \\ x_2 \end{bmatrix} + \begin{bmatrix} 0 \\ \dfrac{1}{T_2} \end{bmatrix} y_{in} \tag{28}$$

$$y_{out} = K \left[\left(1 - \frac{T_4}{T_2}\right) \quad \left(T_3 - \frac{T_4}{T_2}\right) \right] \begin{bmatrix} x_1 \\ x_2 \end{bmatrix} + \frac{T_4}{T_2} y_{in}$$

Assuming that the output y_{out} is known, the initialisation of the input y_{in} and of the two states (x_1, x_2) is:

$$\dot{x}_1 = 0 \quad \Rightarrow \quad x_2^{initial} = 0$$
$$\dot{x}_2 = 0 \quad \Rightarrow \quad x_1^{initial} = y_{in} \tag{29}$$
$$y_{in}^{initial} = y_{out} / K$$

2.3.5 Capacitor-bank control model

The capacitor bank (reactive power) control model is described in the following section. As illustrated in Figure 13, the capacitor-bank, with a specific number of capacitors, is controlled, at each moment, based on information about the measured reactive power. The number of capacitors to be connected or disconnected at each new step is determined by the control system.

Figure 24 illustrates the DIgSILENT block diagram for the capacitor bank controller. The diagram is general for the simulation of capacitor bank switchings, and consequently it can also be used in different wind turbine models. Only the number of capacitors, as well as the averaging time may differ from one wind turbine type to another.
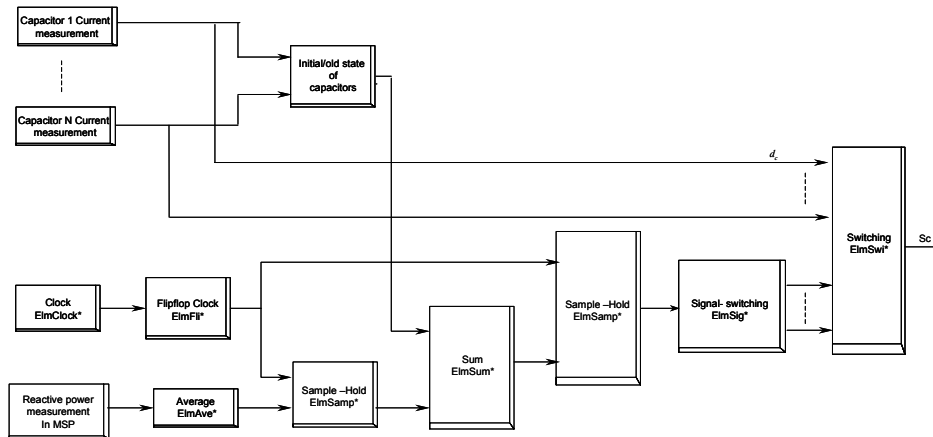
Figure 24: DIgSILENT diagram for capacitor bank controller.

The switching of capacitors is done based on the average value of the measured reactive power during a certain period of time. This average value is used to avoid rapidswitchings of the capacitors, due to the short variations in the reactive power, and thus, to reduce the switching frequency and to protect the contactors. First a moving average of the reactive power is applied, and then a sample-hold function is used to represent block averages. The sample-hold function stores its sampled input signal at the output until the next rising edge of the clock signal appears. The reactive power is measured in the Main Switch Point (MSP), where the reactive power supplied by the already connected capacitors is taken into account. Therefore the control of reactive power is a

closed loop control. Such output average includes the closed loop effect of the reactive power supply from capacitors, which are already connected at a certain moment. The total number of capacitors, which are connected at each step, is obtained by a digital integrator, implemented in the block "Sum", Figure 24. At each time step, this block has information about the closed loop reactive power and the memorised number of capacitors used previously. This information is provided by the block "Initial/old state of capacitors". The output of the digital integrator is first stored and then used to define the switching signals, which are used in the control block "Switching". Based on this process, the control block sends switching control signals S_c to the capacitor-bank contactors of the grid model, in order to operate different capacitors, and thus to supply the required number of capacitors in the grid model, at a specific moment. It is thus at each step determined how many additional capacitors should be further connected or disconnected.

A very simplified version of the control diagram of the capacitor bank is shown in Figure 25. The known and unknown inputs and outputs of the capacitor-bank control model as well as the initialisation direction are shown. The initialisation is performed in the simulation direction, based on electrical characteristics of a grid-connected turbine: the status signal of each capacitor d_c and the measured reactive power Q_{meas} of the turbine.
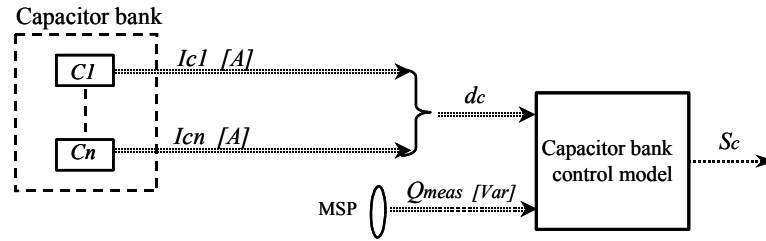
Figure 25: Known and unknown inputs/outputs in the initialisation of the capacitor bank control model.

The initialisation of the switching control signals S_c is based on the status d_c information about the capacitors. The capacitor status signal d_c indicates whether a capacitor is connected or disconnected in the starting moment of the simulation. The status initial information d_c of the capacitors (C_1, …, C_n) is indispensable for a correct initialisation of the capacitor bank control model. The capacitor k is considered connected if its current is positive, $I_{ck} > 0$. Based on how many capacitors are connected at a certain time and on the measured reactive power Q_{meas} ("required" at that moment), the number of capacitors to be further connected or disconnected at the next time step is calculated.

3 Active stall wind turbine concept

An active stall wind turbine is in principle a stall-controlled turbine with variable pitch angle. The generator of an active stall turbine is a simple squirrel cage induction generator directly coupled to the grid. The main difference between stall and active stall turbines is a pitch actuator system for variable pitch angles, which allows the stall effect to be controlled. In addition the power coefficient C_p can be optimised to a certain extend.

The implementation of the controller is done in a general way so that as much as possible is expressed in terms of parameters. The idea is to use this controller model to simulate different existing wind turbines with specific parameters. In-depth knowledge about manufacturer specific controller design is not necessary.

The model described in this report spans the power control during normal operation in the range from start-up wind speed to shutdown wind speed of a single speed generator turbine.

When the wind speed is between start-up wind speed and nominal wind speed the pitch angel is adjusted to optimise C_p i.e. power output.

When the wind speed is above nominal wind speed power output is limited to nominal power by utilising the stall effect. To get a flat power curve, i.e. constant nominal power in the range between nominal wind speed and shut-down wind speed, the pitch angle has to be adjusted accordingly. For comparison: In a stall-controlled turbine the pitch angle is fixed and that means that the power output cannot be held constant. Instead the stall effect leads to a drop below nominal power in the range of high wind speeds. The maximal power of a stall turbine depends on air density, grid frequency and aerodynamic influences e.g. dirt on the blades.

3.1 Active Stall Control Strategy

It is desirable to be able to control the electrical output power of wind turbines. There are different types of wind turbines, which apply different control strategies for controlling the output power of the turbine. One is the active stall controlled wind turbine.

The operation of an active stall wind turbine can be divided into two modes:

- Power limitation: power output is limited to nominal power when wind speed is between nominal wind speed and shut-down wind speed; pitch angle θ is adjusted to control the stall effect. In order to get a flat power curve, i.e. constant nominal power in the range between nominal wind speed and shut-down wind speed, the pitch angle has to be adjusted accordingly.

- Power optimisation: power yield is maximised between start-up wind speed and nominal wind speed; pitch angle θ is adjusted to optimise the power coefficient C_p and hence the power output.

In a passive stall turbine the pitch angle is fixed and that means that the power output can neither be optimised nor controlled limited at wind speeds beyond nominal wind speeds. Instead the stall effect leads to a drop below nominal power in the range of high wind speed.

Although active stall turbines also use the stall effect like passive stall wind turbines, active stall turbines have considerable advantages. The maximum power output of passive stall turbines depends on wind speed, air density, grid frequency, and aerodynamic influences like dirt on the blades, while the maximum power output of active stall turbines can be controlled to a constant value.

3.1.1   Power Limitation

Power limitation is activated whenever the electrical power is above its nominal value, or the wind speed is above its nominal value. In the power limitation mode the power is controlled in a closed control loop, where the measured and averaged generator power is compared with its setpoint, which is the turbine's nominal power.

If the averaged power exceeds the setpoint, θ is increased in negative direction to increase the stall effect and hence to limit the power output. If the averaged power falls below the nominal power, θ is increased in positive direction to reduce the stall effect.

3.1.2   Power Optimisation

The power output of the turbine is optimised whenever the wind speed is below the nominal wind speed and the power is below the nominal power. Optimising power can only be done by finding the pitch angle that corresponds to optimal power coefficient $C_p(\theta,u)$ at a given wind speed u. Optimising power by varying the tip speed ratio λ, which in the simplest case could happen by switching between two different generator speeds, is not considered here.

The pitch angle θ can be adjusted to get optimal $C_p(\theta,u)$ at a given wind speed. In reality this means that the wind speed is averaged over a certain time and θ is adjusted so that it tracks optimal $C_p(\theta,u)$ for this averaged wind speed.

Power optimisation is an open loop control since there is no feedback from θ and power to wind speed.

By adjusting θ not only according to wind speed, but also according to power, side effects like varying air density and dirt on the blades can also be taken into account (Lehnhoff M. et al, 1998). This aspect is not considered in this project, since here focus is on the simulation of short-term operations. Dirt on the blades and varying air densities however are comparatively slow effects. In power optimisation the controller looks up appropriate values of θ in a lookup table. This lookup table consists of wind speed values and corresponding θ values that refer to maximum C_p at the respective wind speed.

3.1.3   Transition between power limitation and power optimisation mode

The transition between the operation modes power limitation and power optimisation is a decision the controller based on the operating point of the wind turbine.
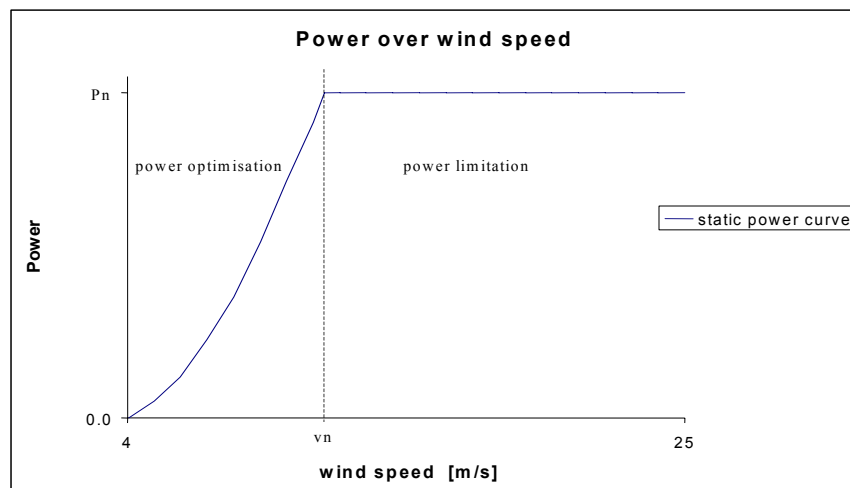

Figure 26: Static power curve with operation modes of an active stall controlled wind turbine.

The static power curve in Figure 26 shows the operation modes: power optimization and power limitation. The dashed line shows the border between the

operation modes, which is where the transition takes place, considering steady state operation.

In the dynamic operation of the turbine the decision whether power optimisation or power limitation mode is to be active has to be made on the basis of averaged wind speed and averaged power values.

3.2 Active stall power controller

In the following subchapters the active stall controller is developed. For this purpose a fictive 2 MW example turbine is used.

The controllers for power optimisation, power limitation and transition are described in the following.

3.2.1   Power optimisation

In the power optimisation mode the pitch θ-values are looked up in a table. The θ-values corresponding to optimal C_p-values have to be found in the C_p table, which describes the aerodynamic properties of the blades.

In order to achieve maximum power yield for each wind speed the maximal C_p and the corresponding θ has to be found, because the aerodynamic power is calculated according to:

$$P = \frac{1}{2} \cdot \rho \cdot \pi \cdot R^2 \cdot u^3 \cdot C_p(\theta, u)$$
(30)

3.2.1.1   Generating θ lookup table

The aerodynamic properties of the blades are applied in the simulation model, as a C_q table. In order to generate a θ lookup table that contains θ-values, which correspond to maximum C_p- and not maximum C_q-values, a C_p table has to be generated from this C_q table. This is done using the following equation:

$$C_p(\theta, u) = C_q(\theta, u) \cdot \lambda$$
(31)

Note that maximising C_q would not achieve maximal power output since maximum C_q and maximum C_p do not necessarily correspond to the same θ.

The lookup table needed in the controller is a θ versus u table. λ is converted to u since in a constant speed turbine the tip speed u_{tip} of the rotor does not vary. u is calculated as follows.

$$\lambda = \frac{u_{tip}}{u}$$
(32)

$$u = \frac{R \cdot \omega}{\lambda}$$
(33)

Note that rotor speed and hence tip speed u_{tip} are considered to be constant, neglecting the fact that the slip in the generator is actually a function of power. (Nominal slip is typically 1% to 2% of nominal speed.)
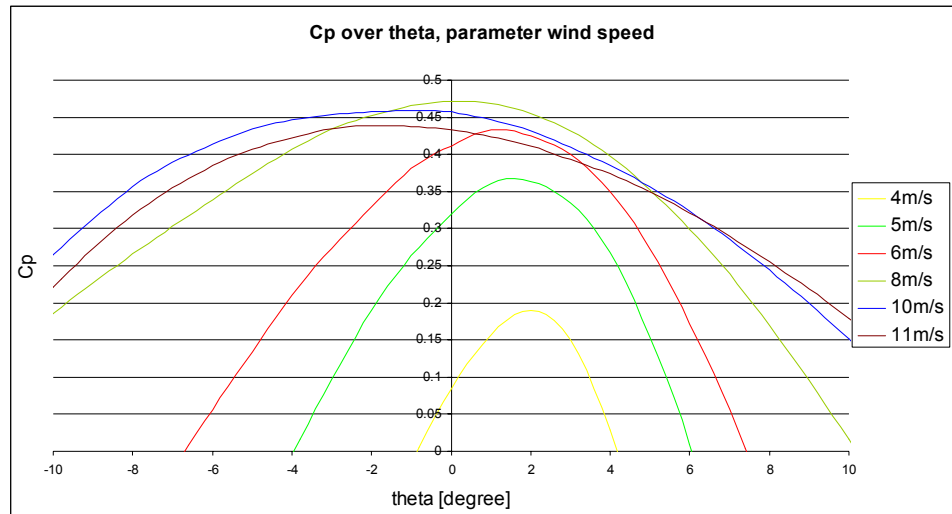
Figure 27: C$_p$ *curve as function of the pitch angle* θ *for different wind speeds.*

To get an idea how accurately the optimal θ should be met, Figure 27 shows C_p curves for different wind speeds as a function of θ. It can be seen that at low wind speeds the C_p over θ curves have rather sharp maxima, i.e. C_p is sensitive to small deviations from optimal θ (optimal θ corresponds to maxima in C_p). At higher wind speeds the curves become flatter and the values of the maxima lie closer to each other, i.e. deviations from optimal θ and slight variations in wind speed make no big differences in C_p.

The graph in Figure 28 shows maximum C_p, optimal θ and linearly interpolated θ over the range of relevant wind speeds (power optimisation range). Optimal θ is the pitch angle required to achieve maximum C_p under any wind speed.

Figure 28: Maximal C$_p$*, optimal* θ *and linearised* θ *over wind speed.*

In Figure 28 the graph of optimal θ shows a lot of discontinuities, especially between 8 m/s and 9.5 m/s. These discontinuities stem from rounding errors and from the discrete data points in the C_p table, which have a rather low resolution (step sizes are: θ = 0.1 degrees and λ = 0.2).
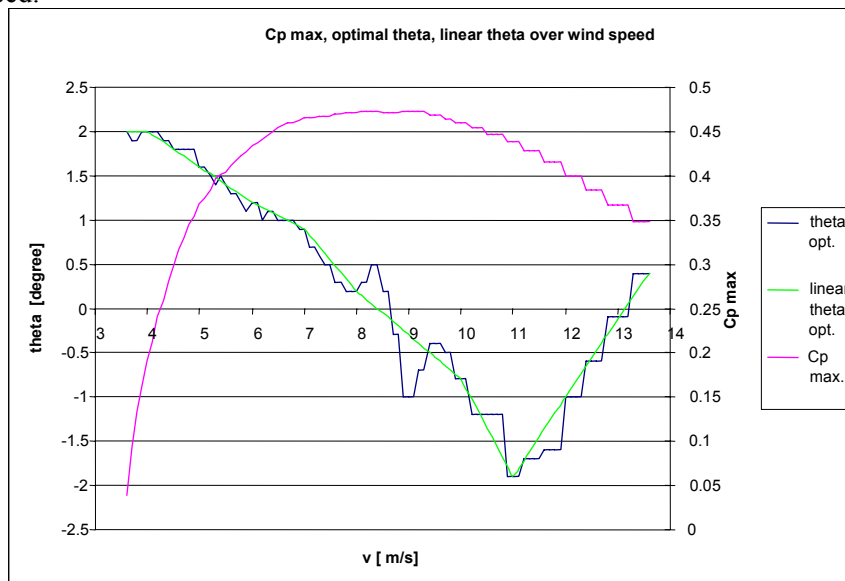
It is not desirable to follow the discontinuities in *theta opt* as depicted in Figure 28 in a wind turbine controller. Looking at Figure 27 it becomes clear that only a little increase in C_p can be achieved from an attempt to follow optimal θ all too accurately. Hence for control purposes a lookup table with the most relevant points and a linear interpolation between these points is used. These values can also be seen in Figure 28 where they are called *linear theta opt*.

When finding the points between which θ shall be linearly interpolated it has to be kept in mind that the optimal θ for lower wind speeds should be met precisely. As it can be seen in Figure 27 the C_p over θ curves have sharp maxima for low wind speeds.

The pitch angle θ is adjusted on the basis of averaged wind speed values instead of instantaneous wind speed values. For this purpose the method of moving average is used. Moving average is a realistic way of filtering the wind signal since this is the method often used in wind turbine controllers.

3.2.2 Power limitation

To get the power limiting stall effect the blades have to be pitched in negative direction when electrical power of the wind turbine exceeds nominal power. Figure 29 illustrates how power over wind speed behaves for different pitch angles.
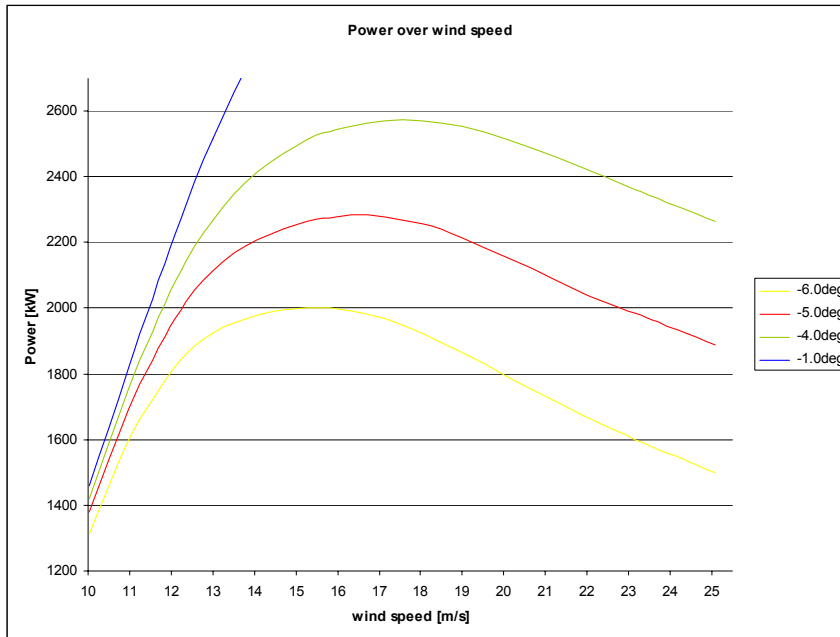

Figure 29: Power over wind speed for different pitch angles.

Figure 30 illustrates how the pitch angle has to be adjusted in order to get nominal power (which is 2 MW in this model) for all wind speed values between nominal wind speed and shut-down wind speed.
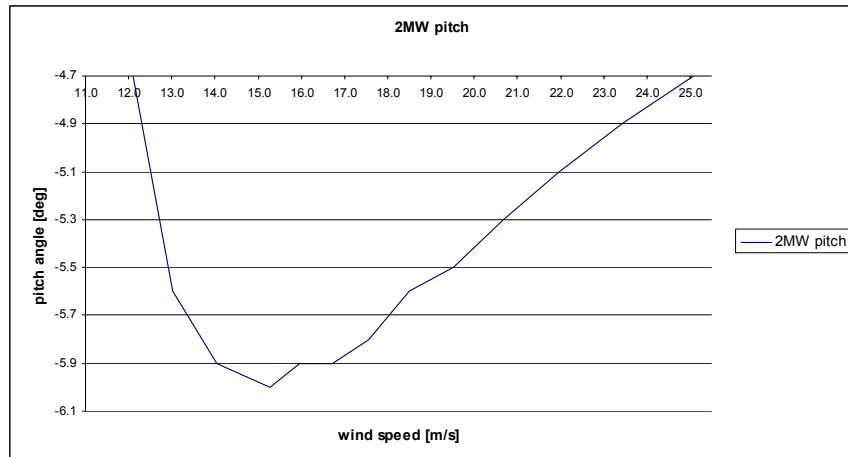
Figure 30: Pitch angle θ *required for constant 2 MW power output in the power limitation wind speed range.*

The pitch angle θ is controlled in a control circuit as shown in Figure 32, where the averaged electrical power from the turbine is compared with the power setpoint i.e. nominal power (2 MW).

The electrical power is filtered using moving average in the same way the wind speed signal is filtered in the power optimisation mode.

3.2.3 Transition between optimisation and limitation

Figure 28 and Figure 30 show that the pitch angle θ at the end of the optimisation range and at the beginning of the limitation range is quite different. The reason for this is that the power curves for different pitch angles in Figure 29 lie close to each other and are very steep in the range between 10 m/s and 12 m/s. To avoid big steps in θ when moving from one operation mode to the other, the θ-values at the end of the power optimisation range have to approach the θ-values at the beginning of the power limitation range. This can be achieved by modifying the θ lookup table, so that θ falls linearly with the slope as in the linearly interpolated θ curve between 10 m/s to 11 m/s. The linearly interpolated and extrapolated θ curve, implemented as a lookup table in the simulation model, are depicted in Figure 31.

This solution is a compromise between maximal power yield in the power optimisation mode and a smooth transition between the operation modes. This compromise reduces the maximum possible power in the range between 11 m/s and 11.8 m/s (which is the nominal wind speed in this example). However, the maximal difference between the practically achieved and the theoretically possible power is only 13.5 kW at 11.8 m/s. This is not only a marginal loss in terms of power, it is also a very small loss in terms of produced energy, since it is reasonable to assume that in most wind power sites a wind speed of 11.8 m/s is a rarely occurring wind speed.
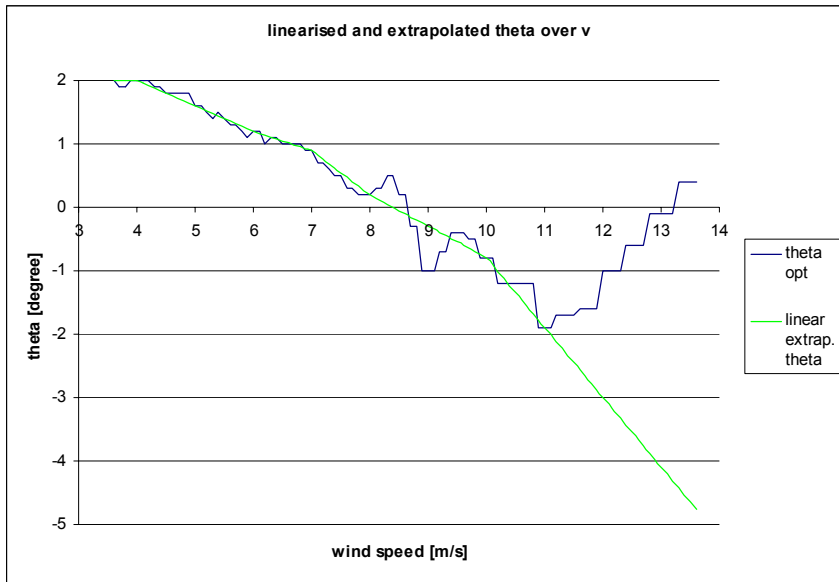
Figure 31: θ_{opt} and θ as implemented in θ-lookup table: Linearly interpolated in power optimisation range and linearly extrapolated for transition between power optimisation and power limitation.

For transition between power optimisation and power limitation the following conditions have to be fulfilled:

- Transition from power optimisation to power limitation: power output has to be greater than nominal power or wind speed has to be greater than nominal wind speed.
- Transition from power limitation to power optimisation: power output has to be less than nominal power and wind speed has to be less than nominal wind speed.

3.2.4   Pitch angle control system

In this subchapter the generation and implementation of the pitch angle setpoint in the pitch control system is described.

Figure 32 shows a diagram of the general control circuit of the pitch control system. The control circuit diagram is divided into four sections, namely "power limitation", "transition switch", "pitch logic" and "pitch system".

The PI-controller for power control (in the section "power limitation" in Figure 32) generates a pitch angle setpoint from the difference between the power setpoint and actually measured and averaged power. The I-part of the PI controller is combined with an anti-windup loop. The task of this anti-windup is to avoid that the integrator keeps integrating while the power control is not active, or while the pitch angle is held constant by the pitch logic. The gain P_{aw} in the anti-windup loop has to be tuned to the normal hold time of the sample and hold (S&H in the section "pitch logic"). When the gain P_{aw} is not tuned correctly the anti-windup either does not work properly, or effectively disables the I-controller. The first case occurs when P_{aw} is too low and the latter case occurs when P_{aw} is too high.

For safety reasons the signal from the PI-controller is limited to a reasonable range, e.g. –2deg to –90deg, which is the range in which θ can be during the power limitation mode.

Also in the section "power limitation" in Figure 32 is a block called "overpower", which detects when the averaged electrical power is excessively above nominal power.

In the section "transition switch" in Figure 32 is the switch, which selects a pitch angle setpoint, either from the power controller for power limitation mode, or from the lookup table for power optimisation mode.
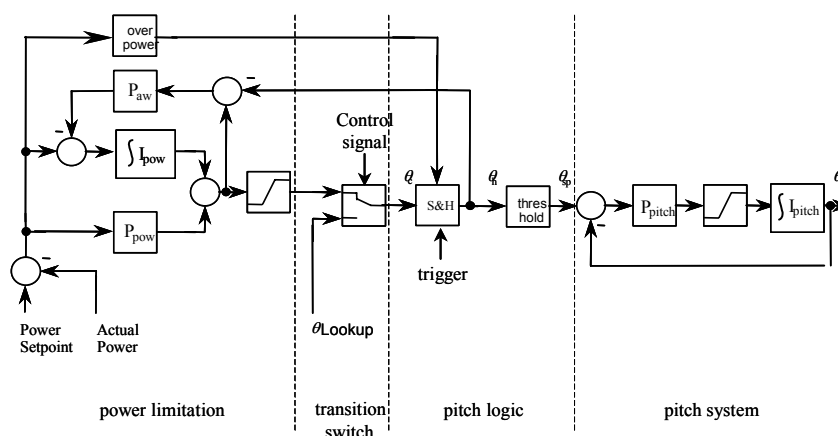

Figure 32: General control circuit of active stall pitch actuator system. PI-power controller, pitch mode selection, sample and hold with a selection of 2 hold times, threshold for pitch angle setpoint and pitch actuator system model.

To the right of the section "transition switch" in Figure 32 is the section "pitch logic". This section contains a sample and hold (S&H) and a threshold block. The desired operation of an active stall wind turbine is to pitch only when necessary. The S&H block has an input from the overpower block in section "power limitation". This input to the S&H block has impact on the hold time, which is needed for overpower protection.

In the section "pitch system" in Figure 32 is a representation of the pitch actuator system. The characteristic of the pitch actuator system is modelled by a pure limitation in the rate of change in pitch angle. The pitch angle setpoint θ_{sp} is compared with the actual pitch angle θ and the difference is multiplied with a factor P_{pitch}, which has the unit $\frac{\text{deg}/s}{\text{deg}}$. This signal is limited to a parameter that defines the maximum rate of change in the pitch angle.

The integrator in section "pitch system" integrates over the limited rate of change in the pitch angle setpoint, which leads to the actual pitch angle of the blades.

The factor P_{pitch} determines the slope of the limiter characteristic in the range between the limits. It is desirable to have the steepest possible slope in order to avoid that the simulation of the pitch actuator system shows a dynamic behaviour in the range of small rates of pitch angle changes. This would mean that the integrator would not integrate fast enough. If however P_{pitch} becomes too big, i.e. the slope becomes too steep; the limiter cannot output small rates of change. In such a case it would permanently jump from one limit to the other instead of staying at a value between the limits.

3.2.4.1   Subsystem to avoid unnecessary pitching

To get pitch actions only once in a specified period the pitch angle setpoint θ_c from either the power controller or from the lookup table, is held in a S&H block.

To further avoid unnecessary pitching a threshold block downstream of the S&H block (in Figure 32) allows a new setpoint θ_{sp} only when the new setpoint differs from the old setpoint by a minimum value.

The function of this combination of S&H and threshold is depicted in Figure 33 where an example θ_c with two different slopes is used to illustrate the function of the system.

The S&H block samples at each positive flank of the rectangular signal. In this example the parameters for threshold, hold time and the slopes of the input signal θ_c are chosen such that the function of the threshold block becomes clear.
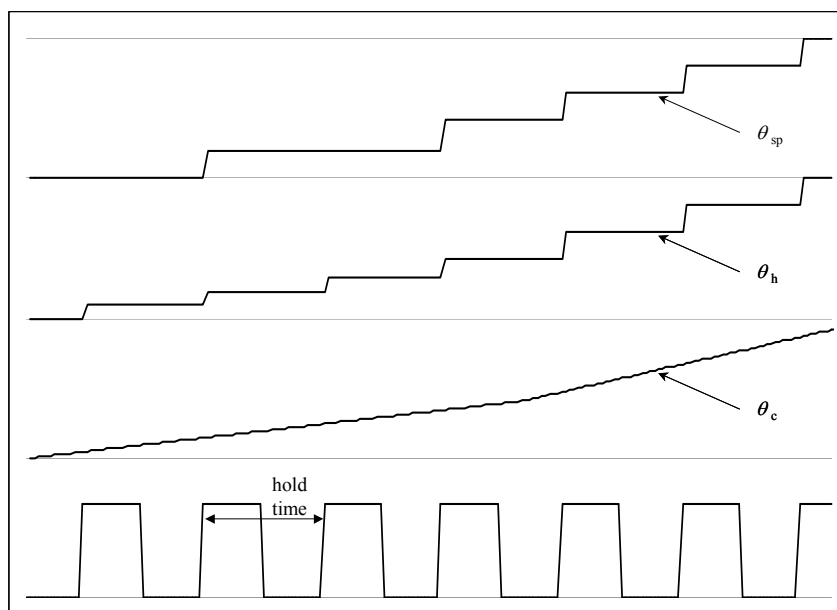
Figure 33: Function of the combination of sample and hold (S&H) and threshold. Input signal θ_c is a ramp, which leads to the output signals θ_{sp} of the S&H and the threshold block. The rectangular signal triggers the S&H at each flank.

The rectangular signal determines at which points in time the S&H block samples a new value. If however the difference between the newly sampled value and the current output value of the threshold block is not bigger than the threshold parameter, the current output of the threshold block is held.

3.2.4.2   Overpower protection

Overpower protection protects the wind turbine from damages due to excessive power production. If under any circumstance the averaged power exceeds a certain level, immediate action has to be taken to limit the power output to avoid damages in mechanical and electrical components of the turbine.

The overpower block in Figure 32 compares the power error with an overpower parameter. If the power error exceeds the value of this parameter the

overpower block effects that S&H uses a much shorter hold time. This means that pitching takes place much more frequently and hence the power output of the turbine can be reduced within a reasonable time.

The power signal that is used for overpower protection (and also for power control) is averaged using a moving average. The averaging time should not be too long but should only make sure that periodic fluctuations in power are filtered out. This avoids that the power controller picks up a setpoint that is not realistic to act on. If the averaging time would be too long, the implied delay would make the overpower protection ineffective.

3.3 Wind turbine controller implementation in power system simulation tool

In the following the implementation of the above-described controller, into the power system simulation tool DIgSILENT PowerFactory is described. During the implementation of the controller care has been taken, that as much as possible is expressed in terms of parameters.

The idea is to simulate different existing active stall wind turbine controllers with this simulation model. The parameters allow the model to be fitted so that it represents the existing controllers of the considered wind turbine. Furthermore the parameters make the program understandable by avoiding constants in the program that are not self-explanatory.

The controller is split up into sub-models as it can be seen in Figure 34.
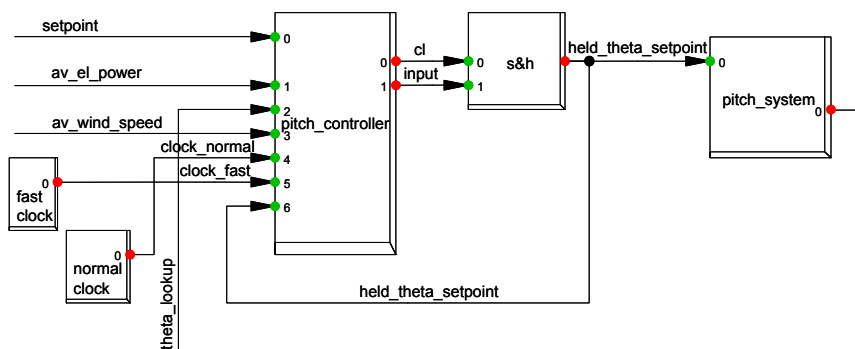
Figure 34: The part of the wind turbine composite model that contains the pitch controller, the pitch actuator system, the sample and hold (S&H) unit and the two clocks that are necessary for the two different hold times in the S&H.

The block "pitch controller" in Figure 34 contains a macro that is depicted in Figure 35. The pitch controller macro contains the PI controller for power limitation, pitch angle setpoint selection (operation mode selection) and clock signal selection for overpower protection.
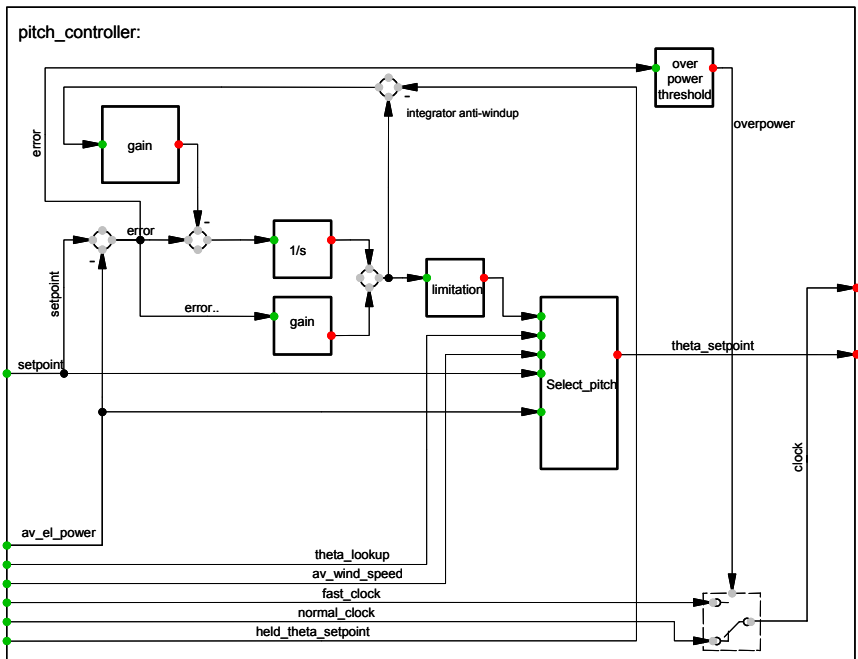
Figure 35: Pitch controller macro.

The block "pitch system" in Figure 34 contains the macro, which is depicted in Figure 36.
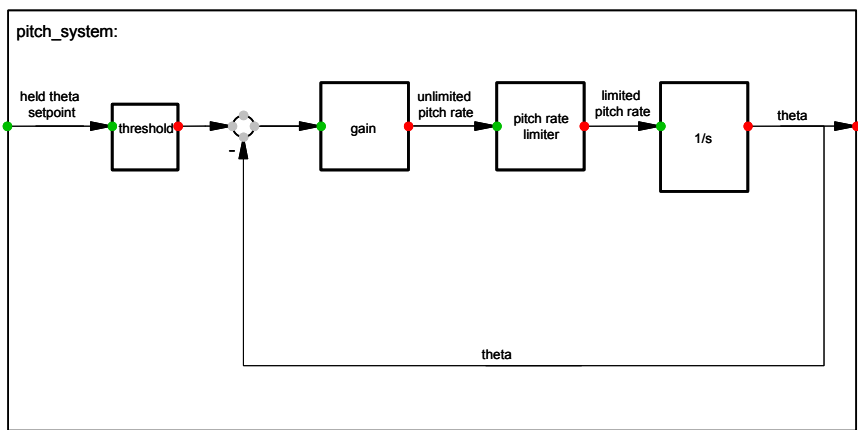
Figure 36: Pitch actuator system macro with threshold and pitch rate limiter.

As it can be seen in Figure 34 the two clocks as well as the S&H block are separate units in the composite model and not a part of the pitch actuator system macro where they would naturally belong. The reason for this is that clocks as well as S&H are built-in DIgSILENT elements and can hence only be used in composite models, but not in macros.

3.3.1 Power optimisation

For power optimisation, i.e. pitch angle from θ-lookup table, the θ versus wind speed table is implemented in the program. In Figure 35 the block select_pitch determines whether or not θ from the lookup table (in Figure 35 it is called *theta_lookup*) is to be chosen. The conditions for choosing *theta_lookup* as *theta_setpoint* are:

av_el_power < setpoint OR av_wind_speed < nominal wind speed
(The variable names are as depicted in Figure 35, and "nominal wind speed" is a parameter.)

Wind speed is averaged using moving average. The averaging time is determined by setting a parameter. The averaging time should be similar to the normal hold time of the S&H block. For θ values corresponding to wind speed values, which lie between two values in the table, linear interpolation is applied.

The moving average function, used for averaging the wind speed and electrical power signal, is implemented into the program as shown in Figure 37 (here at the example of wind speed).

Figure 37: Moving average macro.

For initialisation of the moving average block the assumption is made that the wind speed is constantly on the initial value prior to the start of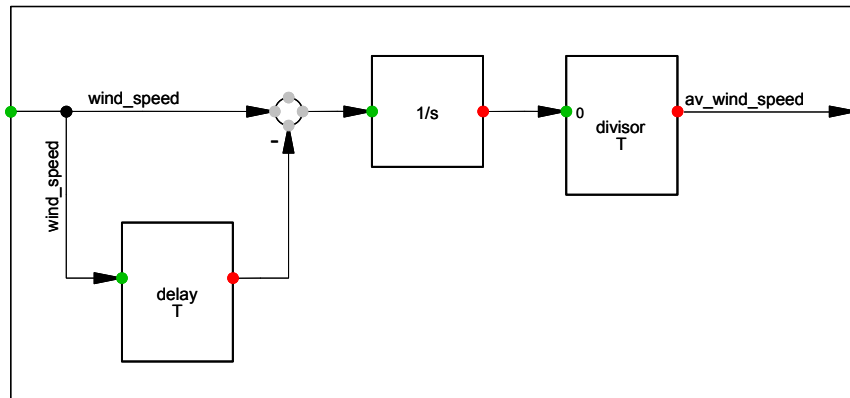 the simulation. This way a moving average with a constant averaging time can be realised, even at the beginning of the simulation i.e. before the simulation time exceeds the averaging time.

3.3.2 Power limitation

The PI-controller of the closed power control loop is split up into a P- and an I-controller.

As explained before, the I-controller is combined with an anti-windup loop. The gain in the anti-windup loop has to be tuned to the normal hold time of the S&H. When the gain is not correctly tuned the anti-windup either does not work properly, or effectively disables the I-controller. The first case occurs when the gain is too low and the latter case occurs when gain is too high.

The power that is controlled (in Figure 35 this signal is called *av_el_power*) is not the instantaneous power but a moving average of the instantaneous electrical power. The averaging time is a parameter and has to be tuned so that fast periodic fluctuations like 3p and fast transient wind speed changes are filtered out, but at the same time overpower can be detected after a tolerable time delay. Therefore it is advantageous to set the power averaging time to a value similar to the short hold time of the S&H because during overpower protection operation these two times have to match each other.

If the averaged power exceeds a certain level of overpower i.e. the condition *error < -(overpower parameter)* is fulfilled the overpower block sets its digital output to high. This effects that the switch in Figure 35 selects the fast clock signal. The clock signal is input to the S&H block where it determines the hold time. By switching between two different clock signals the pitch controller can choose between two different hold times i.e. pitch frequencies.

3.4 Simulations

Different scenarios are simulated to assess the performance of the controller developed.

The impact of the S&H/threshold subsystem on power production is assessed, where applicable, by comparison with a reference turbine. This reference turbine is subject to the same wind speed input but has the least possible restrictions on the pitch action. In both cases i.e. the turbine to be assessed and the reference turbine, the power is averaged over 600 seconds. This allows an effective comparison of the power yields and a quantification of this difference.

3.4.1 Parameter Settings

In all simulations the parameter settings are the same and as listed in Table 1. The parameter settings are chosen such that a fictive example-turbine rated at 2 MW is simulated. By selecting other sets of parameters specific types of active stall turbines could be modelled.

The Power Averaging Time (T_{aP}) is a parameter and has to be tuned so that fast periodic fluctuations like 3p and fast transients from transient wind speed changes are filtered out, but at the same time overpower can be detected after a tolerable delay time. Therefore, it is advantageous to set T_{aP} to a value similar to T_{sh} of the S&H.

u_N	Nominal Wind Speed [m/s]	11.8
P_N	Nominal Power [kW]	2000
ρ	Air Density [kg/m^3]	1.25
R	Rotor Diameter [m]	80
T_{aP}	Power Averaging Time [s]	5
T_{aW}	Wind Averaging Time [s]	60
r	Maximum Pitch Rate [deg/s]	8
P_{pitch}	Gain Pitch System	1000
P_{pow}	Gain Power Controller	0.01
I_{pow}	I-gain Power Controller	0.0025
P_{aw}	Gain Anti-Windup	500
T_{nh}	Normal Pitch Setpoint Hold Time [s]	60
T_{sh}	Short Pitch Setpoint Hold Time [s]	5
P_{over}	Allowed Overpower [kW]	300
$\Delta\theta_{min}$	Minimum Pitch Angle Change [deg]	0.5

Table 1: Parameters of simulation model of an active controlled wind turbine.

The reference turbine, to which the power yield of the turbine described in Table 1 is compared to, has the same parameter settings as in Table 1; only the parameters listed in Table 2 are different.

T_{nh}	Normal Pitch Setpoint Hold Time [s]	5
$\Delta\theta_{min}$	Minimum Pitch Angle Change [deg]	0

Table 2: Parameters of reference turbine.

The reference turbine has the least possible restriction on the pitch actions. As it can be seen in Table 2 the pitch angle setpoint threshold is disabled and T_{nh} is set to the shortest possible value. (Continuous pitch action is not possible since the controller is not designed for that i.e. instabilities might occur under certain conditions.)

3.4.2 Power optimisation

Figure 38 illustrates the simulated operation in power optimisation mode with the mean wind speed set to 8 m/s.
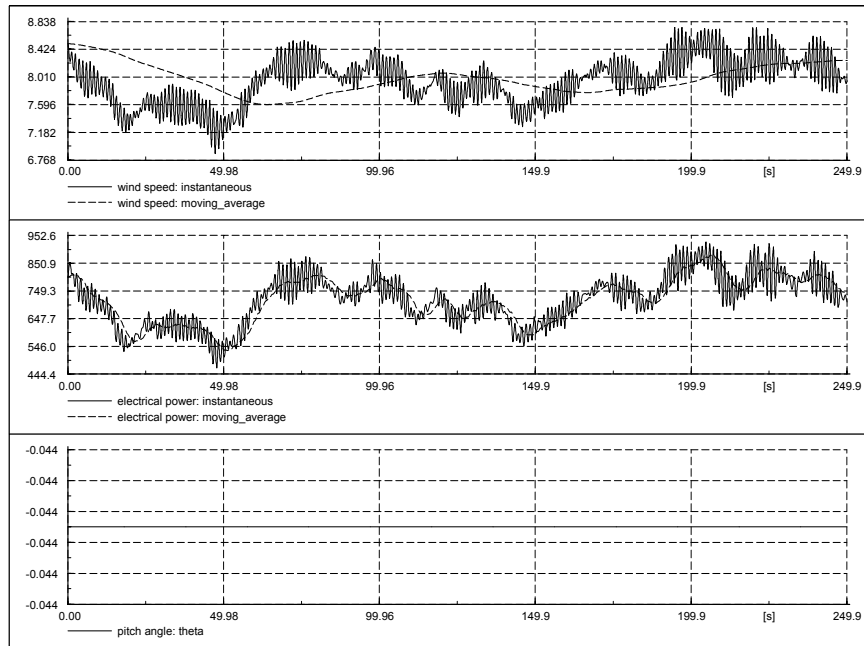
Figure 38: Normal operation in power optimisation mode at mean wind speed 8 m/s. Wind speed, electrical power and pitch angle.

In Figure 38 the pitch angle is held constant since the changes that would be due are below the threshold. The restrictions on pitching implied by the parameters $\Delta\theta_{min}$ and T_{nh} lead to losses in the 10-minute average of power production as it can be seen in Table 3. To calculate the relative difference in averaged power the power of the active stall turbine (restricted pitch action) is used as basis (100%).

600 s power average standard active stall turbine $P1$	600 s power average reference turbine $P2$	Δ averaged power $P2 - P1$	relative Δ averaged power $\frac{P2 - P1}{P1} * 100\%$
684.4 kW	691.1 kW	6.7 kW	0.98 %

Table 3: Comparison of power yield in power optimisation mode.

It can be seen that the pitch angle changes that occur maximum every 5 seconds (when no $\Delta\theta_{min}$ is used) lead to a better power yield of 0.98%. This in-

crease in power yield however has to be paid for with many consecutive pitch actions (every 5 seconds), which means stress for the pitch actuator system.

3.4.3   Transition between optimisation and limitation

To simulate the behaviour of the controller under transition conditions the mean wind speed is set to 12 m/s.
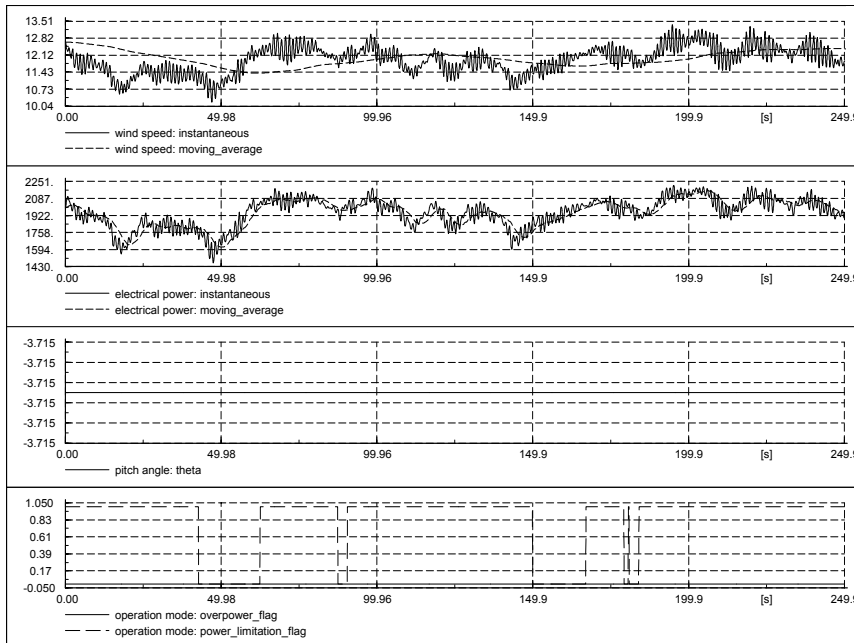
Figure 39: Operation at mean wind speed of 12 m/s. Frequent transition between operation modes. Wind speed, electrical power, pitch angle, overpower indicator and operation mode indicator.

The diagram in Figure 39 shows that transition frequently takes place. The signal "*power_limitation_flag*" is a digital indicator: If on 1 power limitation mode is active; if on 0 power optimisation mode is active.

The power is always around nominal power, intolerable overpower does not occur, nor is power below nominal power, while wind speed is above nominal wind speed. The pitch angle is held constant since the differences implied by the changes in wind speed and by the different operation modes are always below 0.5 degrees. This proves that the linear extrapolation of the θ lookup table leads to a smooth transition between the two operation modes.

Unlimited pitch action leads to no increase in power yield, on the contrary averaged over 10 minutes the power yield is slightly less. Unlimited pitch action avoids not only power deviation below, but also beyond nominal power. However, damages caused by excessive overpower have not to be feared since this is cared for by the overpower protection. Hence pitching every 5 seconds leads to no improvements but to extra stress for the pitch actuator system only.

600s power average standard active stall turbine $P1$	600s power average reference turbine $P2$	Δ averaged power $P2 - P1$	relative Δ averaged power $\dfrac{P2 - P1}{P1} * 100\%$
1918 kW	1916.8 kW	-1.2 kW	-0.06 %

Table 4: Comparison of power yield under operation mode transition condition.

3.4.4 Power limitation

In Figure 40 the performance of the controller in power limitation mode is assessed by applying rather high wind speeds, i.e. mean wind speed is set to 23 m/s.
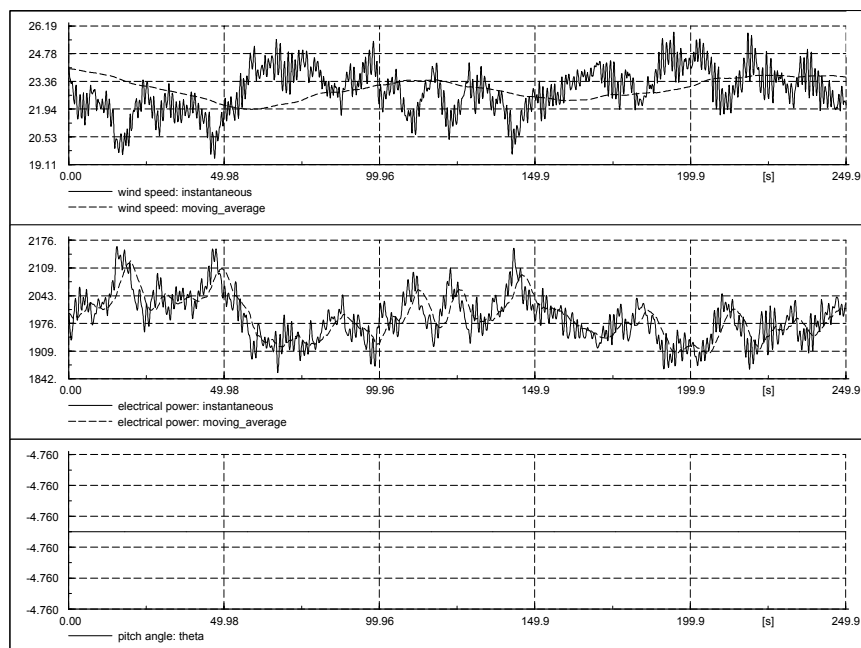
Figure 40: Operation in power limitation mode at mean wind speed 23 m/s. Wind speed, electrical power and pitch angle.

Also for such high wind speeds the controller finds the appropriate pitch angle so that power is always around nominal power. If mean wind speed is at a constant level, pitch angle changes are usually not required as can be seen in Figure 40.

Although it has to be said that the absolute power variations are rather big considering that they exceed ± 100 kW around nominal power, trying to control them out would make little sense in terms of power quality. Considering large wind farms these fluctuations anyway do not exist to such an extent at the terminals of the wind farm, since fluctuations of individual turbines partially offset each other (Rosas, P., 2003).

The operation of the reference turbine is an attempt to control out the power fluctuations. Here the power output of the turbine gets much closer to nominal power, which means less deviation from nominal power. This leads to a decrease in the 10-minute power average of negligible 0.03 % as it can be seen in Table 5.

600s power average active stall turbine $P1$	600s power average reference turbine $P2$	Δ averaged power $P2 - P1$	relative Δ averaged power $\dfrac{P2 - P1}{P1} * 100\%$
2000.9 kW	2000.2 kW	-0.7 kW	-0.03 %

Table 5: Comparison of power yield in power limitation mode for an active stall controlled wind turbine.

While the power limitation is a straightforward task for an active stall wind turbine in the case of moderate wind speed changes only, it becomes a more demanding task when the overall average wind speed increases considerably. To simulate such a situation in the following simulation, the mean wind speed is 11 m/s until the simulation time 60 s, between 60 s and 160 s it is ramped up from 11m/s to 16 m/s. This corresponds to a slope in mean wind speed of 3 m/s per minute. The simulation results of this scenario are depicted in Figure 41.
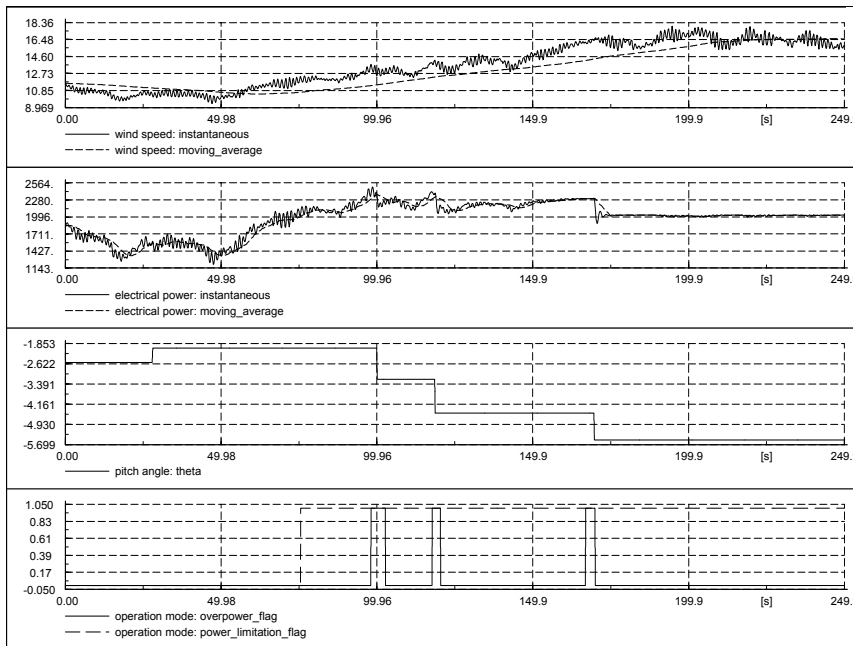
Figure 41: Operation with increasing wind speed implying overpower. Wind speed, electrical power, pitch angle, overpower indicator and operation mode indicator.

The turbine starts off in the power optimisation mode, where an increase in the pitch angle takes place. With an increasing wind speed the turbine enters into power limitation mode and a further increasing wind speed lets the average of the power exceed 2300 kW (300 kW beyond nominal power, which is the maximum allowed level of tolerable overpower). As soon as overpower is detected the pitch angle is adjusted with a maximum delay time of 5 seconds, which is T_{sh}. The signal "*overpower_flag*" is a digital indicator: If overpower is detected it is set to 1.

Due to the steadily increasing wind speed it takes three overpower protection operations to get power permanently down to nominal power.

It can be seen that the controller manages efficiently to limit power to or at least close to nominal power and at the same time does only pitch when it is effective and necessary.

4 Variable pitch, variable speed wind turbine concept

During the last few years, variable speed wind turbines have become the most dominating type of yearly installed wind turbines (Hansen, A.D., 2004), (Hansen, L.H., et al., 2001). The increased interest in the variable speed wind turbines is due to their very attractive features, given by the presence of the power converter, with respect to both the wind turbine itself as well as to more onerous grid requirements.

The variable speed wind turbines have a more complicated electrical system than the fixed speed wind turbines. They are typically equipped with an induction or synchronous generator and a power converter. The presence of the power converter makes the variable speed operation itself possible. The variable speed wind turbines can therefore be designed to achieve maximum power coefficient over a wide range of wind speeds.

The power converter controls the generator speed in such a way that the power fluctuations caused by wind variations are more or less absorbed by changing the generator speed and implicitly the wind turbine rotor speed. Seen from the wind turbine point of view, the most important advantages of the variable speed operation compared to the conventional fixed speed operation are:

- *reduced mechanical stress on the mechanical components such as shaft and gear-box* – the high inertia of the wind turbine is used as a fly-wheel during gusts, i.e. the power fluctuations are absorbed in the mechanical inertia of the wind turbine.
- *increased power capture* – due to the variable speed feature, it is possible to continuously adapt (accelerate or decelerate) the rotational speed of the wind turbine to the wind speed, in such a way that the power coefficient is kept at its maximum value.
- *reduced acoustical noise* – low speed operation is possible at low power conditions (lower wind speeds).

Additionally, the presence of power converters in wind turbines also provide high potential control capabilities for both large modern wind turbines and wind farms to fulfil the high technical demands imposed by the grid operators (Eltra, 2000), (Sørensen,P., et al.,2000), such as:

- *controllable active and reactive power (frequency and voltage control)*
- *quick response under transient and dynamic power system situations*
- *influence on network stability*
- *improved power quality (reduced flicker level, low harmonics filtered out and limited in-rush and short circuit currents)*

All these attractive features make the variable speed wind turbine concept very popular despite some few disadvantages, such as losses in power electronics and increased installation cost due to the power converter. Currently, there are two dominating groups of variable speed wind turbine concepts on the market:

- *Full variable speed concept* – where the generator stator is interconnected to the grid through a full-scale power converter. The generator can be synchronous (WRSG or PMSG) or induction generator (WRIG).
- *Limited variable speed concept* – where the generator stator is connected to the grid. The rotor frequency and thus the rotor speed are controlled. The generator is a wound rotor induction generator (WRIG). There are two such wind turbine concepts (Hansen, L.H, et al., 2001):
  - The variable generator rotor resistance concept, where the rotor is connected to an external optically controlled resistance, whose size defines the range of the variable speed (typically 0-10% above synchronous speed).
  - The doubly-fed induction generator (DFIG) concept, where the rotor is controlled by a partial scale power converter, whose size defines the range of the variable speed (typically +/- 30% around synchronous speed).

Out of all these variable speed wind turbine concepts, the concept with doubly-fed induction generator (DFIG) distinguishes itself as a very attractive option with a fast growing market demand (Hansen, A.D., 2004). The fundamental feature of the DFIG is that the power processed by the power converter is only a fraction of the total wind turbine power, and therefore its size, cost and losses are much smaller compared to a full-scale power converter used in the full variable speed concept.

In this chapter, the attention is drawn to the control strategies and performance evaluation of the variable speed pitch controlled wind turbine with DFIG. The chapter is organised as follows. First, the characteristics of the variable speed wind turbine and of the doubly-fed induction generator are summarized. Then, the overall control system of the variable speed wind turbine with DFIG is described, with focus on the control strategies at the different control levels: DFIG control and wind turbine control.

4.1 Variable speed wind turbine characteristics

A wind turbine is characterised by its power speed characteristics. For a horizontal axis wind turbine, the amount of mechanical power P_{mec} that a turbine produces in steady state is given by:

$$P_{mec} = \frac{1}{2} \rho \pi R^2 u^3 C_p(\theta, \lambda) \tag{34}$$

where ρ is the air density, R the turbine radius, u the wind speed and $C_p(\theta, \lambda)$ is the power coefficient, which for pitch controlled wind turbines depends on both the pitch angle θ and the tip speed ratio λ. The tip speed ratio λ is given by:

$$\lambda = \frac{\omega_{rot} R}{u} \tag{35}$$

where ω_{rot} denotes the rotor turbine speed.

The prime motivation for variable speed wind turbines at lower wind speeds is to adjust the rotor speed at changing wind speeds so that $C_p(\theta, \lambda)$ always is maintained at its maximum value. The power coefficient $C_p(\theta, \lambda)$ has a

maximum for a particular tip-speed ratio λ_{opt} and pitch angle θ_{opt}. This means that for extracting maximum power from a particular wind speed, the control strategy has to change the turbine rotor speed in such a way that the optimum tip speed ratio λ_{opt} is always obtained. The maximum power a particular wind turbine can extract from the wind is a cubic function of the turbine optimum speed, as follows:

$$P_{mec}^{\max} = K_{opt} \left[\omega_{rot}^{opt} \right]^3 \tag{36}$$

where:

$$K_{opt} = \frac{1}{2} \rho \pi R^5 \frac{C_p^{\max}}{\lambda_{opt}^3} \tag{37}$$

K_{opt} depends on the turbine characteristics and the air density. Tracking the maximum power is the goal as long as the generated power is less than the rated power. At wind speeds higher than rated wind speed, the control strategy has to be changed so that the wind turbine no longer produces maximum power but only rated power. The blades are thus pitched to reduce the power coefficient $C_p(\theta, \lambda)$ and thereby to maintain the power at its rated value. Wind gusts are absorbed by rotor speed changes, the wind turbine's rotor behaving as energy storage.

The mechanical power is transformed in the generator into electrical power, the relation between them being given by:

$$P_{el} = \eta_{gen} P_{mec} \tag{38}$$

where η_{gen} is the generator efficiency.

4.2 Doubly-fed induction generator characteristics

The typical DFIG configuration, illustrated in Figure 42 consists of a wound rotor induction generator (WRIG) with the stator windings directly connected to the three-phase grid and with the rotor windings connected to a back-to-back partial scale power converter. The back-to-back converter is a bi-directional power converter. It consists of two independent controlled voltage source converters connected to a common dc-bus. These converters are illustrated in Figure 42, as rotor side converter and grid side converter. The behaviour of the generator is governed by these converters and their controllers both in normal and fault conditions. The converters control the rotor voltage in magnitude and phase angle and are therefore used for active and reactive power control.

Because the optimal voltage of the rotor is typically less than the optimal stator voltage, the transformer connecting the system to the grid has two secondaries: one winding connecting the stator and the other connecting the rotor.
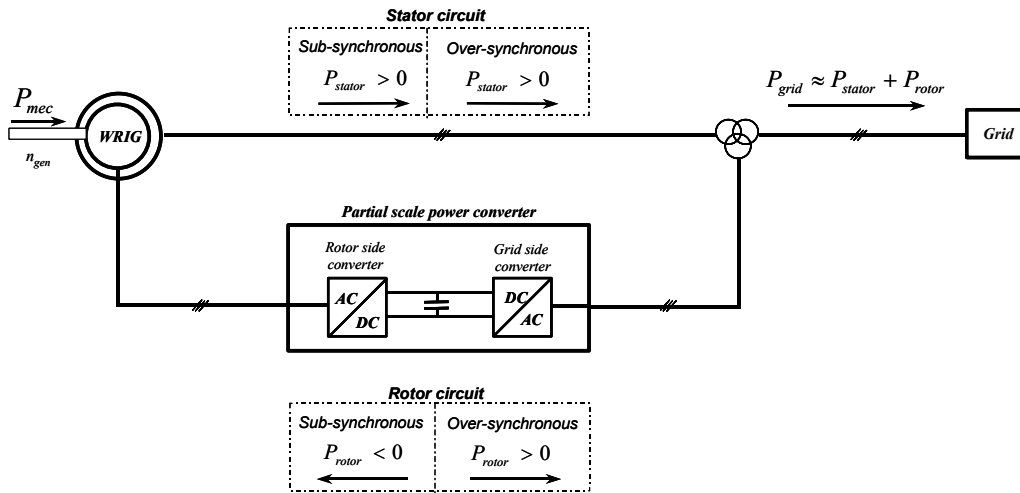
Figure 42: Principle diagram of the power flow in doubly-fed induction generator.

DFIG system allows variable speed operation over a large but restricted range. The smaller the operational speed range the less power has to be handled by the bi-directional power converter connected to the rotor. For example if the speed should be controllable between +/- 30%, the converter must have a rating of approximate 30% of the generator. Thus the size of the converter does not relate to the total generator power but instead to the selected speed range and hence the slip power (Heier, S., 1998), (Leonhard, W., 2001). Therefore, the cost of the power converter increases when the allowed dynamic speed range around synchronous speed increases.

Notice that, since the speed range is restricted, the slip-induced voltage is only a fraction of the grid voltage, depending on the turn-ratio between the stator and rotor. The dc bus voltage is thus relatively low. The operation at a lower dc bus voltage is possible because of the voltage reduction on the rotor side realised by the three winding transformer.

In order to cover a wide operating range from sub-synchronous to over-synchronous speed, i.e. the DFIG is able to work as a generator in both sub-synchronous (positive slip $s>0$) and over-synchronous (negative slip $s<0$) operating area, the power converter has to be able to operate with power flow in both directions. This is the reason why a back-to-back PWM (bi-directional) converter configuration is used. The slip is defined as:

$$ s = \frac{n_{syn} - n_{gen}}{n_{syn}} \tag{39} $$

where n_{syn} and n_{gen} are the synchronous speed and generator speed in rpm, respectively. For a doubly-fed induction machine, it is the sign of the electrical torque, independent of the slip, which indicates if the machine is working as motor or generator.

Assuming that all the losses in the stator and rotor circuit can be neglected, the power through the power converter (through the rotor circuit), known as the slip power, can be expressed as the slip s multiplied with the stator power, P_{stator}. Furthermore, the delivered stator power can be expressed based on the grid power P_{grid} or on the mechanical power:

$$P_{rotor} \approx -s\ P_{stator}$$

$$P_{stator} \approx P_{grid} / (1-s) = \eta_{gen}\ P_{mec} / (1-s) \qquad (40)$$

where η_{gen} is the generator efficiency. Depending on the operating condition of the drive, the power is fed in or out of the rotor: it is flowing from the grid via the converter to the rotor ($P_{rotor} < 0$) in sub-synchronous mode or vice versa ($P_{rotor} > 0$) in over-synchronous mode, as it is indicated in Figure 42. In both cases (sub-synchronous and over-synchronous) the stator is feeding energy to the grid ($P_{stator} > 0$) (Leonhard, W., 2001).

The presence of the power converter allows DFIG a more versatile and flexible operation compared with a squirrel-cage induction machine. The power converter compensates for the difference between the mechanical and electrical frequency by injecting a rotor current with a variable frequency according to the shaft speed. Through collector rings, the power converter supplies thus the rotor windings with a voltage with variable magnitude and frequency. It improves the controllable capabilities of such generator, as for example:

- it provides DFIG the ability of reactive power control. DFIG is therefore capable of producing or absorbing reactive power to or from the grid, with the purpose of voltage control (i.e. in the case of weak grid, where the voltage may fluctuate).
- it can magnetize the DFIG through the rotor circuit, independently of the grid voltage.
- it decouples active and reactive power control by independent control of the rotor excitation current.

4.3 The overall control system of a variable speed wind turbine with DFIG

The control system of a variable speed wind turbine with DFIG has as goals to control the reactive power interchanged between the generator and the grid and the active power drawn from the wind turbine in order to track the wind turbine optimum operation point or to limit the power in the case of high wind speeds.

Each wind turbine system contains subsystems (aerodynamical, mechanical, electrical) with different ranges of time constants, i.e. the electrical dynamics are typically much faster than the mechanical. This difference in time constants becomes even bigger in the case of a variable speed wind turbine, due to the presence of the power electronics. Such more complicated electrical system requires a more sophisticated control system too.

Figure 43 shows the overall control system of a variable speed DFIG wind turbine. Two control levels which have different bandwidths and are strongly connected to each other, can be distinguished in the overall control system:

- Doubly-fed induction generator control (control of active and reactive power)
- Wind turbine control

The DFIG control encompasses the electrical control of the power converters and of the doubly-fed induction generator. Since this controller is an electric one, it works very fast. The DFIG control level has as goal to control the active and reactive power of the wind turbine independently. The DFIG control contains two decoupled control channels: one for the rotor side converter and one for the grid side converter – see Figure 42. As the pulse-width modulation fac-

tor *PWM* is the control variable of the converter, each of these control channels generates a pulse-width modulation factor *PWM*, for the respective converter. This control variable is a complex number and therefore can control simultaneously two variables, such as the magnitude and phase angle of the rotor induced voltage. For example, for a predefined DC voltage and a control variable (pulse-width modulation factor *PWM*), the line-to-line AC-voltage is determined as follows:

$$|U_{AC}| = \frac{\sqrt{3}}{2\sqrt{2}} \cdot |PWM| \cdot U_{DC} \qquad (41)$$

On the other hand, the wind turbine control is a control with slow dynamic responses. The wind turbine control contains two cross-coupled controllers: a speed controller and a power limitation controller. It supervises both the pitch angle actuator system of the wind turbine and the active power setpoint of the DFIG control level. It thus provides both a reference pitch angle θ_{ref} directly to the pitch actuator and a converter reference power signal $P_{grid}^{conv,ref}$ for the measurement grid point M to the DFIG control.

Different line styles are used to provide a quick overview of the signals of the overall control system in Figure 43:
- double-dotted lines mark the measured signals.
- single dotted-lines reveal reference (setpoint) signals
- solid lines reveal the output signals from the controllers

Notice that the overall control system requires information on different measured electrical signals: the active P_{grid}^{meas} and reactive Q_{grid}^{meas} power (measured in the measurement grid point M), the voltage U_{dc}^{meas} on the DC – busbar, the AC- converter current I_{ac}^{meas} (measured in point N), the generator speed ω_{gen}^{meas} and the rotor current I_{rotor}^{meas}.

The DFIG control level has three reference input signals:
- The converter reference active power $P_{grid}^{conv,ref}$ in the measurement grid point *M*. This information is delivered by the wind turbine control level.
- The converter reference reactive power $Q_{grid}^{conv,ref}$ in the measurement grid point *M*. This reference can be extraordinarily imposed by the grid operators (based for example on a certain dispatch control). For example in the case of a weak grid or a grid fault situation, the DFIG can have the extra task to generate reactive power to support the grid voltage.
- The reference DC- voltage U_{dc}^{ref} is a value strictly connected to the size of the converter, the stator-rotor voltage ratio and the modulation factor of the power converter.
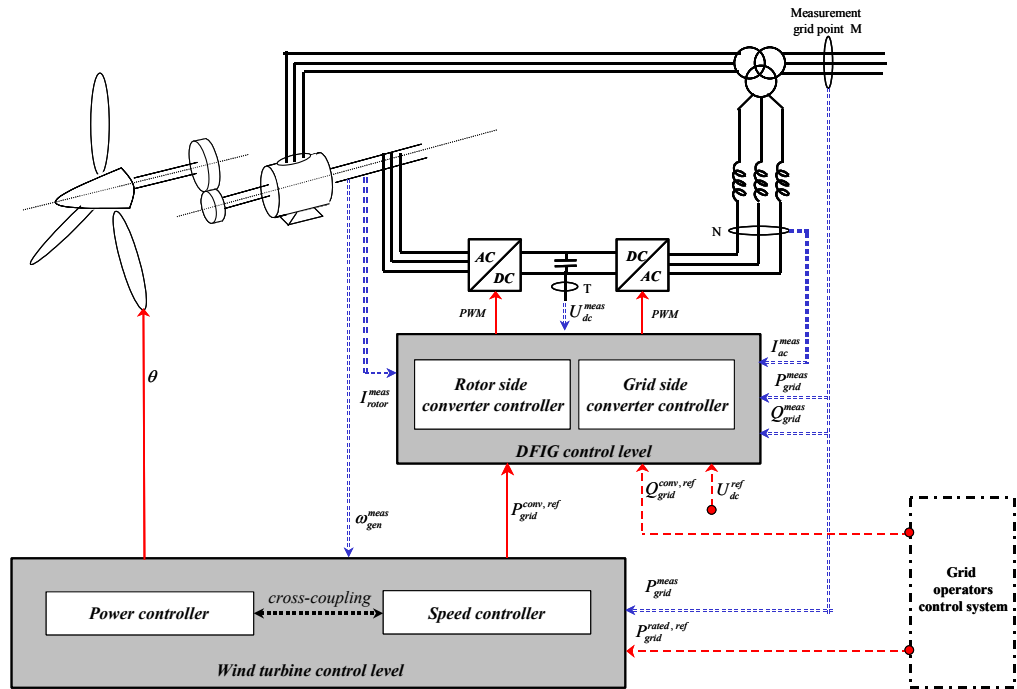
Figure 43: Overall control system of variable speed wind turbine with doubly-fed induction generator.

The wind turbine control generates two control signals:

- The converter reference active power $P_{grid}^{conv,ref}$ - is the setpoint for the active power signal for the DFIG control level. It is generated based on the measured generator speed ω_{gen}^{meas} and the measured grid power P_{grid}^{meas} in the measurement grid point *M.* For example, when the wind speed is less than the rated wind speed, the wind turbine control level generates the converter reference active power $P_{grid}^{conv,ref}$ by adjusting the generator speed in such a way that the turbine captures the maximum power.

- The pitch angle θ - is delivered directly to the wind turbine blades. The pitch angle actuator system is implemented as a part of the power controller. It is generated based on the measured grid power P_{grid}^{meas} and the reference rated active power $P_{grid}^{rated,ref}$. The reference rated active power signal $P_{grid}^{rated,ref}$ is normally the nominal power of the wind turbine. Similarly to $Q_{grid}^{conv,ref}$, $P_{grid}^{rated,ref}$ can be imposed in special situations by the grid operators control system to a power value less then the nominal (rated) power of the wind turbine. The present work considers the case when $P_{grid}^{rated,ref}$ is the nominal (rated) power of the wind turbine.

For example, as long as the power limit $P_{grid}^{rated,ref}$ is not reached (i.e. wind speeds less than the rated wind speed), the wind turbine control keeps the pitch angle to its optimal value and it generates the optimal active power reference $P_{grid}^{conv,ref}$ to the DFIG control level. The DFIG control has then to adjust continuously the generator speed in order to keep the power reference provided by

the wind turbine control level. In the case of wind speeds higher than rated wind speed, the wind turbine control level commands: 1) the pitch actuator system with a pitch angle that prevents the power generation from becoming too large and 2) the DFIG control level with power reference equal to the nominal power. The DFIG control level has then the goal to adjust the generator speed to its nominal value in a predefined dynamic speed range.

In the following sections, the two control levels with their individual controller are described.

4.4 Doubly-fed induction generator control

The doubly-fed induction generator (DFIG) control contains the fast electrical control of the doubly-fed induction generator. Control strategies and performance evaluation of doubly-fed induction generators have been widely discussed in the literature (Leonhard W., 2001), (Mohan N., et al., 1989), (Novotny D.W. et al., 1996), (Pena, R., et al., 1996), and it is therefore beyond the scope of this report to go into details about the vector control of electrical machines and of converters.

4.4.1   System reference frames

Briefly, the vector control techniques allow de-coupled control of active and reactive power. These techniques are based on the concept of d-q controlling in different reference frames, where the current and the voltage are discomposed into distinct components related to the active and reactive power. Each specific reference frame is defined by two orthogonal axes, namely d-axis (direct axis) and q-axis (orthogonal axis). In this report the stator flux oriented rotor current control with decoupled control of active power and reactive power is adopted (Novotny D.W. et al., 1996).
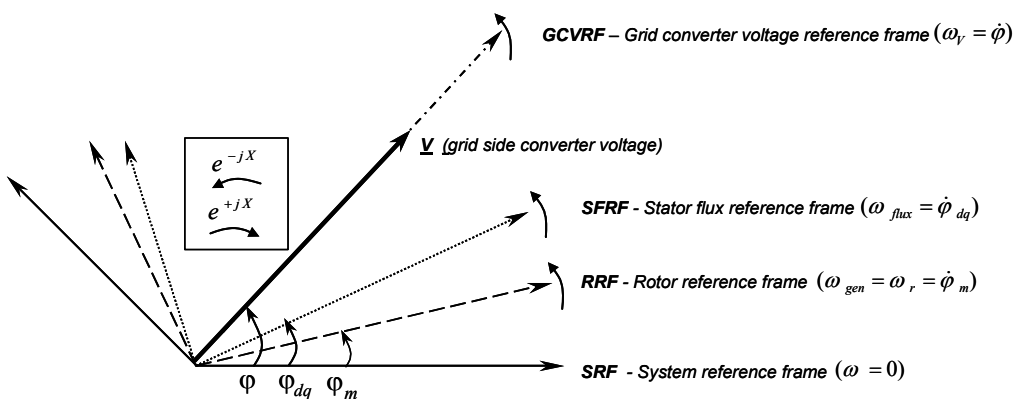

Figure 44: Reference frames used in doubly-fed induction generator control.

The doubly-fed induction generator DFIG and its control in DIgSILENT is using the following reference frames, illustrated in Figure 44:
- System reference frame *(SRF)*– is the reference frame fixed to the grid, and it is rotating with the grid reference voltage. Therefore its relative speed to the grid is considered zero.
- Rotor reference frame *(RRF)* - is the reference frame fixed to the rotor. The d-axis in the rotor reference frame is chosen collinear to the rotor phase winding. The position of the rotor reference frame is the actual position of the rotor φ_m.

- Stator flux reference frame *(SFRF)* – is the reference frame, which rotates synchronously with respect to the stator flux, namely its d-axis is chosen collinear to the stator flux vector. The position of stator flux reference frame is the instantaneous position φ_{dq} of the stator flux vector.

  This is calculated as $\tan(\varphi_{dq}) = \dfrac{\psi_{q,stator}^{SRF}}{\psi_{d,stator}^{SRF}}$ where $\psi_{d,stator}^{SRF}$ and $\psi_{q,stator}^{SRF}$ are its stationary components on *d*- and *q*- axis, respectively in the system reference frame *SRF*. Since the d-axis of this reference frame is chosen to be the instantaneous axis of the stator field, the phase angle φ_{dq} of the stator voltage is generally not a constant, although its frequency and magnitude are constants constrained by the power system. This reference frame is defined with respect to the stator flux and not to the stator voltage because the stator flux basically represents the integral of the stator voltage and is therefore much smoother.

- Grid converter voltage – oriented reference frame *(GCVRF)*– is the reference frame which d-axis is chosen collinear to the voltage grid converter $\underline{V}$. This reference frame is positioned by the voltage angle φ, which is measured with a PLL (phase-locked loop) block.

Once, a reference frame is defined, a vector can be discomposed into distinct components on the axes. For example, the grid converter voltage vector $\underline{V}$, shown in Figure 44, can be expressed in system reference frame *SRF* as:

$$\underline{V} = |\underline{V}|\, e^{j\varphi} = V_d^{SRF} + j\, V_q^{SRF} \tag{42}$$

where V_d^{SRF} and V_q^{SRF} are the components on *d* (real) and *q* (imaginary) axis, respectively, in the system reference frame *SRF*. $|\underline{V}| = \sqrt{\left(V_d^{SRF}\right)^2 + \left(V_q^{SRF}\right)^2}$ is the absolute value of the voltage vector, while φ is the angle of voltage vector $\underline{V}$ in the system reference frame *SRF*.

In the vector control, the signals are typically transformed from one reference frame to another. Such coordinate transformations have as scope to simplify the modelling and the control algorithms. For example, the voltage grid converter vector $\underline{V}^{SFRF}$ expressed in *SFRF* can be transformed in *RRF* by:

$$\underline{V}^{RRF} = \underline{V}^{SFRF}\, e^{jX} \tag{43}$$

where $X = \varphi_{dq} - \varphi_m$ is the angle between the two reference frames, $\underline{V}^{RRF}$ and $\underline{V}^{SFRF}$ are the voltage vectors expressed in coordinates of *RRF* and *SFRF*, respectively. The angle sign convention for the coordinate transformation is also shown in Figure 44.

4.4.2 Control configuration of DFIG in DIgSILENT

Figure 45 shows the overall control configuration of DFIG in DIgSILENT. Notice that the DFIG model and the control of the converters in DIgSILENT are not using the same reference frame, and therefore different coordinate transformations are performed in order to be able to make possible the interconnection between these different blocks.
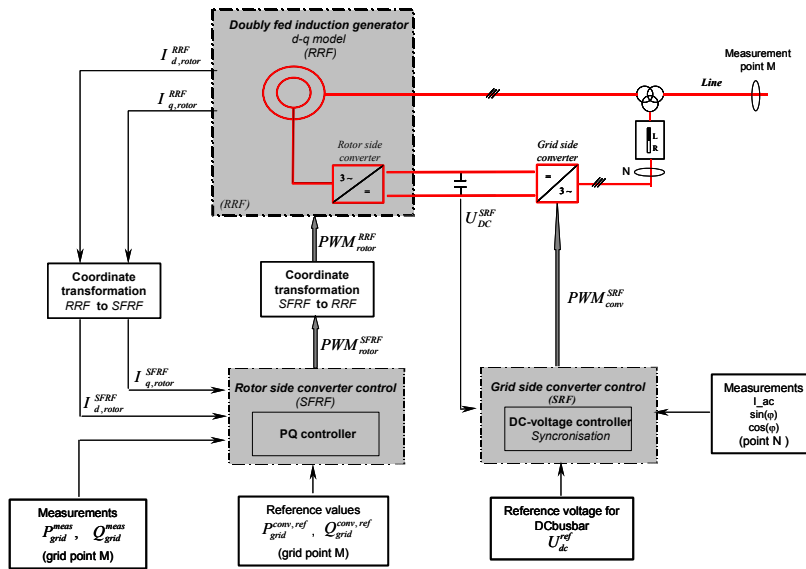
Figure 45: Control scheme of DFIG in DIgSILENT.

As illustrated both in Figure 42 and Figure 45, the configuration of the doubly-fed induction generator contains two converters with a DC link:

1. *Rotor side converter*: is an integrated part of the DFIG model in DIgSILENT together with the usual induction machine d-q model. The DFIG model in DIgSILENT is expressed in the rotor reference frame *RRF* and it is a d-q built-in model with predefined inputs and outputs. The controller of the rotor side converter is expressed in the stator flux reference frame *SFRF*.

2. *Grid side converter* - is an independent component in DIgSILENT's library, which can be added to the machine model to form the DFIG with back-to-back converter. Its controller is expressed in the system reference frame *SRF*.

In the following, it is focus on the control of the two converters existing in the DFIG configuration. Both the rotor- and grid- side controllers are explained only to the necessary extent.

4.4.3 Rotor side converter control

As mentioned before, the rotor windings are connected to the main grid by a power converter allowing controlling the slip ring voltage of the generator in magnitude and phase angle. Figure 46 illustrates the blocks, which are connected with the rotor side converter control block. Notice that some of the block models are built-in type while others are dsl type. The diagram contains the following blocks:

<u>*P, Q measurement block*</u> *(built-in model)* – delivers the measured active P_{grid}^{meas} and reactive power Q_{grid}^{meas} in a predefined grid point *M* – see Figure 43.

<u>*Coordinate transformation blocks*</u> *(dsl model)* –perform different coordinate transformations, as for example:
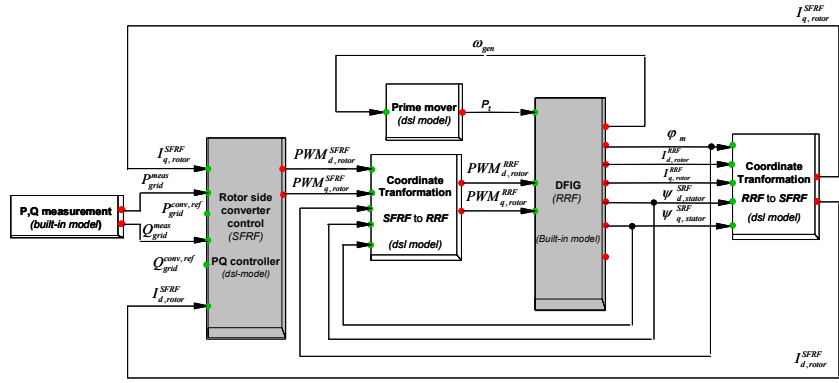
- from *SFRF* to *RRF*:

Figure 46: Inputs and outputs of the rotor side converter control.

The induced controlled rotor voltage is modulated with the pulse-width amplification factor PWM. This modulation factor is the output of the rotor side converter controller and it is expressed in *SFRF*. As the DFIG model is expressed in *RRF*, the output of the rotor side converter's controller has therefore to be transformed to *RRF*:

$$PWM_{rotor}^{RRF} = PWM_{rotor}^{SFRF} \ e^{+j(\varphi_{dq} - \varphi_m)} \tag{44}$$

- from *RRF* to *SFRF*

  The output of the generator model is expressed in *RRF* and therefore it has to be transformed back to *SFRF* in order to be used by the rotor side converter's controller:

$$I_{rotor}^{SRFR} = I_{rotor}^{RRF} \ e^{-j(\varphi_{dq} - \varphi_m)} \tag{45}$$

DFIG block (built-in model) – comprises the model of the doubly-fed induction generator and of the rotor side converter. Notice that its inputs, outputs and equations are expressed in rotor reference frame *RRF*. This block can have as output the rotor current I_{rotor}^{RRF}, the rotor position φ_m and the stator flux ψ_{stator}^{SRF}.

Prime mover block (dsl model) – gets as input the generator speed ω_{gen} and it delivers as output the mechanical power P_t to the generator. In wind turbine applications, the prime mover of the generator is the turbine itself, where the mechanical component model provides the mechanical power to the generator.

Rotor side converter control block (dsl model) – contains the rotor side converter control, which is illustrated in Figure 47. As mentioned before, the aim of the rotor side converter is to control independently the active and reactive power in the measurement grid point M (see Figure 43), and therefore the stator flux oriented rotor current control approach is used. The active and reactive powers are not controlled directly. The impressed rotor current is controlled instead.

The rotor side converter control consists of two PI- control loops in cascade – see Figure 47:

- a slower (outer) power control loop
- a very fast (inner) rotor current control loop.

The power control loop controls the active and reactive power, while the very fast current control loop regulates the machine's rotor currents to the reference values that are specified by the slower power controller.
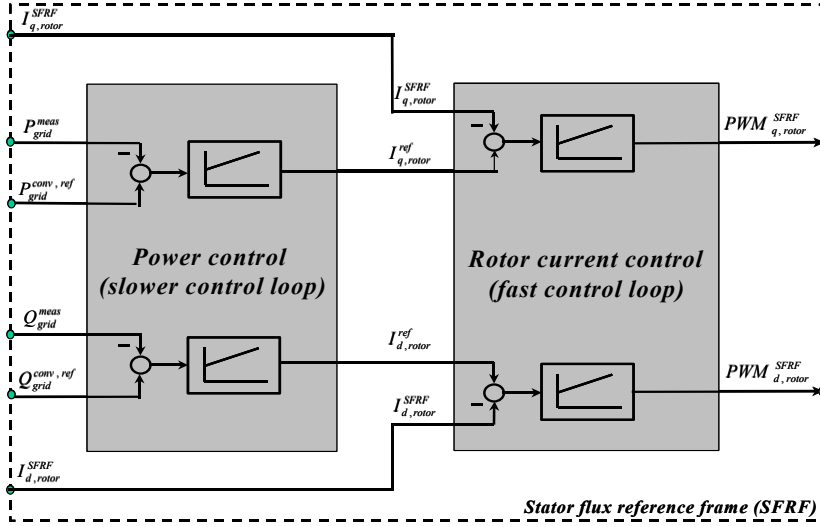
Figure 47: Rotor side converter control scheme using a cascade control structure.

Such cascade control structure is advantageous as the electrical and mechanical dynamics are in different time scales, i.e. the electrical dynamics are much faster than the mechanical dynamics. Since the electrical dynamics are the fastest, the rotor current control loop is the inner loop.

The rotor current is thus split into a parallel and orthogonal component to the stator flux, respectively. In the stator flux reference frame *SFRF*, the d-axis is equivalent to the reactive component and the q-axis is equivalent to the active component. In such a reference frame, the active power (the electromagnetic torque, respectively) is only a function of the q- component of the rotor current, while the reactive power is expressed as function of the *d*- component of the rotor current (Novotny D.W. et.al., 1998):

$$P = func(I_{q,rotor}^{SFRF})$$
$$Q = func(I_{d,rotor}^{SFRF}) \tag{46}$$

This means that the active power *P* control is therefore achieved by controlling the *q*- component of the rotor current $I_{q,rotor}^{SFRF}$ orthogonal on the stator flux, while the reactive power *Q* control is achieved by controlling the *d*- component of the rotor current (the magnetising current) $I_{d,rotor}^{SFRF}$ collinear with the stator flux. Expression (46) illustrates that in *SFRF* the control of active and reactive power is decoupled.

The power control loop generates the reference rotor current components $I_{q,rotor}^{ref}$ and $I_{d,rotor}^{ref}$, respectively, for the rotor current control loop. The rotor current control loop generates the reference rotor voltage components. As the pulse-width modulation factor *PWM* is the control variable of converter, the output of the rotor side converter's controller is expressed in terms of pulse-width modulation factor components $PWM_{d,rotor}^{SFRF}$ and $PWM_{q,rotor}^{SFRF}$, respectively.

Notice that the outputs of the controller are expressed in *SFRF*. As the model of the rotor side converter is comprised in the DFIG model and expressed in the rotor reference frame (*RRF*), the outputs of the rotor side converter controller have to be transformed from stator flux reference frame (*SFRF*) to the rotor reference frame (*RRF*), according to equation (44) and to Figure 46.

Notice that the converter active and reactive power references $P_{grid}^{conv,ref}$ and $Q_{grid}^{conv,ref}$ for the measurement grid point *M*, respectively, used as inputs by the rotor side converter controller (see Figure 43, Figure 47), can be dynamically varied depending on each specific application.

The protection of the rotor side converter against over-currents is an integral part of the doubly-fed induction machine model in DIgSILENT and it is discussed in (Pöller, M., 2003).

4.4.4 Grid side converter control

The aim of the control of the grid side converter is to maintain the dc-link capacitor voltage in a set value regardless of the magnitude and the direction of the rotor power and to guarantee a converter operation with unity power factor (zero reactive power). This means that the grid side converter exchanges only active power with the grid, and therefore the transmission of reactive power from DFIG to the grid is done only through the stator.

Figure 48 illustrates the blocks, which are connected with the grid side converter control block. Similar to Figure 46, the types of model blocks are also specified. The scheme contains the following blocks:

DC - voltage measurement block (built-in model) – measures the DC-voltage in the common dc-busbar of the back-to-back converter.

AC-current measurement block (built-in model) – measures the ac- current of the grid side converter (measurement point *N* in Figure 43).
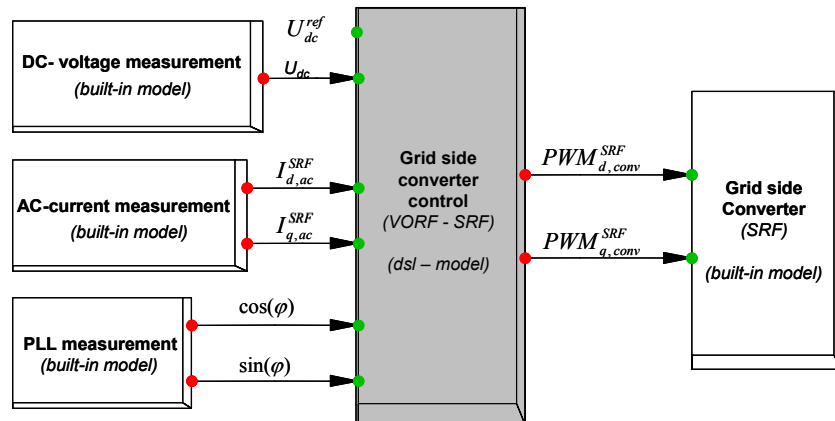

Figure 48: Inputs and outputs for the grid side converter control in DIgSILENT.

PLL measurement block (built-in model) – measures the phase angle φ of the AC-voltage generated by the grid side converter. The voltage phase angle is measured in order to synchronize the AC-converter voltage to the AC-grid voltage.

Grid side converter block (built-in model) –is an independent IGBT converter component in DIgSILENT's library. As mentioned before, DIgSILENT provides several control modes for the control of the converters. The typical control mode used for the grid side converter of the DFIG is U_{dc}-*Q mode,* as its function is to regulate the dc-voltage and the reactive power.

Grid side converter control block (dsl model) – contains the grid side converter control, illustrated in Figure 49. Similarly to the rotor side converter, the grid side converter is current regulated. The dc-voltage and the reactive power are controlled indirectly by controlling the grid side converter current.
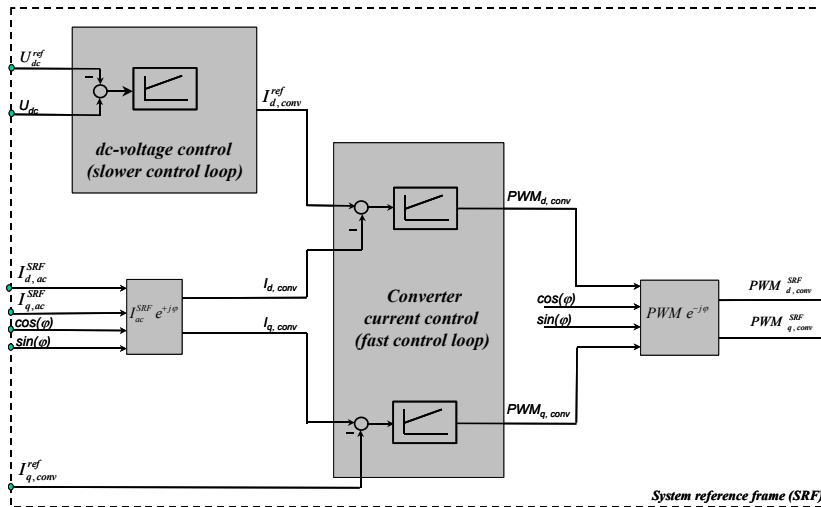

Figure 49: Grid side converter control in DIgSILENT.

The grid side converter control contains two PI control loops in cascade:
- a slower (outer) DC-voltage control loop
- a very fast (inner) converter current control.

The DC- voltage control loop regulates the DC-link voltage to a predefined value U_{dc}^{ref}, while the very fast current control loop regulates the converter current to the reference value specified by the slower dc-voltage controller.

The outputs of the grid side converter controller define the magnitude and phase angle of the AC-voltage terminal of the converter. The converter current control operates in the grid converter voltage oriented reference frame *GCVRF*. The converter current is discomposed into a parallel and an orthogonal component on the grid side converter voltage. In such reference frame the d-axis is equivalent to the active component, while the q-axis is equivalent to the reactive component. The converter current component parallel to the converter voltage (direct phase) $I_{d,conv}$ is used to control the dc-voltage (active power), while the component orthogonal to the converter voltage (quadrature phase) $I_{q,conv}$ is used to control the reactive power.

The DC-link voltage is controlled in the outer slower control loop to its setpoint value U_{dc}^{ref} by the d-converter current component. It generates the reference of the direct phase component of the converter current $I_{d,conv}^{ref}$. The reference of the quadrature component of the converter current $I_{q,conv}^{ref}$ is constant, almost proportional to the reactive power. To operate the converter with unity power factor $(Q_{conv} = 0)$ implies a zero q- current reference $I_{q,conv}^{ref} = 0$.

Notice that the converter current control loop generates the direct $PWM_{d,conv}$ and the orthogonal $PWM_{q,conv}$ component of the pulse-width modulation factor in the grid converter voltage oriented reference frame (*GCVRF*). These components are then transformed into the system reference system *SRF*, as the grid converter requires controlling signals in *SRF*.

Notice in Figure 43 that the grid side converter is connected in series with inductors to the line in order to smooth the converter currents. These inductors may also be integrated into the transformer.

4.5 Wind turbine control

The wind turbine control, with a slower dynamic response than the DFIG control, controls the pitch angle of the wind turbine and the reference active power to the DFIG control level.

4.5.1   Control strategies

Different control strategies of variable speed, variable pitch wind turbine are widely presented in the literature (Novak P., et al., 1995), (Bossany E.A., 2000), (Bindner H., et al., 1997), (Hansen A. D., et al., 1999).

The control method described in this report is close to that described in (Wortmann B., et.al, 2000). The strongest feature of the implemented control method is that it allows the turbine to operate with the optimum power efficiency over a wider range of wind speeds. Moreover, due to the design of this control method, the transition between power optimisation mode and power limitation mode is not dominated by large power fluctuations due to small changes in generator speed.

The present variable speed wind turbine control strategies are fundamentally based on the two static optimal curves, illustrated in Figure 50:

      (a) Mechanical power of turbine versus wind speed

      (b) Electrical power versus generator speed.

These characteristics are determined based on predefined aerodynamically data of the turbine. A parallel presentation of them, as shown in Figure 50 for a 2 MW wind turbine, provides a graphical illustration of the relation between the generated power, the wind speed and the generator speed for each operational stage of the wind turbine. Notice in Figure 50(b) that, as long as the speed can be varied, the maximum power extracted from the wind is a cubic function of the turbine optimum speed, as expressed in (37).

Each wind turbine has some physical operational restrictions, related to the acceptable noise emission, the mechanical loads and the size and the efficiency of the generator and of the frequency converter. It is therefore necessary to limit the stationary wind turbine rotational speed, to a range given by a minimum and a rated (nominal) value $\left[\omega_{rot}^{\min}, \omega_{rot}^{nom}\right]$. Notice that, the graph Figure 50 (b) in also indicates the operational speed range $[n_{gen}^{\min}, n_{gen}^{dyn,\max}]$ for the generator speed. The generator speed can be expressed in [rad/s] or in [rpm] as follows:

$$\omega_{gen}(u) = \eta_{gear}\omega_{rot}(u) \qquad\qquad [rad/s]$$

$$n_{gen}(u) = \frac{60}{2\pi}\omega_{gen}(u) = \frac{60}{2\pi}\eta_{gear}\omega_{rot}(u) \qquad [rpm]$$

(47)

where η_{gear} is the gear-box ratio. The operational speed range $[n_{gen}^{\min}, n_{gen}^{dyn,\max}]$ covers both the stationary generator speed range as well as the dynamical generator overspeed range, which is allowed by the doubly-fed induction generator DFIG's control.
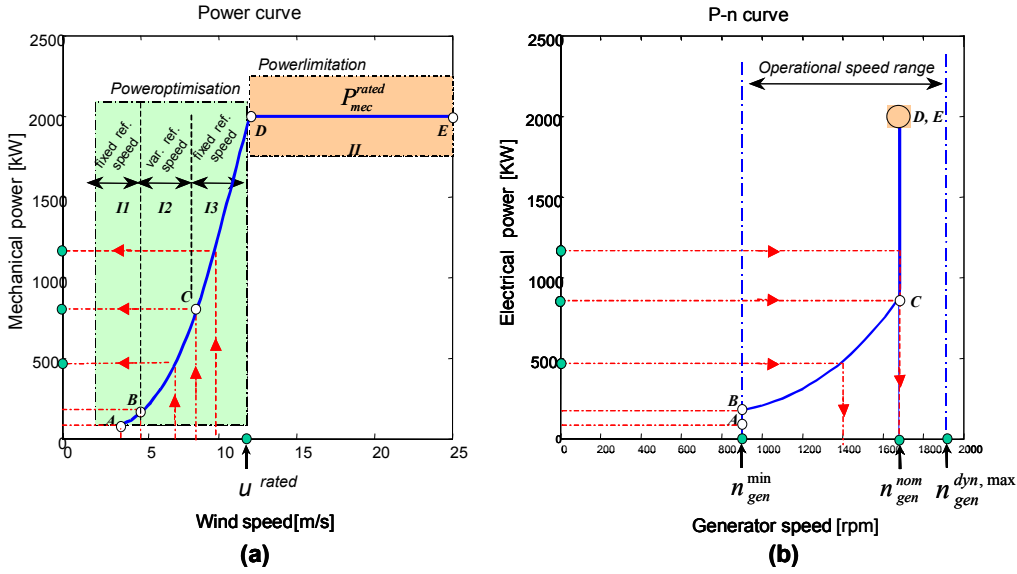
Figure 50: Two static curves used in the design of the control strategies for a doubly-fed induction generator:
(a) mechanical power versus wind speed and (b) electrical power versus wind speed.

Two control strategies for the variable speed wind turbine are indicated in Figure 50:

I. ***Power optimisation strategy*** (below rated wind speed u^{rated})– where the energy capture is optimised. It is depicted by the range *A-B-C-D,* both in Figure 50(a) and in Figure 50(b).

II. ***Power limitation strategy*** (above rated wind speed u^{rated}) – where the goal of the controller is to track the nominal (rated) power reference $P_{grid}^{rated,ref}$ of the wind turbine. It is depicted by the range *D-E* both in Figure 50(a) and in Figure 50(b).

Figure 50 points out four different control algorithms for the control of the variable speed wind turbine:

Algorithm I1. *Partial load operation with fixed reference speed at the lower limit* (power optimisation strategy zone *A-B*)

This case corresponds to the situation when the wind speeds are so small that the rotational speed is less than the lower limit $\omega_{rot} \leq \omega_{rot}^{min}$ (the generator speed $n_{gen} \leq n_{gen}^{min}$). The turbine's reference speed is therefore set to the minimal value $\omega_{rot}^{ref} = \omega_{rot}^{min}$ and the tip speed ratio $\lambda(u)$ is calculated by:

$$\lambda(u) = \frac{\omega_{rot}^{min} R}{u} \tag{48}$$

For each determined tip speed ratio $\lambda(u)$, the optimal power coefficient value $C_p^{opt}(\lambda)$ and then the corresponding pitch angle θ is found in the look-up table $C_p(\theta,\lambda)$. The optimum power is therefore achieved by keeping the turbine speed at the lower limit ω_{rot}^{min}:

$$P_{mec}^{opt}(u) = \frac{1}{2} \rho \pi R^5 \frac{C_p^{opt}(u)}{\lambda^3(u)} \left[\omega_{rot}^{min}\right]^3 \qquad [W] \qquad (49)$$

Algorithm I2. *Partial load operation with variable reference speed* (power op-timisation strategy zone *B-C*)

This case corresponds to the situation when the rotational speed is higher than the lower limit and less than the nominal rotational speed $\omega_{rot}^{min} < \omega_{rot} \leq \omega_{rot}^{nom}$ (the generator speed $n_{gen}^{min} < n_{gen} \leq n_{gen}^{nom}$). The goal here is to maximise the energy capture by tracking the maximum power coefficient C_p^{max} curve. The maximum power coefficient value C_p^{max} corresponds to one pitch angle θ_{opt} and one tip speed ratio λ_{opt}. The pitch angle is therefore kept constant to the optimal value θ_{opt}, while the tip speed ratio is tuned to the optimal value λ_{opt} over different wind speeds by adapting the rotor speed ω_{rot} to its reference, expressed by:

$$\omega_{rot}^{ref}(u) = \frac{\lambda_{opt} u}{R} \qquad [rad/s] \qquad (50)$$

The maximal mechanical power is therefore achieved by tracking the reference rotational speed:

$$P_{mec}^{max}(u) = \frac{1}{2} \rho \pi R^5 \frac{C_p^{max}}{\lambda_{opt}^3} \left[\omega_{rot}^{ref}(u)\right]^3 \qquad [W] \qquad (51)$$

Algorithm I3. *Partial load operation with fixed reference speed at the higher limit* (power optimisation strategy zone *C-D*)

This case corresponds to the situation when the turbine speed is restricted to the nominal value $\omega_{rot}^{ref} = \omega_{rot}^{nom}$ and when the generated power is less than the rated value ($P_{mec} < P_{mec}^{rated}$). The control algorithm is similar to ***Algorithm I1*** (presented for zone *A-B*), with the only difference that the tip speed ratio, the optimal power coefficient value $C_p^{opt}(\lambda)$, the optimal pitch angle θ and the op-timal power are determined based on ω_{rot}^{nom} instead for ω_{rot}^{min}. In this case, the highest efficiency is obtained by operating the turbine at nominal speed ω_{rot}^{nom}.

Algorithm II. *Full load operation* (power limitation strategy zone *D-E*)

This case corresponds to the situation of wind speeds higher than the rated wind speed. The reference output power is the rated mechanical power $P_{mec}^{ref} = P_{mec}^{rated}$ while the reference rotor speed is the nominal rotor speed $\omega_{rot}^{ref} = \omega_{rot}^{nom}$. Thus, for each wind speed *u*, the power coefficient is calcu-lated as:

$$C_p(\lambda) = \frac{2 P_{mec}^{rated} \lambda^3(u)}{\rho \pi R^5 \left[\omega_{rot}^{nom}\right]^3} \qquad (52)$$

Once the power coefficient value $C_p(\lambda)$ is calculated and the tip speed ra-tio $\lambda(u) = \omega_{rot}^{nom} R/u$ is known, the static pitch angle θ can then be determined by interpolation in the power coefficient table $C_p(\theta, \lambda)$.

An example of the pitch angle and rotor speed versus wind speed, determined based on the presented control strategies for a variable speed 2 MW wind turbine, is shown in Figure 51. Similar to Figure 50, Figure 51 also points out the wind turbine operation ranges (*A-B*, *B-C*, *C-D*, *D-E*). The pitch angle values in the power optimisation strategy are all found close to zero for the given wind turbine, while at higher wind speeds in order to limit the power, the pitch angle is increasing by a non-linear function. The static reference values of the rotor speed are, as expected, varying in zone *B-C* and otherwise are kept constant. However, as the DFIG control design allows overspeed in the case of a wind gust, the rotor speed can vary dynamically in zone C-D-E. Therefore, the ability to vary the rotor speed ω_{rot} is used in both strategies (power optimisation and power limitation), but it is mostly exploited below rated wind speed (in the power optimisation strategy). The ability to vary the pitch angle θ with wind speed is mostly used above rated wind speed to prevent over rated power production.
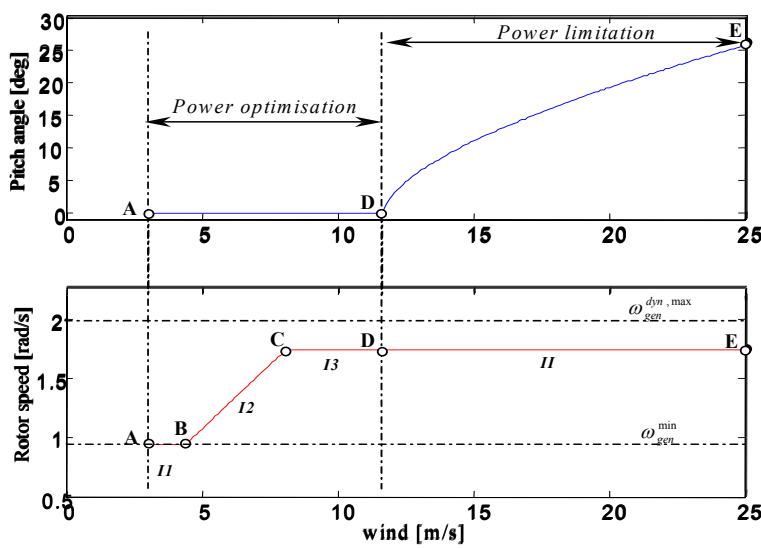

Figure 51: Generic static pitch angle and rotor speed versus wind speed - result of the control strategies.

4.6 Wind turbine control system

As illustrated in Figure 43, the wind turbine control contains two controllers, which are cross-coupled to each other:
1. Speed controller
2. Power limitation controller

The design of these two controllers is based on the previous described control strategies. The speed controller is the main controller in the power optimisation strategy, while in the power limitation strategy both controllers are active and cross-coupled to each other. This interconnection can be exemplified as follows.

If the wind speed is less than the rated wind speed u^{rated}, the pitch angle is kept constant to the optimal value θ_{opt}, while the generator speed ω_{gen} is adjusted by the wind turbine control in such a way that the maximum power is captured out of the wind. If a wind gust appears, the rotor speed ω_{rot} and thus also the generator speed ω_{gen} will increase due to the increased aerodynamic

torque. In this moment, the speed control loop reacts by increasing the power reference $P_{grid}^{conv,ref}$ to the DFIG control, see Figure 52. If the wind speed increases further beyond the rated wind speed, then the power limitation control loop, see Figure 53, reacts by increasing the pitch angle to prevent the power generation becoming too large. Meanwhile, the speed control loop controls the rotor speed to its nominal value, but allows rotor speed dynamic variations in a predefined speed range. The changes in the aerodynamic power are thus absorbed as changes in the rotational speed instead of as changes in torque and therefore the impact of the wind speed variations on the drive train loads is reduced.

4.6.1 Speed controller

The *speed controller* has as main tasks:

   1. to achieve the optimum power by keeping the generator speed at the lower limit $\omega_{gen}^{\min}$ (***Algorithm I1***) in power optimisation *A-B* zone with fixed low reference speed limit.

   2. to keep the optimal tip speed ratio λ_{opt} over different wind speeds *u*, by adapting the steady state generator speed to its reference ω_{gen}^{ref} (***Algorithm I2***) in power optimisation *B-C* zone with variable reference speed.

   3. to control the generator speed to its nominal value, allowing however dynamic variations in the predefined speed range indicated in Figure 50(b). For wind speeds above rated wind speed u^{rated} (in power limitation), the speed control loop prevents the rotor/generator speed becoming too large.

   Figure 52 shows the implemented speed control loop. It has as input the difference between the reference generator speed and the measured generator speed. The reference generator speed ω_{gen}^{ref} is obtained from the predefined static characteristic (see Figure 50(b)), and it corresponds to the generator speed at which the measured active power P_{grid}^{meas} on the grid is optimal. The error $\Delta\omega_{gen} = \omega_{gen}^{ref} - \omega_{gen}^{meas}$ is sent to a PI controller and then further to a power gradient limitation block. Unbalance between turbine torque and generator torque will result in an accelerating torque until the desired speed is reached. The output of the speed controller is the reference power value on the grid $P_{grid}^{conv,ref}$ to the DFIG control.
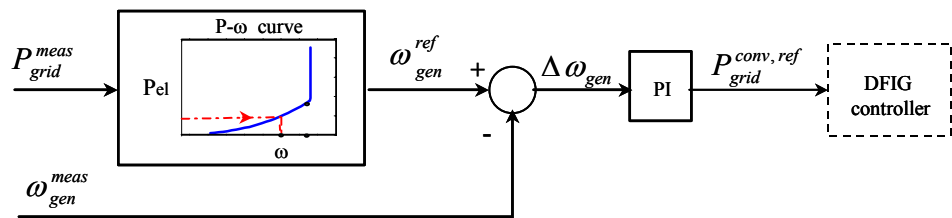

Figure 52: Speed controller of the wind turbine control.

   Notice that the speed controller is active both in the power optimisation and power limitation operating modes. The parameters of the speed controller are changed depending on the wind turbine-operating mode (power optimisation or power limitation).

4.6.2 Power limitation controller with gain scheduling

The *power limitation controller* has as task to increase or decrease the pitch angle in the power limitation strategy, i.e. in order to limit the generated power to the rated power.

Figure 53 shows the power limitation control loop. The error signal $\Delta P = P_{grid}^{meas} - P_{grid}^{rated,ref}$ based on the measured power in the grid point M, is sent to a PI-controller. The PI controller produces the reference pitch angle θ_{ref}. This reference is further compared to the actual pitch angle θ and then the error $\Delta\theta$ is corrected by the servomechanism. In order to get a realistic response in the pitch angle control system, the servomechanism model accounts for a servo time constant T_{servo} and the limitation of both the pitch angle and its gradient. The output of the power limitation controller is the pitch angle of the blades.
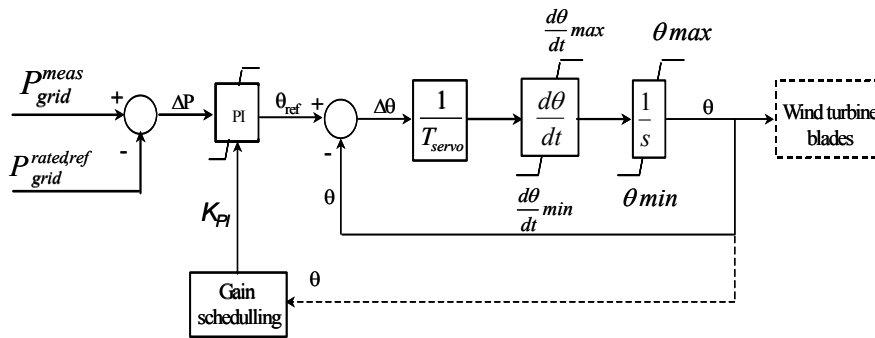

Figure 53: Power limitation controller of the wind turbine control, which controls the pitch.

Notice that both speed and power limitation controllers do not need a wind speed measurement. Only the generator speed and the generator active power are required. Ideally, the control parameters would be chosen as a function of the wind speed, but this is not an appropriate procedure due to the fact that it is not possible to measure the wind speed precisely. Assuming that the wind turbine system is well controlled, then the pitch angle and the active power can be used as gain-scheduling parameters instead of wind speed. Therefore, the implementation of the gain scheduling is performed based on knowledge of the pitch angle, which can be thus used to express the non-linear aerodynamic amplification in the system.

The non-linear variation of the pitch angle versus wind speed for high wind speeds, illustrated in Figure 51, implies the necessity of a non-linear control (gain scheduling) – as indicated in Figure 53. A linear control would result in instabilities at high wind speeds.

The total gain of the system in the power control loop K_{system}, can be expressed as a proportional gain K_{PI} in the PI controller times aerodynamic sensitivity of the system $\frac{dP}{d\theta}$:

$$K_{system} = K_{PI}\ \frac{dP}{d\theta} \tag{53}$$

The aerodynamic sensitivity $\frac{dP}{d\theta}$ of the system depends on the operating conditions (the setpoint power value, the wind speed or the pitch angle). There-

fore, in order to maintain the total gain of the system K_{system} constant, the proportional gain of the PI controller K_{PI} is changed in such a way that it counteracts the variation of the aerodynamic sensitivity $\dfrac{dP}{d\theta}$. The gain of the controller K_{PI} must therefore incorporate information on the dependency of the variation of the power with the pitch angle. The variation of the aerodynamic sensitivity with the pitch angle for a 2 MW wind turbine is illustrated in Figure 54(a). It increases numerically (absolute value) with the pitch angle and it can vary with a factor up to 10.
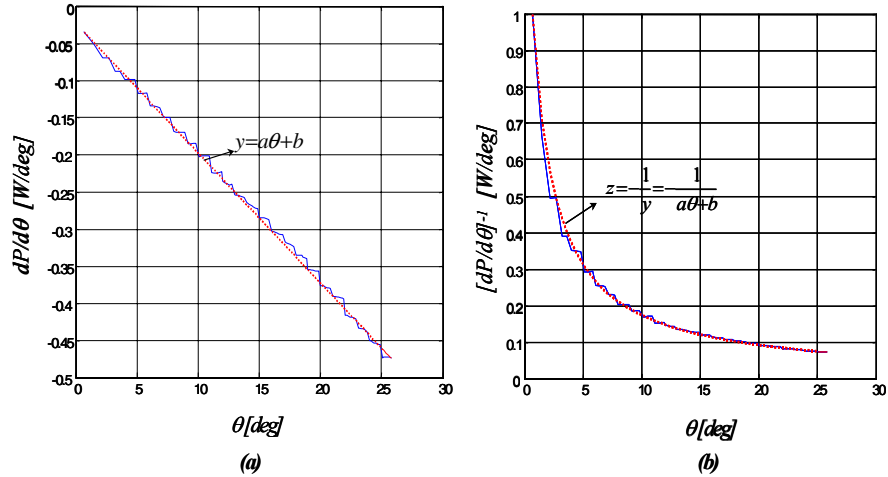

Figure 54: Sensitivity function and the inverse sensitivity function of the wind turbine. (a) sensitivity function dP/dθ *versus pitch angle* θ *. (b) inverse sensitivity function [*dP/dθ]⁻¹ *versus pitch angle* θ.

Observe that the variation of the aerodynamic sensitivity is almost linear in the pitch angle θ and therefore a linear expression with the parameters *a* and *b* can be estimated:

$$\frac{dP}{d\theta} = a\,\theta + b \tag{54}$$

This linear description makes it possible to determine the reciprocal of the aerodynamic sensitivity, defined as follows:

$$\left[\frac{dP}{d\theta}\right]^{-1} = -\frac{1}{a\,\theta + b} \tag{55}$$

where the negative sign compensates for the negative ramp of the aerodynamic sensitivity and thus assures that the sign of the total gain of the system does not change. Notice that the reciprocal sensitivity function $\left[\dfrac{dP}{d\theta}\right]^{-1}$, illustrated in Figure 54(b), is non-linear with the pitch angle. It is used in the definition of the controller gain K_{PI} to counteract the mentioned variation, as follows:

$$K_{PI} = K_{basis}\ \left[\frac{dP}{d\theta}\right]^{-1} \tag{56}$$

where K_{basis} is the constant proportional gain of the PI- controller, determined to be appropriate for one arbitrary wind speed. Notice that the more sensitive the system is (larger pitch angles θ / higher wind speeds) the smaller the gain for the controller should be and vice versa. The introduction of the gain scheduling

enables the PI- controller to perform an adequate control over the whole wind speed range.

4.6.3 Cross-coupled control

Both the speed control loop and the power control loop are cross-coupled in the power limitation strategy. Notice that these two strategies do not need a wind speed measurement. Only the generator speed and active power are required.

The interconnection between speed control loop and power control loop can be exemplified as follows. If the wind speed is less than the rated wind speed u^{rated}, the pitch angle is kept constant to the optimal value θ_{opt}, while the generator speed ω_{gen} is adjusted by the frequency converter control in such a way that the maximum power is obtained. If now a wind gust appears, the rotor speed ω_{rot} and thus also the generator speed ω_{gen} are increasing due to the increased aerodynamic torque, and the speed control loop reacts by increasing the power reference $P_{grid}^{conv, ref}$ (in Figure 52). If the wind speed increases further over the rated wind speed, then the power control loop reacts by increasing the pitch angle to prevent the power generation becoming too large. Meanwhile, the rotor speed is also prevented to become too large by the speed control loop, which tries to keep the rotor speed to its nominal value. DFIG control has the advantage to permit a dynamical variation range of the generator/rotor speed around the nominal value. Thus the impact of the wind speed variations on the drive train loads is reduced. The changes in the aerodynamic power are absorbed as changes in the rotational speed instead of as changes in torque.

4.7 Simulation results

Different scenarios are simulated to asses the performance of both the DFIG controller and of the overall control of the variable speed /variable pitch wind turbine.

A. **DFIG control**

Using the stator flux control approach, the active power control is decoupled from reactive power control. As mentioned before the active and reactive power can be controlled using the impressed rotor currents in the stator flux reference frame. Thus, the active power control is achieved by controlling the rotor current q- component $I_{q,rotor}^{meas}$ orthogonal to the stator flux, while the reactive power control is achieved by controlling the d- component of the rotor current referred to the stator flux $I_{d,rotor}^{meas}$. Figure 55 illustrates the control of the active power on the grid when a step in the reference active power signal $P_{grid}^{conv, ref}$ on the grid is imposed and when the reference reactive power signal $Q_{grid}^{conv, ref}$ remains unchanged.
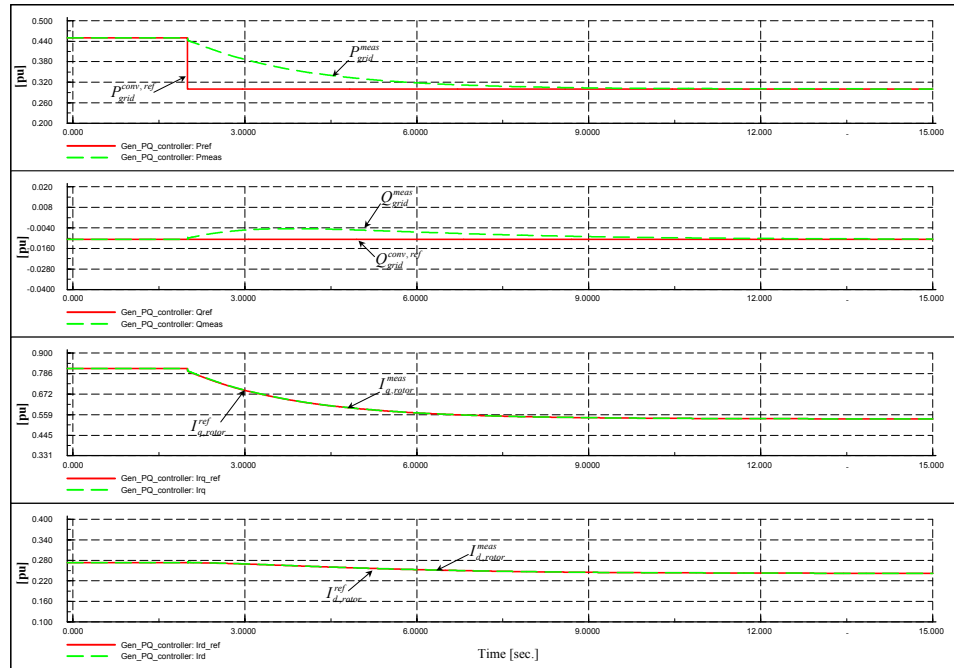
Figure 55: Decoupled control of active and reactive power of DFIG.

The active power step response, measured on the grid (30 kV), exhibits good dynamic performance. A little coupling with the reactive power control is observed in the transient phase. However, in steady state the reactive power is not affected by the active power step, as it is back to its reference value. As expected, the step in the reference of the active power is reflected only in the q-component and not in the d- component of the rotor current, as the reactive power is controlled by the d- component.

B. **Power flow inside DFIG**

Both Figure 56 and Figure 57 illustrate the results of a simulation, where a fictive non-turbulent wind speed with fixed mean value and a sinusoidal variation with a 3p frequency is used. A variable speed DFIG wind turbine with 2 MW rated power is considered. A step in the mean speed value from 7 m/s to 9 m/s is performed to force the system from sub-synchronous to over-synchronous operation. The purpose of this simulation is to illustrate:

- the power flow through the grid, stator and rotor when the DFIG changes between sub-synchronous and over-synchronous operations, due to a step in the wind speed.
- the filter effect of the mechanical 3p fluctuations in the electrical power.

Notice in Figure 56 that during sub-synchronous operation the power delivered to the grid is less than that delivered by the stator P_{stator}, as in the rotor circuit the power is flowing from the grid to the rotor via power converter ($P_{rotor}<0$). Meanwhile in over-synchronous operation, the power delivered to the grid is higher than that from the stator because of the power contribution from the rotor. The rotor power flows from the rotor to the grid in over-synchronous operation ($P_{rotor}>0$).
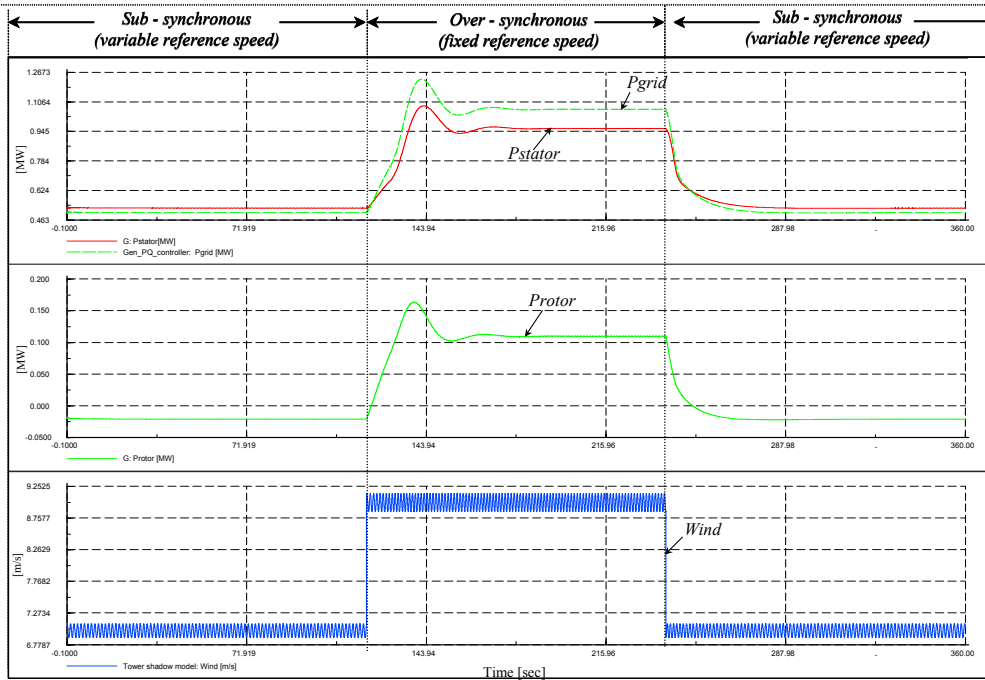
Figure 56: Simulated power through the grid, stator and rotor in sub-synchronous and over-synchronous operations.

The 3p fluctuations of the wind speed are present in the mechanical part of the system, i.e. in the aerodynamic torque, but not on the electrical part, i.e. in the electrical torque – see Figure 57. The 3p fluctuations in the wind are thus not visible in the electrical power. They are reduced substantially by the control of the DFIG. For this wind speed range (7 m/s to 9 m/s), the wind turbine operates in the power optimisation mode (zone B-C-D), where the speed controller seeks to maximise the power captured from the wind according to Figure 50(b). It thus adjusts the generator speed to its predefined reference (variable or fixed) to be able to capture as much energy from the wind as possible. The power limitation controller is not active here, as the rated power is not reached. The pitch angle is kept constant to its optimal value determined with the control **Algorithm I2** and **I3**.
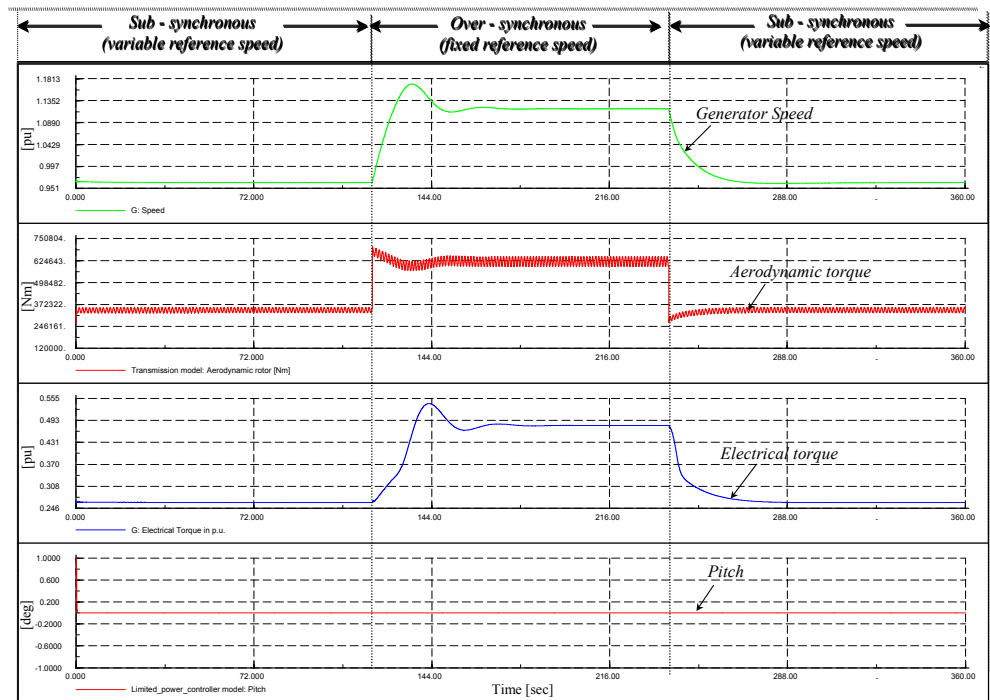
Figure 57: Simulated generator speed, aerodynamic torque, electrical torque and pitch angle.

C. **Overall control of the wind turbine**

Both Figure 58 and Figure 59 illustrate how the control algorithms are working at different operating conditions. Again a variable speed wind turbine with a rated power of 2 MW is used. The rated wind speed is 11.5 m/s and the rated generator speed ω_{gen}^{nom} is 1686 rpm. Typical quantities are shown: wind speed, generator speed and reference generator speed, the pitch angle and the generator power on the grid.

Figure 58 illustrates the simulation operation at 7 m/s mean value turbulent wind speed with turbulence intensity of 10%. This operation corresponds to the power optimisation with variable generator speed reference (zone B-C in Figure 50).
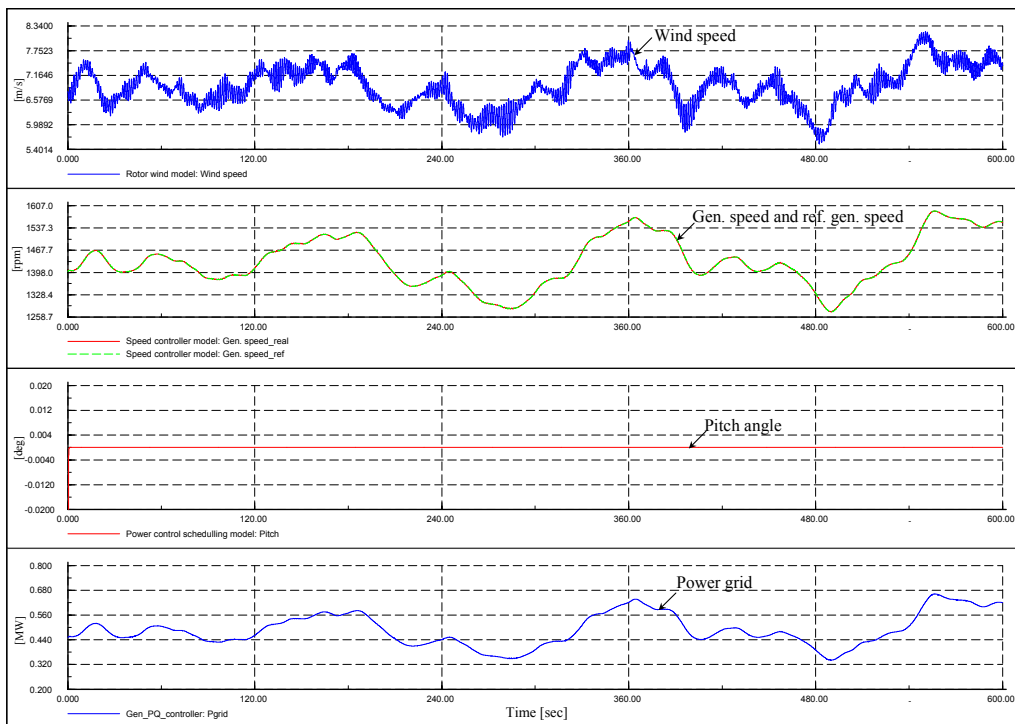
Figure 58: Simulation with turbulent wind speed, with mean 7m/s and turbulence intensity of 10%.

In power optimisation, the main turbine controller is the speed controller. As the rated power is not reached, the power limitation controller is not active. The speed controller has here to be strong and fast in order to seek to the maximum power. It has to assure that the generator speed follows very well the variable generator speed reference in order to be able to absorb the maximum energy from the wind. The speed reference is generated based on the static curve illustrated in graph (b) of Figure 50 and it corresponds to the generator speed for which the measured power is optimal. As expected for this wind speed range (7 m/s mean value), the pitch angle is not active, being kept constant to its optimal value (i.e. zero for the considered wind turbine). Notice that the fast oscillations in the wind speed are completely filtered out from the electrical power.

Figure 59 shows the simulation results when a turbulent wind speed with a mean value of 18 m/s and a turbulence intensity of 10% is used. In order to illustrate the elasticity of the variable speed DFIG wind turbine, some gusts about 5 m/s up and down, respectively, are introduced in the wind speed at each 150s.

This simulation case corresponds to the power limitation strategy, where both the speed controller and the power limitation controller are active. The power limitation control loop is strong and fast, while the speed control loop is deliberately much slower, allowing dynamic variations of the generator speed in the speed range permitted by the size of the power converter.
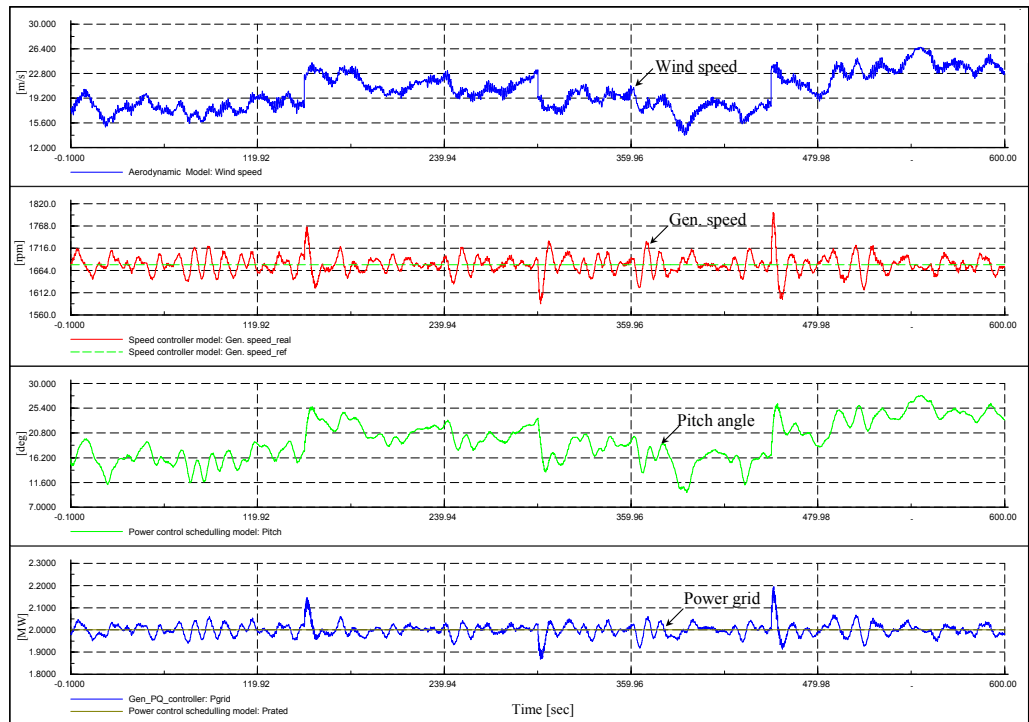
Figure 59: Simulation with turbulence wind speed, with mean speed 18 m/s, turbulence intensity 10% and gusts.

The power limitation controller changes the pitch angle to keep the rated power, while the speed controller prevents the generator speed from becoming too high. Contrary to the power optimisation, illustrated in the previous simulation, the speed controller allows here deviations of the generator speed from its reference (rated) value. For example, at the time instant t=150 s, the wind speed rapidly reaches 22 m/s. The generator speed increases quickly due to the increased aerodynamic torque. The electrical power increases too, until the pitch controller reacts modifying the pitch angle. The pitch controller is not fully capable of capturing this fast wind speed change. The pitch angle follows the slow variation in the wind speed, while fast gusts in the wind speed are absorbed as variation (peaks) in generator speed. The rotational speed of the turbine rotor is thus allowed to increase storing energy into the turbine's inertia.

5 CONCLUSIONS

The report presents the wind turbine modelling in the power system simulation program DIgSILENT, both at component level and at system level. The report contains an overview over some electrical models (induction generator, power converters, transformers), already integrated components in the power system tool, but also over the newly developed and implemented wind turbine models (mechanical model, aerodynamical model, wind model, control model).

The wind turbine dynamic model includes the main effects that contribute to the fluctuation of the power from a wind turbine. It comprises the mechanical model, the aerodynamic model (improved with a model for dynamic stall effects) and the electrical model: induction generator, power converter (converter, soft-starter, capacitor bank) and transformer.

The built-in electrical models in DIgSILENT are initialised automatically by the load flow calculation, while the user developed models, must be initialised by the user. If the initialisation is not done properly, it results in large fictive transients, which must decay before the actual dynamics can be simulated. This costs simulation time and in some cases the fictive transients even can cause numerical instabilities. An initialisation method is therefore developed and implemented. This method allows immediately an accurate simulation of the dynamic performance, without fictive transients in the beginning of the simulation.

At the system level, two wind turbine concepts have been implemented in the power system simulation program DIgSILENT:

- Active stall wind turbine (fixed speed) with induction generator
- Variable speed/variable pitch wind turbine with doubly-fed induction generator DFIG

These wind turbine concept models can be used or even extended for the study of different aspects, e.g. assessment of power quality, control strategies, connection of the wind turbines at different types of grid.

The goal has been to build generic models, which are not restricted by confidentiality, but as a consequence, the performance of the simulation models may differ some from the performance of a specific wind turbine.

Since wind turbine controllers can be designed in several ways, and since the design details are normally confidential, new control methods have been proposed and implemented, their performance assessed and discussed by means of simulations. The design as well as the evaluation of the controllers was carried out, in the first place, for normal continuous operations (for both power optimisation and power limitation operations).

The control during grid faults has not been investigated in the present project. This is an important issue, as wind turbines are replacing other generating units in the system, and as thus the wind turbine control must be able to both support the grid stability and to protect the wind turbine.

Active stall wind turbine controller

Characteristic for the implemented active stall wind turbine controller is that it achieves good power yield with a minimum of pitch actions. Once the overall mean wind speed is at a constant level, pitch angle adjustments are hardly necessary. Allowing the controller to control the pitch angle most fast and optimal, a 10-minute simulation shows that the potential increase in power would be 1% for wind speeds below nominal wind speed. Considering wind speeds beyond nominal wind speed the power yield is not improved at all.

Depending on the pitch system, the lost power (due to slow control) may be justified by reduced stress and wear in the pitch system and reduced fatigue loads in the wind turbine. This applies to power optimisation, where the controller strives for maximum power yield by using moving average of the wind speed signal for finding the appropriate pitch angle in a lookup table. This applies also to power limitation where the power output is controlled in a closed control loop.

With a slow control system, substantial overpower in the power limitation mode may cause problem. This is avoided by an overpower protection feature.

The simulations conducted show that the controller manages to run the turbine efficiently in many conceivable wind speed situations. The system has no tendency to become unstable in which situation ever, since the controller does not attempt to respond to fast transients instantaneously.

Variable speed, variable pitch wind turbine with doubly-fed induction generator DFIG

The overall control of the variable speed, variable pitch wind turbine with DFIG has as goal to track the wind turbine optimum operation point, to limit the power in the case of high wind speeds and to control the reactive power interchanged between the wind turbine generator and the grid.

In the overall control method of the variable speed, variable pitch wind turbine with DFIG, two hierarchical control levels, strongly connected to each other, can be depicted: DFIG control level (control of active and reactive power) and wind turbine control level.

A vector control approach is adopted for the control of the DFIG, while the control of the wind turbine is a result of two cross-coupled controllers: a speed and a power limitation controller. The strongest feature of the implemented control method is that it allows the turbine to operate with the optimum power efficiency over a wider range of wind speeds. Moreover, due to the design of this control method, the transition between power optimisation mode and power limitation mode is not dominated by large power fluctuations due to small changes in generator speed. A gain scheduling control of the pitch angle is also implemented in order to compensate for the non-linear aerodynamic characteristics.

The performed simulations show that the implemented control method is able to control efficiently the variable speed DFIG wind turbine at different normal operation conditions. At wind speeds lower than the rated wind speed, the speed controller seeks to maximise the power according to the maximum coefficient curve. As result, the variation of the generator speed follows the slow variation in the wind speed. At high wind speeds, the power limitation controller sets the blade angle to keep the rated power, while the speed controller permits a dynamic variation of the generator speed in a predefined speed range in order to avoid mechanical stress in the gear-box and the shaft system. As a result, the pitch angle follows the slow variation in wind speed, while fast gusts are absorbed in variations of the generator speed.

One future research step is to investigate and enhance the controller's capabilities of DFIG to handle grid faults. Another interesting issue is to explore the present controller in the design of a whole wind farm controller with variable speed, variable pitch wind turbines with doubly-fed induction generators, where focus is drawn on the voltage and frequency regulation of the grid.

The two implemented wind turbine concept models are an important step towards the long-term objective of developing tools for study and improvement of the dynamic interaction between wind turbines/wind farms and power systems to which they are connected. These models can be easily extended to model different kinds of wind turbines or wind farms.

Acknowledgements

REFERENCES

Bindner H., Rebsdorf A., Byberg W. (1997) *Experimental investigation of combined variable speed/variable pitch controlled wind turbines.* EWEC, Dublin, 4p.

Bossany, E.A. (2000) *The design of closed loop controllers for wind turbines.* Wind Energy, vol. 3, p. 149-163.

DEFU (1998). *Connection of wind turbines to low and medium voltage networks*, Report no. KR111-E, Elteknikkomiteen (1998-10-09).

DIgSILENT GmbH (2002). *"DIgSILENT PowerFactory V13 – User Manual"*

DIgSILENT note on power converter, 2003

Eltra (2000). *Specifications for Connecting Wind Farms to the Transmission Network.* ELT 1999-411a, Eltra, http://www.eltra.dk.

Hansen, L.H.,Helle L., Blaabjerg F., Ritchie E., Munk-Nielsen S., Bindner, H., Sørensen, P. and Bak-Jensen, B. (2001) *Conceptual survey of Generators and Power Electronics for Wind Turbines*, Risø-R-1205(EN).

Hansen A. D., Bindner H., Rebsdorf A. (1999) *Improving transition between power optimisation and power limitation of variable speed/variable pitch wind turbines*. European Wind Energy Conference, Nice, France, 1-5 March, p. 889-892.

Hansen A. D., Sørensen P., Blaabjerg F., Bech J. (2002) *Dynamic modelling of wind farm grid interaction*. Wind Engineering, Vol. 26, No.4, p. 191-208.

Hansen A. D., Sørensen P., Iov F., Blaabjerg F. (2003) *Initialisation of grid-connected wind turbine models in power-system simulations*. Wind Engineering, Vol. 27, No.1, p. 21-38.

Hansen A.D. (2004). *Generators and Power Electronics for wind turbines*. Chapter in "Wind Power in Power systems", John Wiley&Sons, Ltd, 24 p, to be published in 2004.

Heier S. (1998). *Grid Integration of Wind Energy Conversion Systems*, ISBN 0 471 97143.

IEC 61400-21 (2001). *Wind turbine generator systems - Part 21: Measurement and assessment of power quality characteristics of grid connected wind turbines*. Final Draft International Standard 88/144/FDIS International Electrotechnical Commission, IEC 2001-07-01, Ed.1.

Krause P.C., Wasynczuk O., Sudhoff S. D. (2002) *Analysis of Electric machinery and drive systems*, IEEE Press

Langreder W. (1996) *Models for variable speed wind turbines* CREST, Dept. of Electrical Engineering, Loughborough University, UK and Risø National Laboratory, Denmark.

Lehnhoff M., Böhmeke G., Trede A. (1998) *Active-Stall / Passive-Stall Vergleich und Betriebsergebnisse*, aerodyn Energiesysteme GmbH, Husumer Schiffswerft, DEWEK'98 Tagungsband, p. 78-81

Leonhard, W. (2001) *Control of electrical drives*, Springer Verlag, ISBN 3540418202.

Pöller, M. (2003) *Doubly-Fed Induction Machine Models for Stability Assesment of Wind Farms*, Power Tech. Conf., Bologna.

Mohan N., Undeland, T.M. and Robbins, W.P. (1989) *Power Electronics: converters, applications and design*.

Novak P., Ekelund T., Jovik I., Schmidtbauer B. (1995) *Modelling and control of variable speed wind turbine-drive-system dynamics.* IEEE Control Systems, August.

Novotny D.W., Lipo T.A. (1998) *Vector control and dynamics of AC drivers*, Oxford University Press.

Pena, R., Clare, J.C. and Asher, G.M. (1996) *Doubly-fed induction generator using back-to-back PWM converters and its application to variable speed wind-energy generation.* IEE proceedings on electronic power application, 143(3), p. 231-241.

Rosas P.A.C. (2003) *Power Quality and Stability Issues of Integration of Large Wind Farms.* Ph.D. thesis

Sørensen P., Bak-Jensen B., Kristiansen J., Hansen A.D., Janosi L., Bech J. (2000) *Power plant characteristics of wind farms.* Wind Power for the 21st Century. Proceddings of the International Conference held at Kassel, Germany 25-27 September.

Sørensen P., Hansen A.D., Janosi L., Bech J., Bak-Jensen B. (2001a) *Simulation of interaction between wind farm and power system.* Risø-R-1281, Risø National Laboratory.

Sørensen P., Hansen A.D., Rosas P.A.C. (2001b) *Wind models for prediction of power fluctuations from wind farms.* Journal of Wind Engineering no 89, p. 9-18 .

Wortmann B., Hansen L.H. (2000) *Multipole generator wind energy converter without gearbox and with variable speed.* Project EFP 96 report. Partners: Risø national Laboratory, Elkraft AmbA, Siemens A.G., NEG Micon A/S.

Øye,& S. (1991). *Dynamic stall - simulated as time lag of separation.* In Vol. Proceedings of the 4th IEA Symposium on the Aerodynamics of Wind Turbines, McAnulty, K.F- (Ed.), Rome, Italy.

Abstract (max. 2000 characters)

The present report describes the dynamic wind turbine models implemented in the power system simulation tool DIgSILENT (Version 12.0). The developed models are a part of the results of a national research project, whose overall objective is to create a model database in different simulation tools. This model database should be able to support the analysis of the interaction between the mechanical structure of the wind turbine and the electrical grid during different operational modes.

The report provides a description of the wind turbines modelling, both at a component level and at a system level. The report contains both the description of DIgSILENT built-in models for the electrical components of a grid connected wind turbine (e.g. induction generators, power converters, transformers) and the models developed by the user, in the dynamic simulation language DSL of DIgSILENT, for the non-electrical components of the wind turbine (wind model, aerodynamic model, mechanical model). The initialisation issues on the wind turbine models into the power system simulation are also presented. However, the main attention in this report is drawn to the modelling at the system level of two wind turbine concepts:

1. **Active stall wind turbine with induction generator**
2. **Variable speed, variable pitch wind turbine with doubly-fed induction generator**

These wind turbine concept models can be used and even extended for the study of different aspects, e.g. the assessment of power quality, control strategies, connection of the wind turbine at different types of grid and storage systems. For both these two concepts, control strategies are developed and implemented, their performance assessed and discussed by means of simulations.